

Shear resistance of tongued-and-grooved timber panels

Laboratory tests and FE analysis

Master's Thesis in the International Master's Programme Structural Engineering

ERIK HANSSON

MARCUS PETERSSON

Department of Civil and Environmental Engineering

Division of Structural Engineering

Steel and Timber Structures

CHALMERS UNIVERSITY OF TECHNOLOGY

Göteborg, Sweden

Master's Thesis 2006



Shear resistance of tongued-and-grooved timber panels


Laboratory tests and FE analysis

Master's Thesis in the International Master's Programme Structural Engineering

ERIK HANSSON

MARCUS PETERSSON

Department of Civil and Environmental Engineering
Division of Structural Engineering
Steel and Timber Structures
CHALMERS UNIVERSITY OF TECHNOLOGY
Göteborg, Sweden 2006

Shear resistance of tongued-and-grooved timber panels 

Laboratory tests and FE model

Master's Thesis in the International Master's Programme Structural Engineering

ERIK HANSSON

MARCUS PETERSSON

© ERIK HANSSON & MARCUS PETERSSON, 2006

Master's Thesis 2006:20

Department of Civil and Environmental Engineering

Division of Structural Engineering

Steel and Timber Structures

Chalmers University of Technology

SE-412 96 Göteborg

Sweden

Telephone: + 46 (0)31-772 1000

Cover:

Picture from laboratory test and figure of model from ABAQUS.

Chalmers Reproservice  Department of Civil and Environmental Engineering
Göteborg, Sweden 2006

Shear resistance of tongued-and-grooved timber panels
Laboratory tests and FE analysis
Master's Thesis in the International Master's Programme Structural Engineering
ERIK HANSSON
MARCUS PETERSSON
Department of Civil and Environmental Engineering
Division of Structural Engineering
Steel and Timber Structures
Chalmers University of Technology




ABSTRACT

Timber has long traditions as a construction material in Sweden. The Swedish government has presented a report with a aim of increasing the use of timber as a construction material. In Sweden of the present time tongued-and-grooved (t&g) timber is primarily used in roof constructions and also sporadically as board material in walls. There are no good models to calculate the shear resistance of a panel with t&g timber boards, although evidence of a certain effect does exist. If a good model for calculating the shear capacity could be developed, t&g timber could partly replace other timber-based panel materials in some constructions. A higher use of t&g timber is a good economic solution both for the users and also for sawmill industries because of the high availability of t&g timber and the low production volume of board materials. This master's thesis is intended as a pilot project in order to investigate whether it is possible to calculate any shear resistance in a panel with t&g boards and how it is affected by attaching wallpaper. The study is divided into two parts, a part with laboratory work that investigates the behaviour between two individual boards and a part that develops a model with the commercial Finite Element software ABAQUS for analysing larger size panels in order to make comparisons with existing constructions.

Introductory studies were conducted in order to be able to investigate how the shear resistance in a panel with t&g timber could be seen as friction behaviour between the individual boards in the panel. A laboratory test was carried out with a laboratory test procedure of the capacity in shear of the panel materials as the starting point. Tests in the laboratory were performed in order to measure how the value of the friction was changed with repeated loading, at varying moisture content and with wallpaper attached to the panel. The modelling started from a model of the same size as the panel that was tested in the laboratory. On the basis of a verified model, the modelling was expanded to including a model of an entire panel, a shear wall. The shear capacity of the wall could now be compared with modelled and hand-calculated walls with plywood as the board material.

The results of the modelling show that, with wallpaper attached to a wall, the shear resistance can be comparable to that of a wall with plywood. The wallpaper in our experiments was shown to be too elastic and, in the service limit state, the deformation in the wall becomes too large. However, the results show a striking and interesting increase in the capacity with wallpaper attached, so that future studies have to be recommended.

Keywords: Tongued-and-grooved timber, board materials, shear resistance, friction, moisture content, spruce

Bärförmåga i skjuvning för råspontpaneler
Laboratorie test och FE modulering
Examensarbete inom Konstruktionsteknik 
ERIK HANSSON
MARCUS PETERSSON
Institutionen för bygg- och miljöteknik
Avdelningen för Konstruktionsteknik 
Stål- och Träbyggnad 
Chalmers tekniska högskola

SAMMANFATTNING

Trä har en lång tradition som konstruktionsmaterial i Sverige. Sveriges regering har uttryckt en önskan om ökad användning av trä som konstruktionsmaterial. Råspont används idag i Sverige främst i takkonstruktioner och även sporadiskt i väggkonstruktioner. Det finns inga bra modeller för att räkna på bärförmågan i skjuvning för en råspontpanel, dock finns bevis för en viss effekt. Skulle en bra modell för beräkning utvecklas skulle råspont i viss mån kunna ersätta skivmaterial i olika konstruktioner. En ökad användning av råspont skulle vara lönsamt både för den enskilde användaren och för sågverksindustrin som har låg produktion av skivmaterial men en hög tillgång till råspont. Examensarbetet är tänkt som ett pilotprojekt för att utröna om möjligheten finns att tillgodoräkna sig skjuvverkan i råspontpanel och hur skjuvverkan påverkas med t.ex. en tapet fäst på panelen. Arbetet är uppdelat i två delar, en laboratoriedel som utreder beteendet mellan två enskilda brädor och en del som utvecklar en modell med hjälp av det kommersiella Finita Element programmet ABAQUS för en större panel för att kunna jämföra med befintliga konstruktioner.

Inledande studier gjordes för att kunna utreda hur skjuvverkan i en råspontpanel kunde ses som ett friktionsbeteende mellan de individuella brädorna i panelen. Ett laboratorietest utfördes med utgångspunkt från laboriemodell av skivor för skjuvning. Test i laboriet gjordes för att mäta hur värdet på friktionen ändrades vid upprepning av last, vid varierande fuktkvot och med en tapet fastlimmad på panelen. Med resultat och utvärderingar från denna del av undersökningen kunde nu arbetet fortsätta med modellering. Modelleringen utgick ifrån en modell i samma storlek som panelen som testades i laborietestet. Utifrån en verifierad modell expanderades modellen till att innefatta en modell av en hel panel i form av en vägg. Bärförmågan i skjuvning på väggen kunde nu jämföras med modellerade och handberäknade väggar med plywood som skivmaterial.

Resultaten från modelleringen visar att med en tapet pålimmad på en vägg kan bärförmågan i skjuvning bli jämförbar med en vägg med plywood. Tapeten i genomförda försök visade sig dock vara lite för elastisk och i bruksstadiet blir deformationerna i väggen för stora. Dock visade resultaten en så markant och intressant höjning av kapaciteten med tapet pålimmad på råspont att framtida studier på området bör rekommenderas.

Nyckelord: Råspont, skivmaterial, bärförmåga i skjuvning, friktion, fuktkvot, trä, gran

Contents

ABSTRACT	I
SAMMANFATTNING	III
CONTENTS	V
PREFACE	IX
NOTATIONS	X
1 INTRODUCTION	1
1.1 Background	1
1.2 Aim	2
1.3 Problem description	3
1.4 Method	5
2 T&G MATERIAL PROPERTIES	6
3 THEORY AND MODELS	8
3.1 Friction theory	8
3.2 The elastic model according to Källsner	10
4 LABORATORY TESTS	12
4.1 Test standard EN594	13
4.2 Panel shear method C	15
4.2.1 Evaluation of background theories for laboratory tests	17
4.3 Description of test procedure	21
4.3.1 Clamp force device.	22
4.3.2 Calibration of the pressure springs	27
4.3.3 Results of spring calibration	28
5 LABORATORY TEST OF T&G TIMBER PANELS AND THE RESULTS	30
5.1 Influence of moisture content on friction	30
5.2 Conditioning of test material	31
5.3 Timber to timber friction coefficient	32
5.3.1 Stiffness behaviour for friction	33
5.4 Effect of varied load level	34
5.5 Effects of varied moisture content	35
5.6 Effects of repeated loading	39
5.7 Effects of varying load rate	43
5.8 Effects of wallpaper attached to the panel	44
	V

6	EVALUATION OF LABORATORY TESTS	49
6.1	Test of timber friction coefficient	49
6.2	Varied horizontal load level	49
6.3	Varied moisture content	49
6.4	Repeated loading	50
6.5	Varied load rate	51
6.6	Wallpaper attached to panel	52
6.6.1	Strength Capacity	53
6.6.2	Stiffness behaviour	55
6.6.3	Summary effects of wallpaper	56
7	FE MODELLING	57
7.1	Modeling the laboratory test of friction with t&g panel	57
7.1.1	Model of t&g board	57
7.1.2	Material properties	58
7.1.3	Time step	58
7.1.4	Interactions	59
7.1.5	Loads and boundaries	61
7.1.6	Mesh	62
7.1.7	Results	63
7.2	Simplified model of performed laboratory test	64
7.2.1	Boards	64
7.2.2	Friction modelling with Slot+Align connectors	65
7.2.3	Load and Boundary Conditions	67
7.2.4	Results from ABAQUS simulation	68
7.3	Panel with wallpaper added	68
7.3.1	Results from wallpaper simulation	69
7.4	Shear wall with plywood	70
7.4.1	Frame	71
7.4.2	Plywood sheathing	71
7.4.3	Nails	71
7.4.4	Boundary conditions	72
7.4.5	Load acting on shear wall	72
7.4.6	Results	73
7.4.7	Verification of model	74
7.5	Modelling of full scale shear wall with t&g	75
7.5.1	Frame	75
7.5.2	T&g sheathing	75
7.5.3	Nails	75
7.5.4	Interaction properties	76
7.5.5	Boundary conditions and loads	78
7.5.6	Results from ABAQUS	78
7.5.7	Evaluation	79
7.5.8	Parametric study	80

8	CONCLUSION	82
9	REFERENCES	84
10	APPENDIX A - DIAGRAMS AND VALUES FROM LABORATORY	86
11	APPENDIX B - REPEATED LOADING	147

Preface

In this study, the shear resistance of tongued-and-grooved timber panels has been investigated using laboratory tests and FE analysis. The thesis can be regarded as a pilot project to encourage future studies. It has been written for the Division of Structural Engineering, Steel and Timber Structures, at the Department of Civil and Environmental Engineering at Chalmers University of Technology in Göteborg, Sweden. It was produced during the cold winter of October 2005 to March 2006.

We would like to express our gratitude to Professor Robert Kliger, supervisor and examiner of this thesis. He has been a great support throughout the process from choosing a subject to the examination and this support has been given through many inspiring, enjoyable meetings.

We would like to thank Lars Wahlström for his great support and many helpful hours in the laboratory.

We would also like to thank Lennarth Stave at Annebergs Hus for support in form of material and good advice and BoråsTapeter for supplying material and test data.

Finally, we would like to thank family and friends for supporting and feeding us during our time at Chalmers.

Göteborg, March 2006

Erik Hansson

Marcus Petersson

Notations

H	Racking load
h	Panel height
k	Fastener slip modulus
δ	Displacement
γ_s	Frame rotation
x'_i	x-coordinate of fastener i in x',y' system
y'_i	y-coordinate of fastener i in x',y' system
u_{frame}	Displacement of frame corner
F_N	Normal force
F_F	Friction force
μ	Friction coefficient
A_{stud}	Cross section area of studs
$A_{t\&g}$	Cross section area of t&g
E_{stud}	E-modulus longitudinal for stud
$E_{t\&g}$	E-modulus tangential for t&g
α	Ratio between E-moduli
$F_{ratio,t\&ge}$	Load ratio
$\mu_{loading1}$	Friction coefficient loading cycle 1
$\mu_{loading2}$	Friction coefficient loading cycle 2
R_F	Reaction force
R_x	Reaction force x direction
R_y	Reaction force y direction
E_L	E-modulus longitudinal
E_R	E-modulus radial
E_T	E-modulus tangential
E_{mean}	E-modulus, average
G_{LT}	Shear modulus longitudinal-tangential
G_{LR}	Shear modulus longitudinal-radial
G_{TR}	Shear modulus tangential-radial

1 Introduction

1.1 Background

Timber has for a long time been used as a construction material and Sweden has an extensive forestry and fine tradition of timber houses. Even though timber is easily available as a building material, other materials are more frequently used. A report by Von Platen from the Swedish ministry of industry, employment and communications from 2003 was written to promote the use of timber structures and Swedish forestry. The report both includes strategies for a more frequent use of a timber but also strategies for promotion of new innovations in timber structures. A natural step is to increase the use, and find new applications for Swedish products.

The tongued-and-grooved (t&g) principle is used in many types of wood based products. T&g is used to increase interaction and prevent movement in normal direction, but it's still not used with any consideration to diaphragm action, this due to lack of knowledge and no available design models for calculations. If there is a possibility to increase knowledge about t&g and develop a working model it might be possible not only slim existing constructions but also in some elements replace boards with t&g elements.

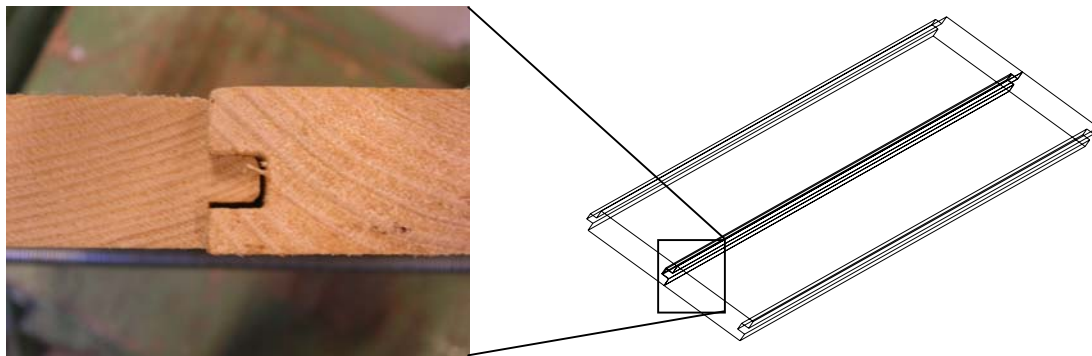


Figure 1.1 Two tongued-and-grooved timber panels

T&g timber is the most frequent used material to cover the roof trusses in roof construction in family houses in Sweden. The boards are easily assembled one after each other on top of the roof trusses and nailed. T&g boards are easy to assemble and the low price combined with the high availability of t&g boards also makes t&g suitable for walls. The problem when using t&g panels instead of for example plywood is that no interaction between the boards is assumed and therefore no diaphragm action can be used. This leads to the fact that in roof constructions you have to brace the roof truss in the lateral direction and in wall constructions with t&g timber no racking resistance of the panel can be assumed.

Previous experience from the landslide in Tuve 1977 (Johannesson and Johansson, 1979) has shown on an extremely good structural behaviour and diaphragm action then t&g timber is used in houses. One house with t&g timber on frame walls slid a few hundred metres from its slab foundations and the paintings were still left on the walls. This house acted as a stiff box and the t&g boards were only stiffened with a few layers of wallpaper.

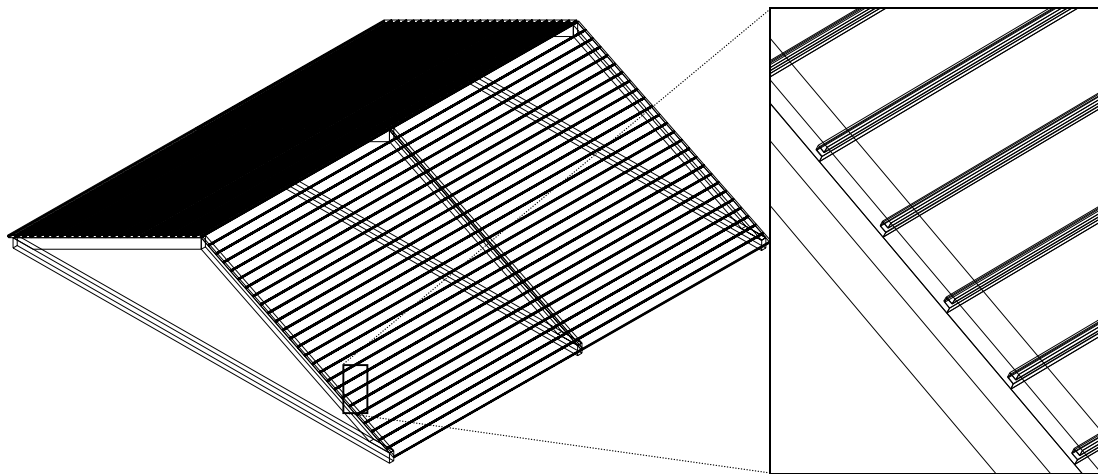


Figure 1.2 Typical roof construction, roof truss attached with t&g timber panels

T&g timber is easy produced from sideboards of timber logs and can therefore be produced for a low cost and be cheap for users. The most common used logs for sawn timber used for building timber houses are Norway spruce (*Picea abies*). The Swedish production of plywood, MDF- and particleboards has decreased and only five factories are now active. Because of the relatively low production of different kinds of construction boards in Sweden, t&g timber boards can be a good economic solution to decrease import of boards and increase the use of own produced t&g timber. This development is also in line with the guidelines from the Swedish ministry of industry, employment and communications.

1.2 Aim

The main aim of this master's thesis is to increase understanding of the diaphragm action for t&g timber boards attached to a construction frame. The aim also includes the following questions:

- How the interaction between t&g boards work and how can it be translated to shear capacity for a panel?
- How the interaction between the t&g timber boards change by variation in moisture content?
- How the interaction is affected with for example wallpaper attached to a panel of t&g boards?
- Is there any use for future studies about the t&g timber boards?

The answers to these questions are elaborated in this thesis and a contribution to the general discussion on how to make construction of timber houses cheaper in Sweden (Local and Global reflections) is presented.

1.3 Problem description

A good start is to study simple shear panel with a construction frame and a board material attached on each side.

If this panel with t&g is going to work in a proper way a number of different conditions must be fulfilled. According to existing models for calculating of shear panels with wood-based material the nail capacity is decisive for the resistance of the panel. The wood based panel in comparison to the t&g boards can be regarded as a continuous element. With t&g boards as panel material studies have to be made to see if the nails are decisive. The most interesting condition studied in this thesis is to control that the shear capacity of a panel with t&g timber have sufficient shear capacity to act as a web in the “I beam” as a the wall with the head joists. The shear capacity is often described with the shear modulus G . The problem is to understand how the t&g boards act as a wood-based panel material. Which are the factors deciding the capacity of the panel loaded in shear.

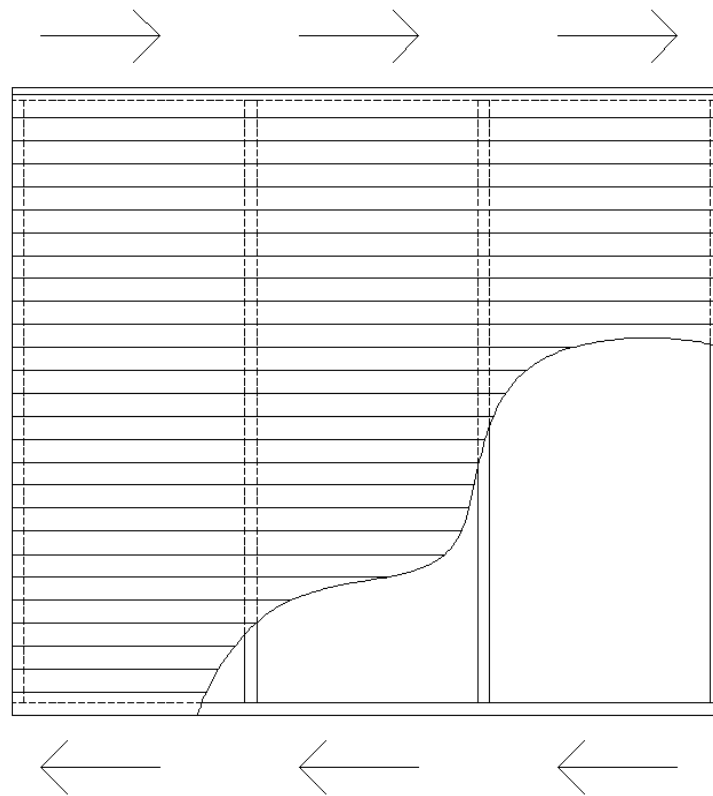


Figure 1.3 Wall frame attached with t&g timber panels

To understand the structural behaviour of a t&g timber panel, a study of the geometry of each board and how they interact have to be performed. An obvious and an important condition for the panels in designing of shear panels is that the t&g effect prevents movement between the panels in the normal direction so that buckling in a single panel is prevented. In Figure 1.4 the dimensions according to SIS standard (SIS 232813,1992) are shown for a t&g timber board with the dimensions 95x22 mm.



Figure 1.4 Dimensions of a t&g panel 95x22 mm

The size of the tongue and the grooved are designed to make it easy to assemble boards during construction. With longer boards, a small twist or bend can be enough to make it very hard to assemble two boards. The disadvantage with the difference in dimension between the tongue and the groove is the gap found in the interaction as seen in Figure 1.5.

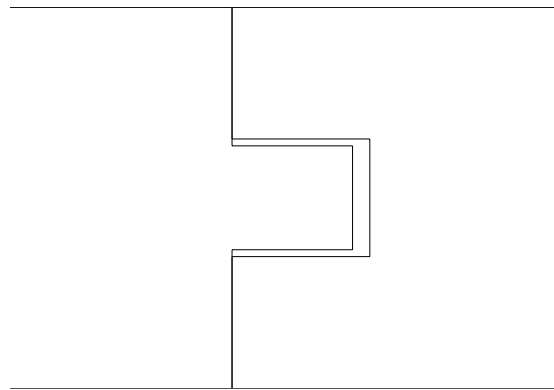
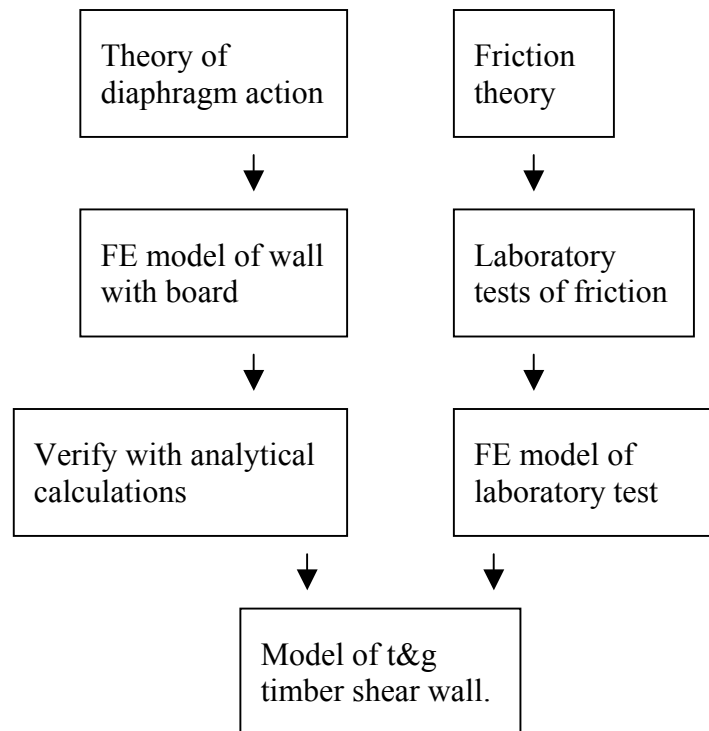


Figure 1.5 The gap inside the groove

All distortion modes can give both positive and negative effect of the interaction between the boards. The shear capacity of a panel of t&g timber is interaction between the boards and the major force in the interaction is the friction between two boards.

1.4 Method



The aim is to be achieved by developing and verifying a numerical FE model.

- With a laboratory test investigate the shear/interaction behaviour for 95 x 22 mm t & g boards assembled to a panel. The tests will be made based on known theories of friction and testing of shear in panels to obtain some reliable data for the thesis and for future studies. During laboratory test the required data will be collected for the modelling and for evaluating the effects at different moisture content. The laboratory test will also investigate how the capacity will be affected with wallpaper attached to the t&g boards.
- Create a FE model that describes the shear/interaction behaviour observed in the laboratory. The model is to be verified with the laboratory tests and with hand-calculations. By simplifying interactions used in the FE model it will be optimised for later and more advanced models. The parameters can be changed to simulate the affect of difference in moisture content and interaction with wallpaper.
- Extend the model to a wall with horizontal t&g boards attached to a frame to investigate the racking resistance of an entire wall. By using the same frame with plywood sheet assembled the model can be verified with hand-calculations.
- Analyse the results from the FE model of the t&g boards attached to a frame and compare the results with existing types of shear walls used in constructions to see if there is a need for future studies

2 T&g material properties

The raw timber is a complex material with a number of varying properties such as anisotropic values of elasticity and shear modul. Since timber is a biological material it also shows an exceptional individual variation between each specimen.

The rectangle in the middle of the log is used for construction timber. Outside the rectangle are the sideboards; this is normally the material used for t&g boards (Figure 2.1). The reason for this use is both economical and geometrical, first the sawmills wants to optimize the profit of the log and second the dimensions sideboards is not large enough to produce any construction timber. Unfortunately, it is the material in the sideboards which sometimes is abandoned, that has the highest material stiffness, (Kliger et al. 1997) and this is an additional reason to increase the use of these boards.

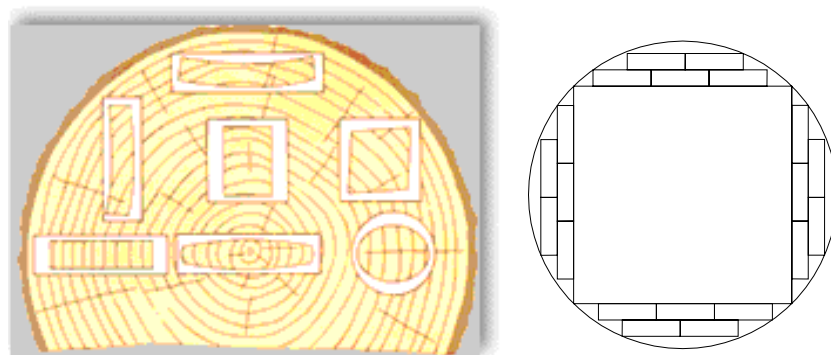


Figure 2.1 Cross section of timber log (Hoffmeyer, 1995) and principle drawing over the sideboards

The Figure 2.1, does not only show how sawmills are using a log, but also shows on the effects of anisotropic shrinkage due to differences in moisture content.

Earlier studies (Kliger et al. 1997) describe how differences in material properties are affected by the radial position in a tree. By testing studs made from a log and categorize them dependent of their radius from the center of the log different material properties were revealed. The studs were divided into three groups, core, intermediate and mature. The tests were made on Norway spruce timber, fast grown and slow grown.

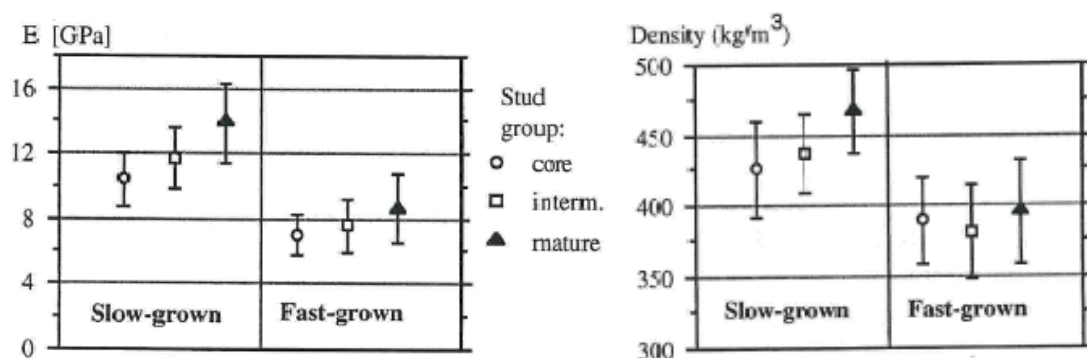


Figure 2.2 Modulus of elasticity and density of Norway Spruce depending on the radial position of timber. (Kliger et al. 1997)

The value for E-modulus of Norway spruce timber can vary from 5 GPa in fast-grown wood core to more than 16 GPa in mature slow grown spruce. These differences are interesting and important to consider in this thesis since t&g timber is mostly produced from mature wood.

The strength classes with their characteristic values according to EN 338 (Anon. 2003) are illustrated in Table 2.1. By investigating the density/E-modulus relationship together with knowledge about the radial position of a stud a realistic value for E-modulus of t&g timber board with known density can be approximated. The value for $E_{90,mean}$ can be approximated to $E_{0,mean} / 30$ according to EN 338 (Anon. 2003).

Table 2.1 Strength classes with E-modulus according to EN 338 (Anon. 2003), Coniferous species

	C14	C16	C18	C22	C24	C27	C30	C35	C40
$E_{0,mean}$ [kN/mm ²]	7	8	9	10	11	12	12	13	14
$E_{90,mean}$ [kN/mm ²]	0,23	0,27	0,30	0,33	0,37	0,40	0,40	0,43	0,47
ρ_k [kg/m ³]	290	310	320	340	350	370	380	400	420

T&g timber is normally produced of coniferous species and therefore material properties of t&g is from Norway spruce. In all experiments and calculations from now on in this thesis the values in Table 2.2 and Table 2.3 will be used.

Table 2.2 Anisotropic material properties for spruce (Ormarsson 1999)[Pa]

E_L	E_T	E_R	G_{LT}	G_{LR}	G_{TR}
9.9E+009	4E+008	2.2E+008	4E+008	2.5E+008	2.5E+007

Table 2.3 Isotropic material properties for spruce (Polverini 2000) [Pa]

E_L	E_T	E_R	G_{LT}	G_{LR}	G_{TR}
9E+009	9E+009	9E+009	3,3E+009	3,3E+009	3,3E+009

3 Theory and models

3.1 Friction theory

The Columb friction model described by Grahn and Jansson (1997) is the interaction between two surfaces with the non-dimensional friction coefficient μ . This coefficient gives the relationship between the normal force (F_N) acting in the normal direction of the friction plane and the friction force (F_F) acting as a tangent force in the friction plane.

$$\mu = \frac{F_F}{F_N} \quad (3.1)$$

The friction force is equal to force F , required to move the body in the opposite direction (Figure 3.1).

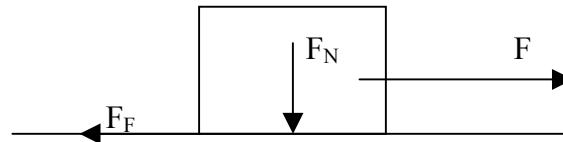
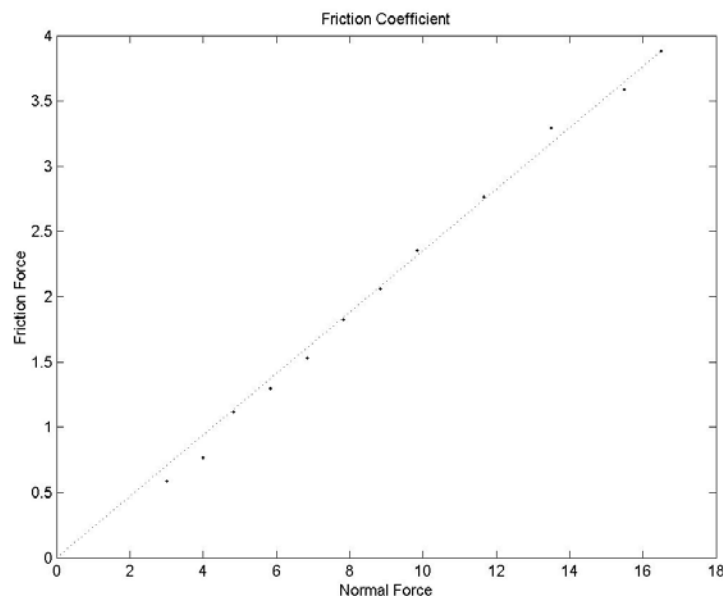


Figure 3.1 Columb friction model

The friction law is simply defined and according to the law two important statements can be assured. The friction coefficient μ is independent of the friction area, with the same normal force F_N , the friction force F_F is the same with different size of the surface. A corollary is that μ is independent of the normal force, the friction force is proportional to the normal force (Figure 3.2).



*Figure 3.2 Test of friction for a paper-paper interface with $\mu=0.24$
(Baumberger 1996)*

The dynamic behaviour is more complex to understand, by testing with a model like in Figure 3.1 with a spring in the force direction the required force can be measured. An ideal model of the behaviour from static to dynamic mode, steady sliding is shown in Figure 3.3, the plot illustrates the spring force as a function of time. F_a is the static friction force and F_b is the kinetic friction force. The spring force corresponds to the friction force from the surface.

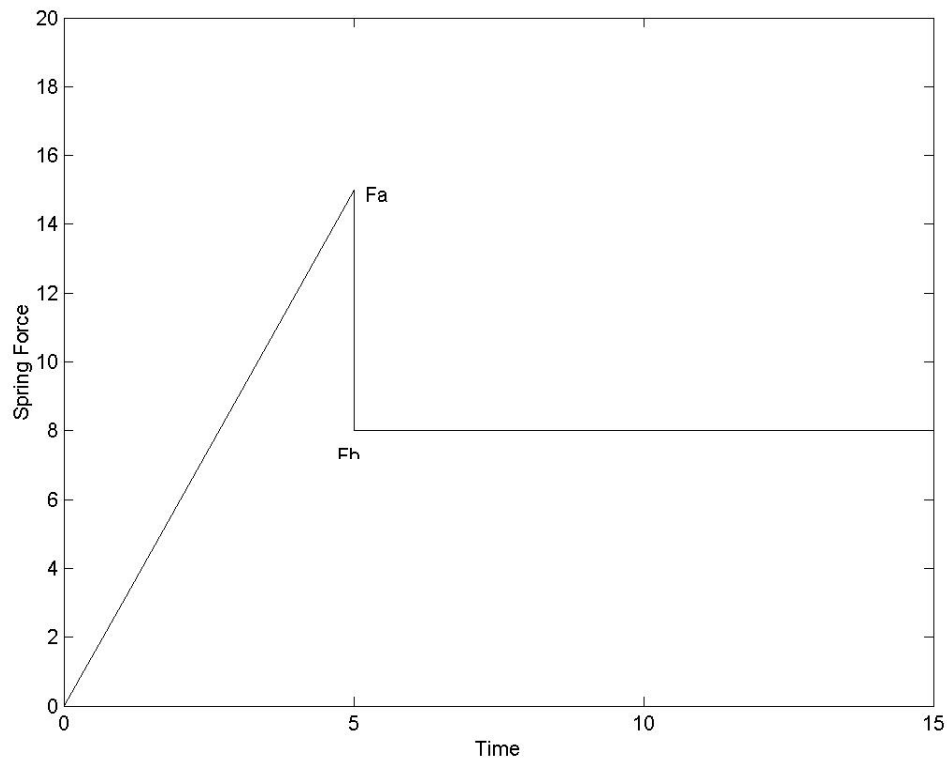


Figure 3.3 Friction curve (Baumberger, 1996)

The friction behaviour of plain timber panels according to Coulomb friction theory reveals a value for the static friction coefficient μ between 0.3 and 0.6 (Nordling and Österman, 1999) for dry timber to timber. According to the Coulomb theories the friction coefficient is approximated to a constant.

3.2 The elastic model according to Källsner

Källsner (1984) made a large study of structural behaviour of diaphragm and shear walls made of timber and wood-based panels. The method for his study was to build a large number of full-scale walls with different types of sheeting and geometry, and then perform laboratory tests to investigate their structural behaviour. Källsner has proposed an elastic model for analytical treatment of this kind of structural problems. The model was for calculating horizontal displacement of the upper corner of the shear panel but it can also be used to calculate the maximum racking capacity of a panel. The elastic model is based on a number of assumptions and simplifications that needs to be stated before moving further with the model. These assumptions that will be stated below are not only simplifying the problem but are of course also introducing uncertainties to the final result.

- The vertical and the horizontal parts of the structural frame are considered as rigid and they are connected to each other with hinges.
- The board material is assumed to be rigid as well and no contact is assumed to neighbouring sheets or frame members.
- The fasteners that act between the frame and the sheet are supposed to have linear elastic behaviour until they reaches failure.
- The horizontal displacement due to loading of the shear panel is supposed to be small in comparison to the dimensions of the panel.

Vertical studs that are attached to horizontal top and bottom rails combined with some sheeting generally build up a shear panel. The bottom rail is fastened with nails or some other connector to the foundation and can therefore be seen as pinned to the ground from a structural point of view. This means, taken the rigid elements into account and the hinged frame, that the structural behaviour of the panel will be similar to a cantilever with force acting on the outer edge to simulate the shear behaviour. In this model the displacement is related to the only deformable part, the fasteners.

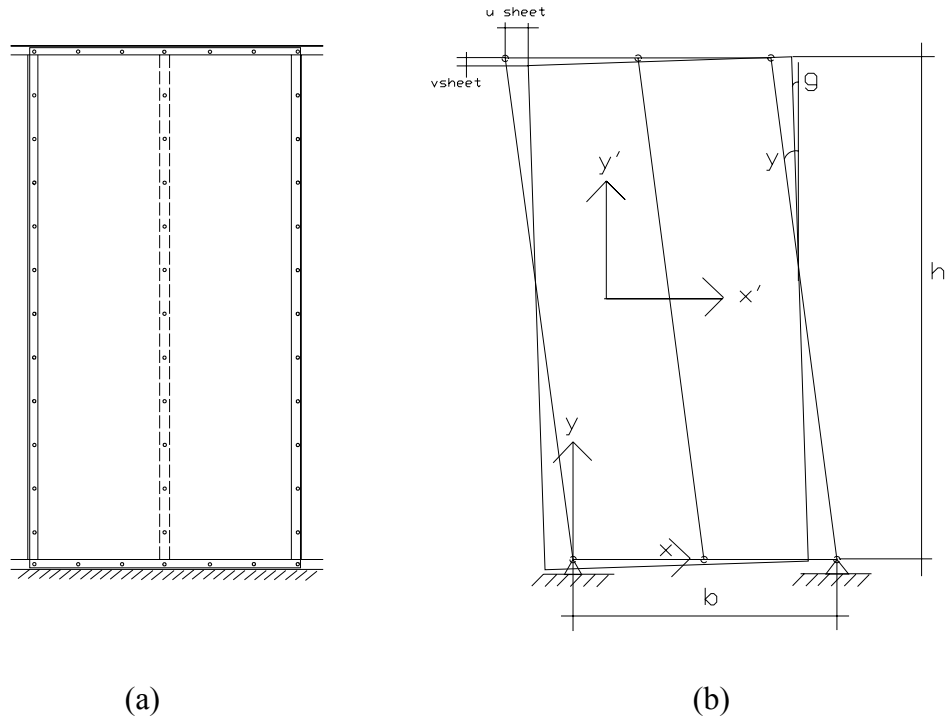


Figure 3.4 (a) Generalized picture of a shear panel (b) Deformation geometry for the elastic model in static loading

When studying the work made by Källsner (1984) a derivation from the energy principle, stating that the inner energy will be equal to the outer energy, to the complete expression for the relative displacement of the top rail can be found. The expression can be seen in Equation 3.2.

$$u_{frame} = (1/k)Hh^2 \left[\left(1 / \sum_{i=1}^n x_i'^2 \right) + \left(1 / \sum_{i=1}^n y_i'^2 \right) \right] + \gamma_s h \quad (3.2)$$

This equation will be used later to verify parts of the ABAQUS model.

4 Laboratory tests

To the best of our knowledge no previous study has been made to measure the shear strength of t&g connected timber. Therefore a series of laboratory tests have been performed to study the interaction between the boards. In order to develop a method for the laboratory test a number of test methods used for similar tasks were studied and evaluated. The first thing to define before starting to investigate the methods is the factors needed to know for further work.

The major factors are as follows:

- Variation of the normal force
- Effects of repetition
- Effects of different loading rate
- Wallpaper, (interlayer effects)
- Variation of moisture content

4.1 Test standard EN594

This chapter will shortly summarize parts of the European standard EN594 (Anon. 1995) that is important for the understanding of the design of the ABAQUS models and the laboratory test method. The standard was approved by CEN on 1995-11-04 and was made national standard before June 1996. The major purpose of the standard is to specify the methods used to determine the racking strength and stiffness of timber wall panels. The Figures 4.1 to 4.3 describe the geometry of the standard model and application of loads and anchorage.

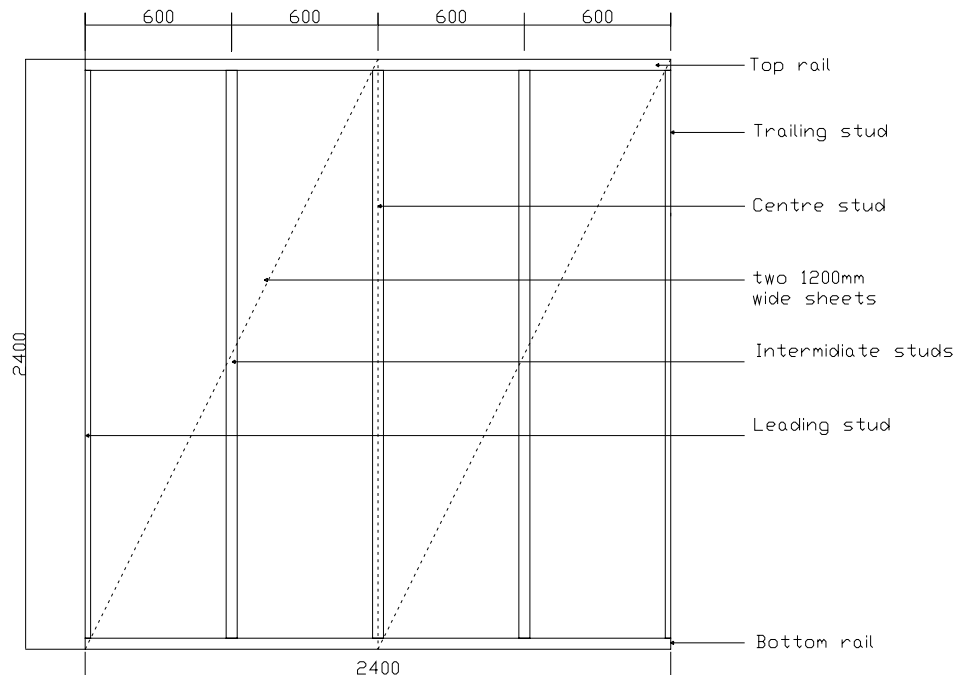


Figure 4.1 Details of test panel, EN 594 (Anon. 1995)

The vertical load is evenly distributed over the top rail. It is represented by evenly distributed concentrated loads applied to each vertical stud. The vertical load applied closest to the racking load F is displaced towards the centre of the panel to allow 100 mm maximum racking deflection. The top rail is laterally restrained so only in-plane displacements are allowed.

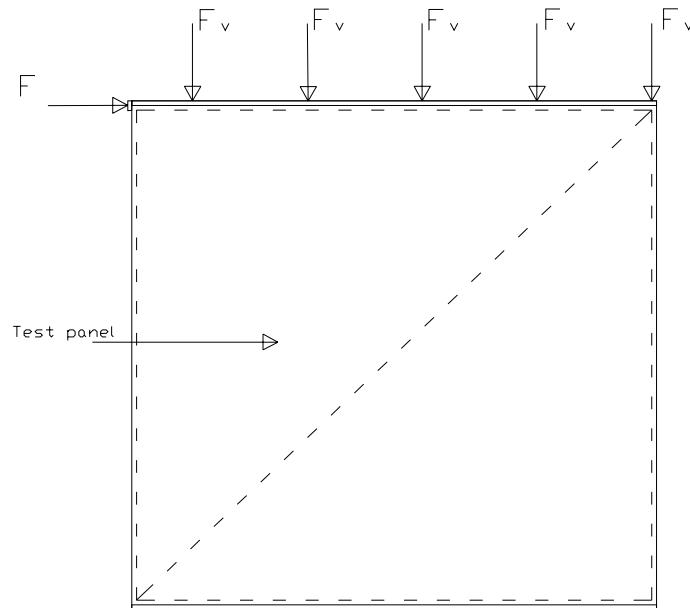


Figure 4.2 Loading geometry with vertical loading (Anon. 1995)

If using the normal load application procedure recommended in EC5 (Anon. 2004), method A, some of the timber studs will be subjected to tension forces due to the moment subjected to the shear panel. Tension forces will also occur in parts of the t&g panel where no capacity to handle vertical tension forces exists. If the boards in the t&g panel are separated, a failure will occur due to the loss of the interacting friction forces. The reason to include the permanent vertical load coming from structures above is chosen for the laboratory and the FE models to secure interaction between the boards.

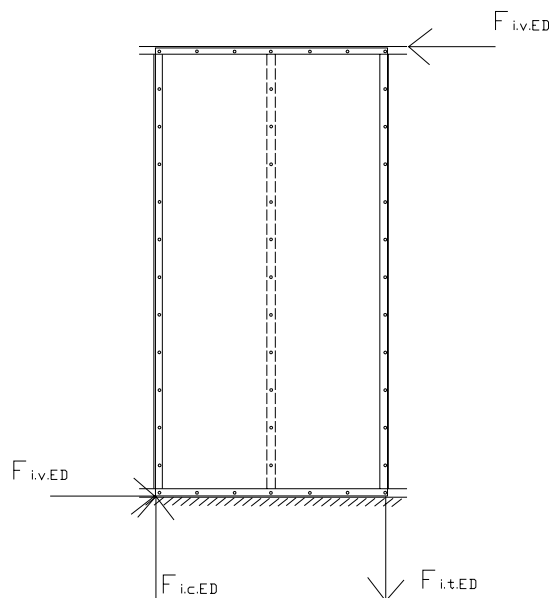


Figure 4.3 Load application and anchorage according to EC5 (Anon. 2004)

4.2 Panel shear method C

Literature studies of previous work by Johannesson (1979) revealed three different test methods to measure the shear strength of a board material. In his evaluation of the models, Johannesson makes some recommendations when to use which model.

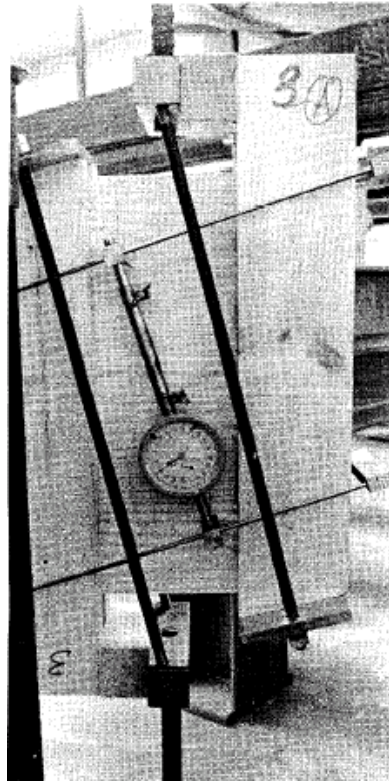


Figure 4.4 Panel shear method (Johannesson, 1979)

The one most suitable for measuring of the short-term shear strength and also the most accurate one is panel shear method C, it is used as a standard method to measure short-term shear strength.

By applying forces as shown in Figure 4.5 results for the shear stress in middle of the plate without any effect of moment forces is obtained. The forces should be applied with a speed that limits the deformations to $1 \pm 0,25$ mm/min. The shear modulus is received by calculations from the force – displacement diagram plotted from the test. The shear capacity is obtained by dividing the maximum load with the area of the cross section of the test specimen.

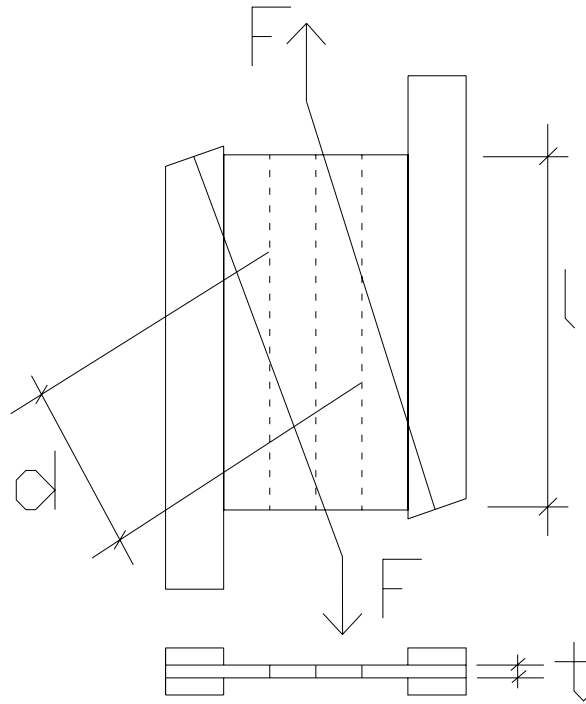


Figure 4.5 Static system of panel shear method C

$$\tau = \frac{F}{l \cdot t} \quad (4.1)$$

τ = calculated shear capacity

F = measured maximum load

l = length of test body

t = thickness of plate

$$G = \frac{F \cdot d}{a \cdot l \cdot t} \quad (4.2)$$

G = shear modulus

d = distance between measuring points

a = measured displacements between points

If the test is used with t & g timber the received value for shear capacity corresponds to friction constant between the timber pieces.

4.2.1 Evaluation of background theories for laboratory tests

To be able to utilize t&g timber as a board material on the shear wall it is essential to make the boards to act together. As can be seen in Chapter 1.3, the tongue is fabricated in a smaller dimension than the groove, therefore no additional force holding the pieces together will be found but only the friction force between the two connecting surfaces.

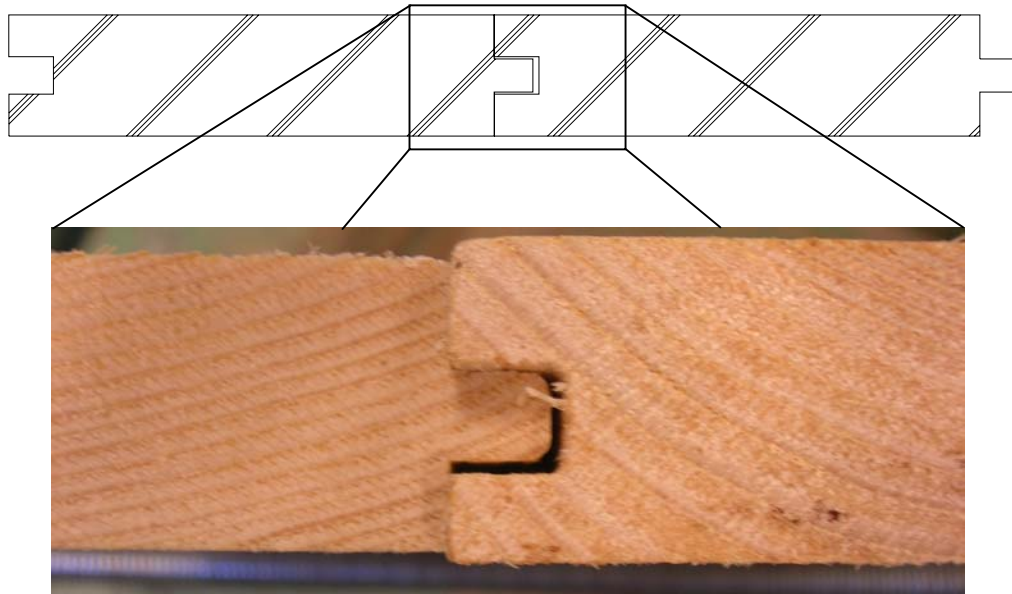


Figure 4.6 Cross section of interacting 22mm t&g boards

The size of this friction force is however totally depending of the normal force also called clamping force that is applied to the interaction surface. If a more detailed study is performed of the structural system, it can be found that the way the shear panel acts is strongly depending on where it is positioned and if other forces than the horizontal racking force is applied. In the work of Källsner (1984) it is proved that even for a continuous timber-based panel material such as plywood, the racking resistance of the wall can be increased if adding vertical loads to the panel.

Starting from the panel shear method C developed by Johannesson (1979) a new test method for testing the shear capacity of t&g boards assembled into panels was designed. The problem with the panel shear method C is that it does not allow preloading of normal force which is essential for the shear capacity of t&g panels. The new testing procedure proposed in this thesis is described in Chapter 4.3. In the evaluation of the panel shear method C, Johannesson (1979) describe the importance of avoiding additional moment due to the loading of the panel. This problem was solved in the new model by creating a symmetric system as can be seen in Figure 4.7.

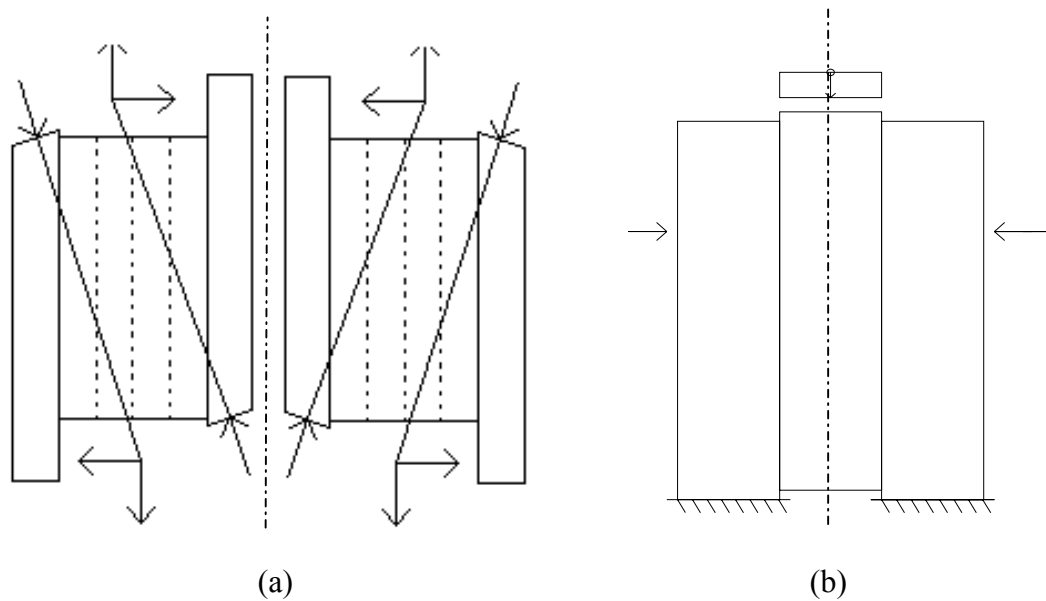


Figure 4.7 (a) Panel shear method C (b) New model for t&g testing, both models with symmetry line

If a normal structure of two-stored house is considered, a wall on the first floor will be affected of vertical and horizontal load. The vertical load will mainly depend on self-weight and snow and the horizontal load on the wind load. The vertical load will increase the horizontal load capacity. For a normal shear wall similar to the one showed in Figure 4.1 with plywood and timber studs, the assumption is normally made that the studs transfer the vertical load and the horizontal load is transferred by shear in the plywood. If the plywood is changed to t&g timber boards this assumption can be hard to make. The studs will transfer some of the vertical load and some of the t&g boards creating a normal force on the interacting surfaces between the boards, see Figure 4.8. The relation between the amount of force transferred by the studs and by the t&g boards can be approximated by the assumption of effective area, se the Equations 4.3 to 4.5. The choice of geometry of the wall was made according to the standard wall used in EN594 (Anon. 1995).

The force applied on the wall is decisive to the amount of friction and interaction between the boards. To find the exact load on the boards the ratio between the forces applied to a wall and the force distributed to the t&g boards have to be calculated.

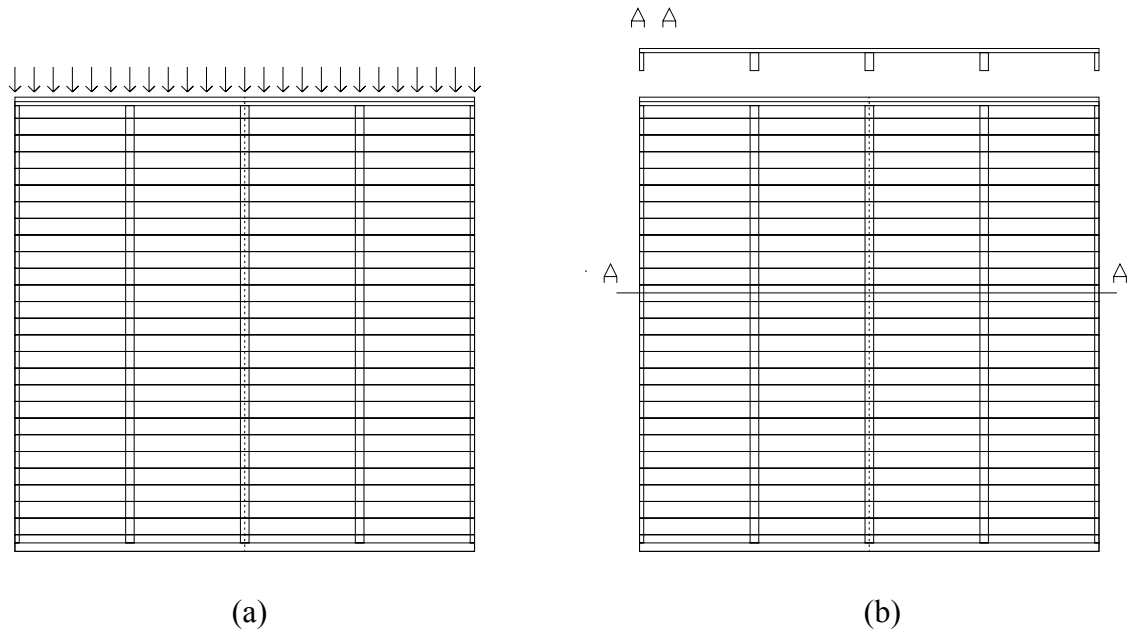


Figure 4.8 (a) Wall with load applied (b) Wall with cross-section

If the nails are placed close to each other, almost full interaction can be assumed between boards and studs. The ratio between the different E-modulus can be decisive in the similar way as equivalent area is calculated in a reinforced concrete beam (Engström 1994).

A_{stud} = Cross section area of studs

$A_{t\&g}$ = Cross section area of t&g

E_{stud} = E-modulus, longitudinal, for a stud

$E_{t\&g,T}$ = E-modulus, tangential, for a t&g board

$E_{t\&g,L}$ = E-modulus, longitudinal, for a t&g board

The ratio α between the E-moduli, α is calculated. With α , the equivalent cross section area for the studs with E-modulus for the longitudinal direction of t&g timber can be calculated.

$$\frac{E_{stud}}{E_{t\&g}} = \alpha \quad (4.3)$$

$$A_{eqv} = \alpha \cdot A_{stud} \quad (4.4)$$

By dividing the cross section area of the t&g with the total area of the cross-section the ratio $F_{ratio,t\&g}$ is obtained.

$$\frac{A_{t\&g}}{A_{eqv} + A_{t\&g}} = F_{ratio,t\&g} \quad (4.5)$$

The density of the t&g boards is measured to a mean value 420 kg/m³, (Chapter 5). The investigation in Chapter 2 recommends that for timber with the density of 420 kg/m³ the E-modulus of 14 GPa should be used. The choice of material will have a great influence of the behavior of the wall, to illustrate this the Table 4.1 lists some choices for various configuration.

Table 4.1 Effects of varying E modulus for the behaviour of the wall

$A_{stud} \quad [m^2]$	0,021375	0,021375	0,021375
$A_{t\&g} \quad [m^2]$	0,0528	0,0528	0,0528
$E_{stud} \quad [GPa]$	7	8	12
$E_{t\&g,L} \quad [GPa]$	14	13	12
$E_{t\&g,T} \quad [GPa]$	0,467	0,433	0,4
$\frac{E_{stud}}{E_{t\&g,T}} = \alpha$	15,0	18,5	30,0
$\frac{A_{t\&g}}{A_{eqv} + A_{t\&g}} = F_{ratio,t\&g}$	0,14	0,12	0,08

If the different ratios obtained from Table 4.1 is used to calculate the magnitude of the vertical load per length metre that is transferred to the t&g boards' results according to Table 4.2 can be obtained. The left column is representing the magnitude of the vertical loading of the wall according to Figure 4.8.

Table 4.2 Vertical load transferred by t&g boards [N/m]

Vertical load on the wall	F _{ratio t&g}	F _{ratio t&g}	F _{ratio t&g}
	0,14	0,12	0,08
1000 [N/m]	141	118	76
3000 [N/m]	424	354	228
5000 [N/m]	707	590	380

4.3 Description of test procedure

The test model is built up by three t&g connected pieces of timber each one with the measurements 400 x 22 x 95 mm. The centerpiece is placed with a 10 mm vertical displacement relative to the other two. The outer two is then fixed to the ground in order to be able to counteract the load applied to the top of the centerpiece. Then on each of the outer two timber pieces the external pressure is applied to act as normal force on the interacting surfaces.

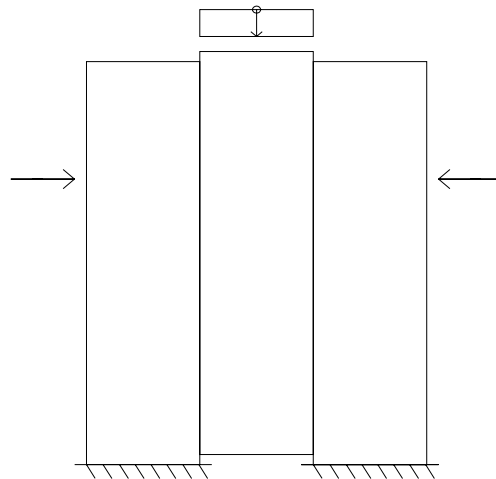


Figure 4.9 Static system over laboratory model

The vertical load is applied using a universal testing machine type alpha accuracy class 1. The applied load is registered by a 50kN, (type CVDT HBN W20TS), load cell. This will later be described in form of plots of force versus displacement. The plots were made on a XY-printer (type Graphtec) connected to the amplifier (type HBM MGC). The horizontal load is applied with small construction described in Chapter 4.3.1. This construction will further on be referred to as the “clamp device”.



Figure 4.10 Laboratory testing of t&g panel

4.3.1 Clamp force device.

In cooperation with experienced laboratory personnel a small device for applying the horizontal forces to the specimen was designed. This small device, as it is illustrated in the Figures 4.11, was designed in such a way that the horizontal load is distributed evenly over the interaction surface.

To eliminate the non-symmetric effects when applying the horizontal load two 13 mm thick steel plates was used to apply the load to the test specimen. The reason for using this relatively thick steel plate was to obtain rigidity in the span of loads applied in the tests. In order to transmit the forces from the plane surface of the steel plates to the test specimen one board was split into half creating two small boards with one long side with a plane surface and one with either a tongue or a groove (Figure 4.11 and Figure 4.12 b). By using this small board the test specimen is loaded only on the surfaces of the board that is interacting in reality.

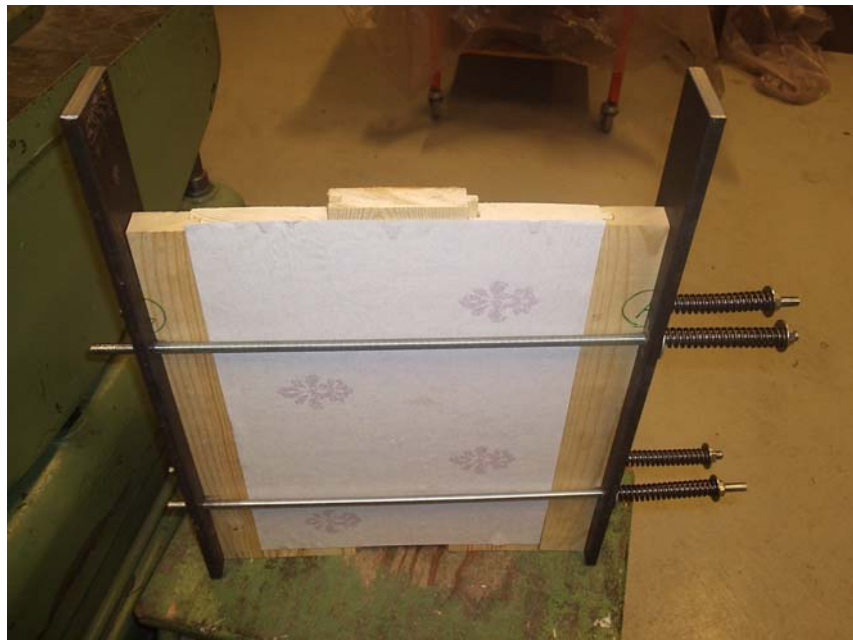
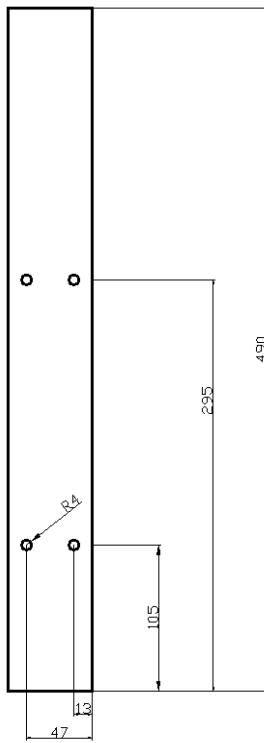


Figure 4.11 T&g panel with wallpaper loaded in the clamp device.

Four holes with a diameter of 8 mm were drilled in each steel plate in order to connect them to one and another. The plates were assembled to a load applier with four 500 mm long M8 threaded steel rods with one bolt and a washer on each side of the plates to (Figure 4.12 a). The reasons for adding the washers are that they spread the load from the nut on to the steel plates, which helps the steel plate to act as a rigid element, but they also makes it easier the tightening of the nuts.



(a)



(b)



Figure 4.12 (a) Drawings over the steel plates used in the load applicier (b) Divided t&g board used to apply horizontal load

4.3.1.1 Calibration of the device which define the clamp load

4.3.1.1.1 Preliminary test procedure

The idea was to tighten the nut by a moment key and apply the load this way. In order to do this the moment key needed to be calibrated to establish a relationship between the level of the moment applied with moment key and the level of the horizontal load applied to the test specimen by the nut. Positioning of the load cell and other parts used to calibrate the device which produce the clamp force can be seen in Figure 4.13.

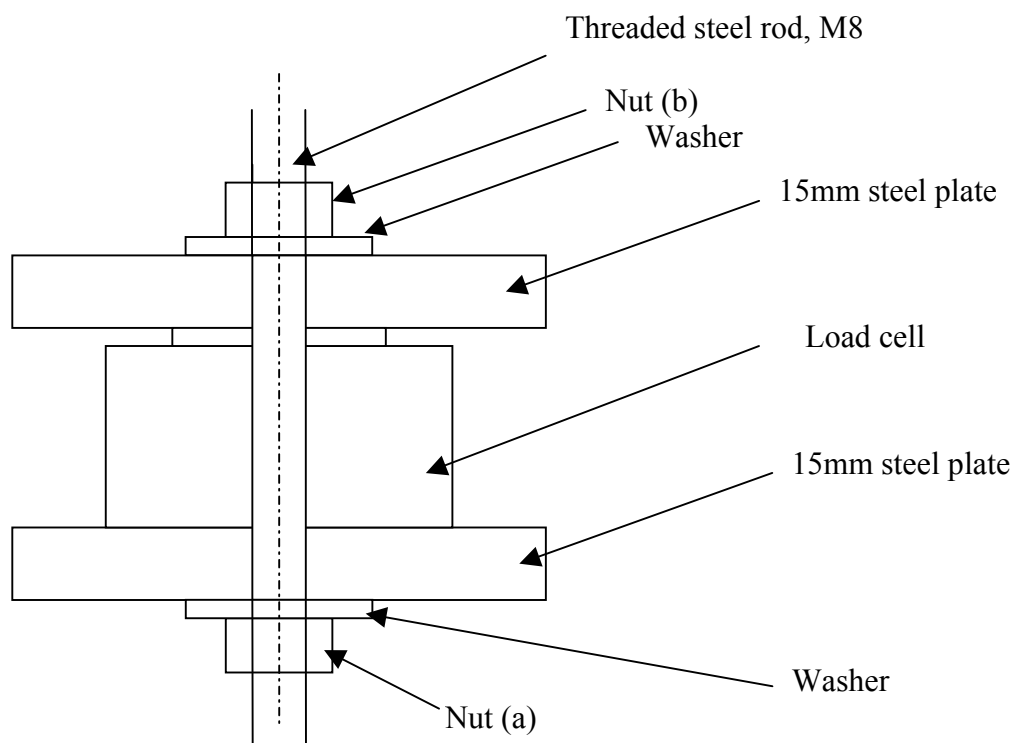


Figure 4.13 Schematic sketch of the calibration of the moment key

After mounting the lower nut (a) the top nut (b) was tighten by the moment key creating a pressure over the load cell. This pressure force was registered by the load cell and transmitted over an amplifier to a digital display. The moment key used for the test was a standard key graded with a scale running from number 3 to 12 where 3 was the lowest force. When tightening a nut with a moment key it works in that way that a small lock inside the key unlocks when the set load level reaches and the nut socket starts to rotate. A number of tests were made to calibrate the key but the results were all showing a very large variation. Depending on how fast the load was applied with the moment key the results when the key was set on load level no. 3 varied from 300 N to 1800 N. The test was repeated with another moment key and at load level no. 5 but the results showed an even greater variation than the previous. A test was made with a small panel according to Figure 4.11 to see if it was possible to use the moment key to apply the clamp force. The result from this small test was that cracks occurred in the boards before the moment key unlocked. The conclusion made from this test was that a new test procedure needed to be developed.

4.3.1.2 Final test procedure

The major problem with the preliminary test procedure was that the level of the applied load was very difficult to control. In order to adjust this problem four well defined pressure springs that were added in between the steel plates and the nut with a washer on each side of the spring. The reason for the additional washer was to eliminate rotation of the springs when tightening the nuts which can cause asymmetric loading. The springs offered the opportunity to control the applied load with much higher accuracy. In the preliminary test procedure the load increased very rapidly when tightening the nut because of the fact that the deformation constant K for this model was the E-modulus of timber. In the final model the deformation constant K was instead the deformation constant of the springs and therefore the loading process became easier to handle. The two sketches in Figure 4.14 illustrate the problem.

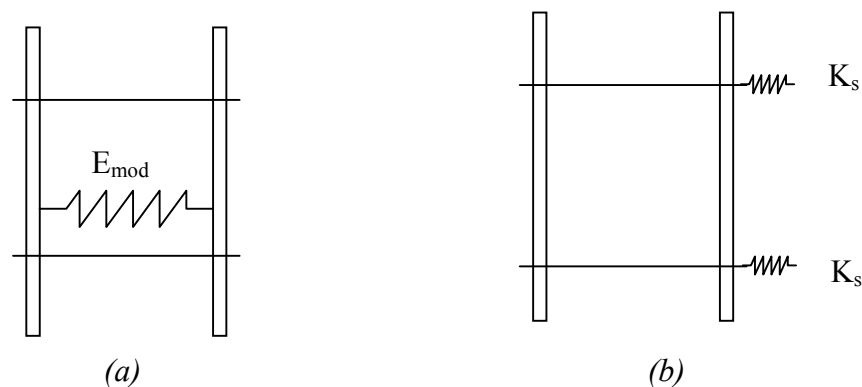


Figure 4.14 Device for applying the clamp load to the t&g panels (a) Preliminary configuration (b) Final configuration

In this way the simple relationship between deformation and force for the springs could be used. By tightening the bolts the load level could be controlled and an evenly distributed load could be applied.



Figure 4.15 Clamp load applier final version

4.3.1.3 The Pressure springs

The springs used for the tests are standard pressure springs with a linear load deformation property (Figure 4.16). The decisive parameters for the choice of these springs were load capacity, length and inner diameter. The inner diameter and the length of the springs had to fit properly with the M8 threaded steel bar. The load capacity for the spring had to be large enough to be able to give the decided load span (0-1600 N). The data needed to define the spring is presented in Table 4.3. The most important parameter for further work in this thesis is the spring constant marked in the bottom right corner of the table. The following type of spring was used:



Figure 4.16 Pressure spring used in laboratory tests

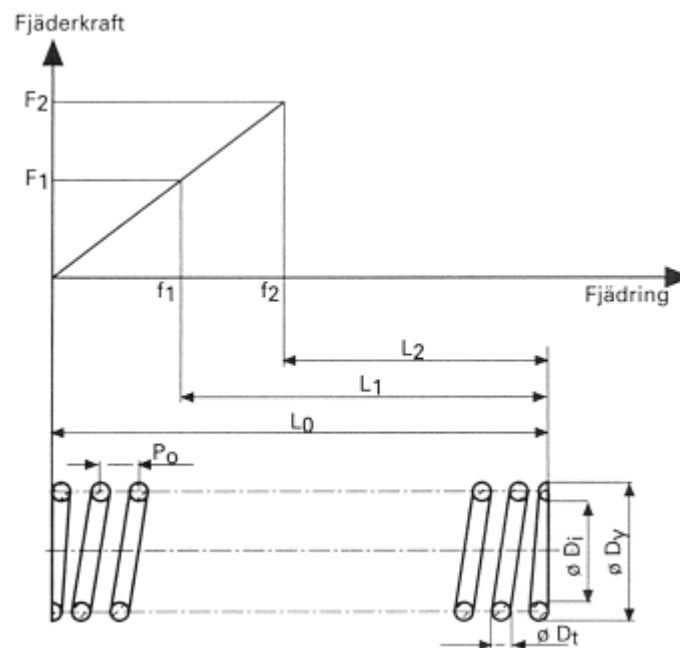


Figure 4.17 Variables for the pressure spring given by the manufactory (x-axis, spring length[mm], y-axis, spring force[N])

Table 4.3 Characteristic values for spring

Dt	Dm	Lo	L1	Sn = (Lo-L1)	Di	Dy	n* ¹	Fn* ²	R* ³
2,5	12,5	98	55,1	42,9	9,4	15,6	18,5	468,78	10,98

*¹ Number of rotations of the spring: *² Maximum spring force: *³ [N/mm] Spring constant

Dt = Thread diameter

Di = Inner diameter for the spring

Dy = Outer diameter for the spring

Dm = Medium diameter for the spring

Lo = Unloaded length

L1 = Max loaded length

Sn = Lo-L1 active length

R = Spring constant

4.3.2 Calibration of the pressure springs

To verify the spring capacity given by the manufacturer, a series of tests similar to the ones described Chapter 4.3.1.1 was performed. Preliminary model was conducted. A total load span of 0-1600 N was chosen for investigation. The reason for choosing this load span is that it represents the reasonable span of vertical loads occurring in the t&g panel attached on a frame described in Chapter 4.1. The new configuration of the calibration method can be seen in Figure 4.18.

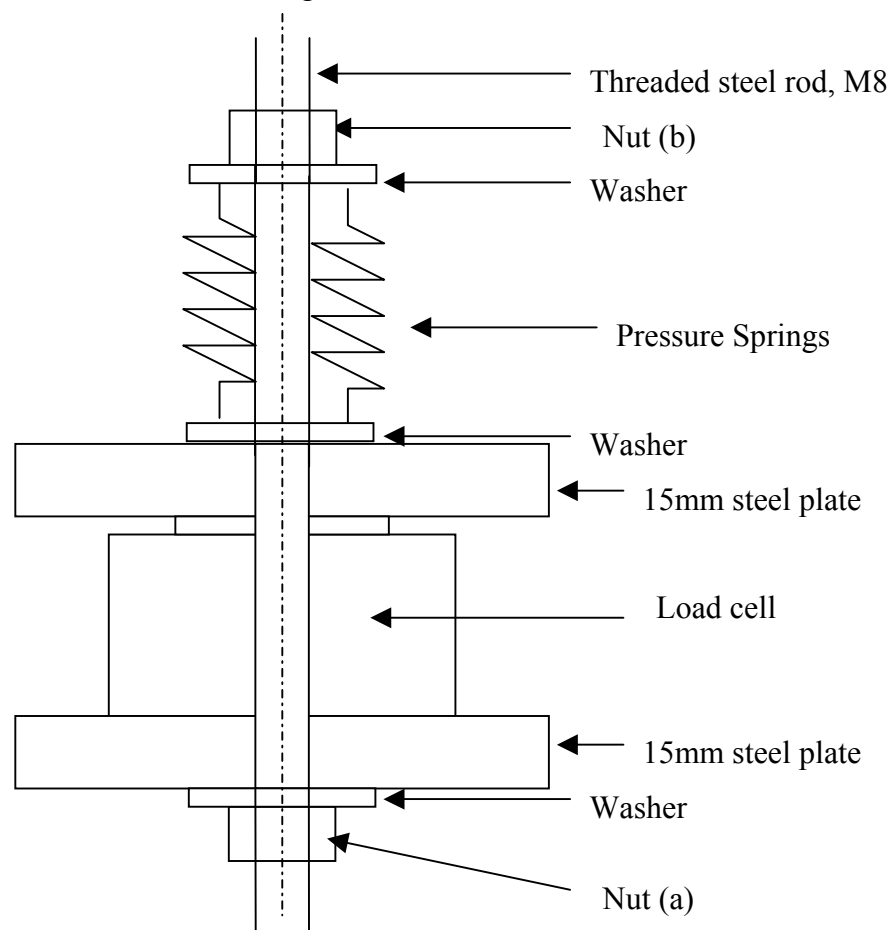


Figure 4.18 Configuration of the spring calibration model

The principle for the calibration is the same as for the first testing procedure. The top nut (b) Figure 4.18, is tightened by a key and deformation is introduced to the spring. The pressure force is then applied to the load cell by a washer and a steel plate in order to eliminate asymmetric loading. The weights of the top steel plate and the washers were withdrawn to eliminate the effects of self-weight on the results.

4.3.3 Results of spring calibration

The results from the calibration tests are shown in Table 4.4. The deformation of the spring was measured at a number of predefined load levels to control the accuracy of the spring constant given by the manufacture. In the second column from the left the measured spring length is presented and in the third the calculated according to Equation 4.6.

$$L = \left(L_o - \frac{F}{R} \right) \quad (4.6)$$

The spring constant used was the one given by the producer shown in Table 4.4. In the last column the total level of load applied by the clamp load device. As shown in Figure 4.19 the accuracy is very close to the calculated value. A thin line compared to the test results marked by dots represents the calculated values.

Table 4.4 Results of spring calibration

Load level (F) [N]	Measured spring length from laboratory [mm]	Calculated spring length according to Equation 4.6 [mm]	Total load applied by the clamp load applier [N]
0	98,0	98,0	0
50	91,2	93,4	200
100	88,7	88,9	400
200	79,3	79,8	800
300	70,0	70,7	1200
400	60,3	61,6	1600

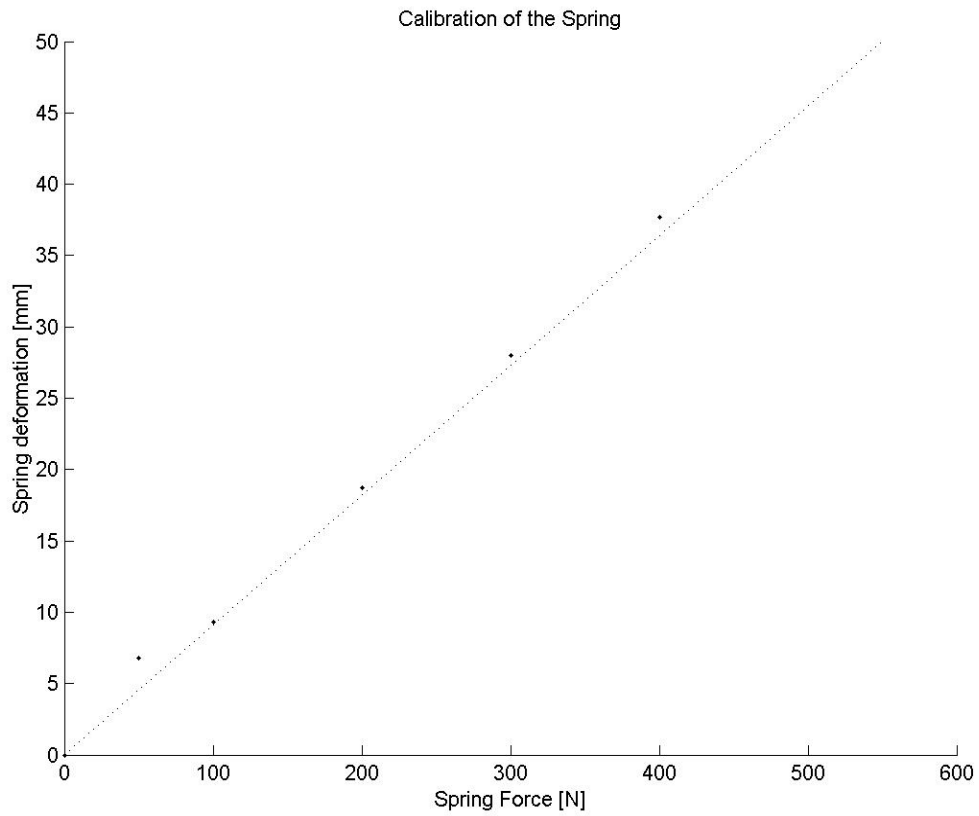


Figure 4.19 Diagram displaying the measured spring length at predefined load (dots), compared to the calculated values with manufactory spring constant (line).

5 Laboratory test of t&g timber panels and the results

5.1 Influence of moisture content on friction

Since the boards are in contact with the surrounding air the moisture content in the boards will be affected by the relative humidity of the air. During a year the relative humidity of the air in Sweden can vary from 55-90% RH outdoors (SMHI, 2004). This variation will affect the moisture content of timber according to the Figure 5.1. Another reason that the moisture content in the boards might vary is the fact that some parts of timber may have been exposed to water during the construction time. The test was performed according to the method described in Chapter 4.3. The horizontal load levels will be varied according to the spring calibration Table 4.4 with an initial load of 4x50 N and a final load of 4x400 N.

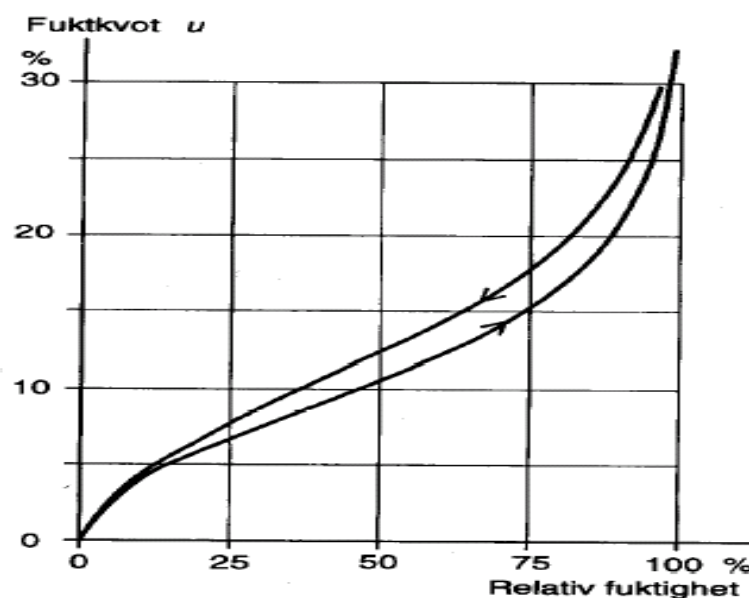


Figure 5.1 Hygroscopic sorption curve for wood and wood material (x-axis relative humidity y-axis moisture content), (Nevander and Elmarsson, 1994)

The test is divided into two phases. In the first phase all material data was collected for each specimen including moisture content, geometry and weight, all the boards was assembled into small panels of three boards in each. The configuration of the panels was randomly assembled. In the second phase, all the panels were tested according to the test procedure as described in Chapter 4. This testing procedure was repeated for three different levels of moisture content.

5.2 Conditioning of test material

To obtain a homogeneous group of specimens concerning the moisture content, the 27 t&g timber boards were numbered and placed in a conditioning room. The panels were dried prior to conditioning to 12% moisture content. The room was set for 80% relative humidity and a temperature of 32°C. The positioning pattern of the boards in the room where made to get as much exposure of the boards to the air inside the room as possible, Figure 5.2 Continuous controls of the weight of the boards were made to see where equilibrium with the humidity of the room was reached. The boards were kept in the conditioning room for a time period of 64 days. By obtaining the dry weight of seven boards after all tests were finished, according to standard procedure the mean moisture content could be calculated. The weight of the boards were measured after 24 hours in 103°C and divided by the volume of the board to obtain dry density. Mean moisture content for all the boards at equilibrium with surrounding air could be determined to 14.85%. Also the densities for each board was calculated and plotted as can be seen in Figure 5.3. This was done to obtain an approximation of how fast the timber has grown and what properties to expect. The boards show a variation of density at the moisture content of 14.85% between 380-480 kg/m³. The mean and the median values are 420 kg/m³ and the 410 kg/m³ respectively.



Figure 5.2 Photo of mass control and acclimatization process

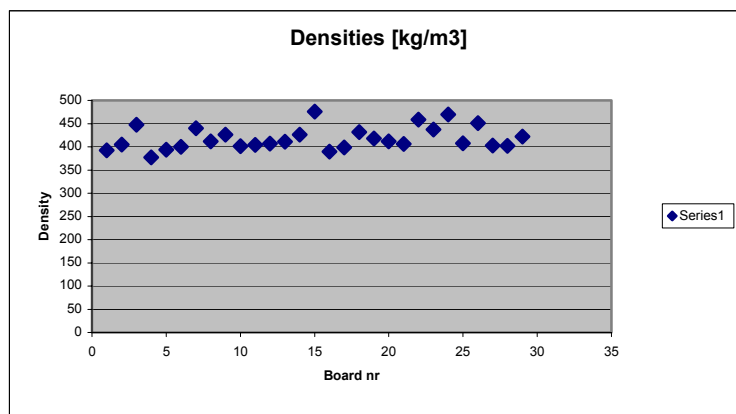


Figure 5.3 Varying of dry densities in boards

5.3 Timber to timber friction coefficient

The first test was made to investigate the variation of the timber-to-timber friction coefficient between different boards. Eight panels containing three boards each were assembled and tested. The configuration of the panels was made randomly mixing all the board numbers to simulate reality. The panel configurations used can be seen in Table 5.1.

Table 5.1 Panel configuration

Panel number	Board 1	Board 2	Board 3
1	16	18	21
2	1	25	15
3	17	24	20
4	26	27	29
5	11	6	8
6	13	12	10
7	14	7	9
8	19	22	23

The Panels were preloaded with a horizontal clamp load from the load applier of 4x50 N representing the normal force in a wall described in Chapter 4.2.1. In order to maintain the predefined moisture content only one panel at the time were tested before put back into an isolated environment.

The panels were one at the time loaded vertically in the alpha machine according to the method described in Chapter 4. For every panel a load displacement plot was obtained as shown in Appendix A. From these plots a maximum load capacity could be obtained and the friction coefficient be calculated according to Coulomb's formula for friction Equation 6.1. The results can be seen in Table 5.2. The mean value is 0,58 and the median is 0,54.

Table 5.2 Friction coefficients

Panel number	1	2	3	4	5	6	7	8
Friction coefficient	0,45	0,51	0,46	0,70	0,57	0,75	0,69	0,50

5.3.1 Stiffness behaviour for friction

The stiffness behaviour of the friction between boards is decided by two parameters, the force applied and the displacement caused by the force. The relationship between the displacement and the force can easily be seen in the diagrams from the laboratory tests (Figure 5.4 b). This curve can be seen as the behaviour of a spring force. The spring constant, k can then be calculated according to Equation 5.1.

$$k = \frac{F}{d} \quad (5.1)$$

Calculations from diagrams in Appendix A reveals an average value for the spring constant between t&g boards with an interaction length of 780mm (2x390) to 7,2 kN/mm.

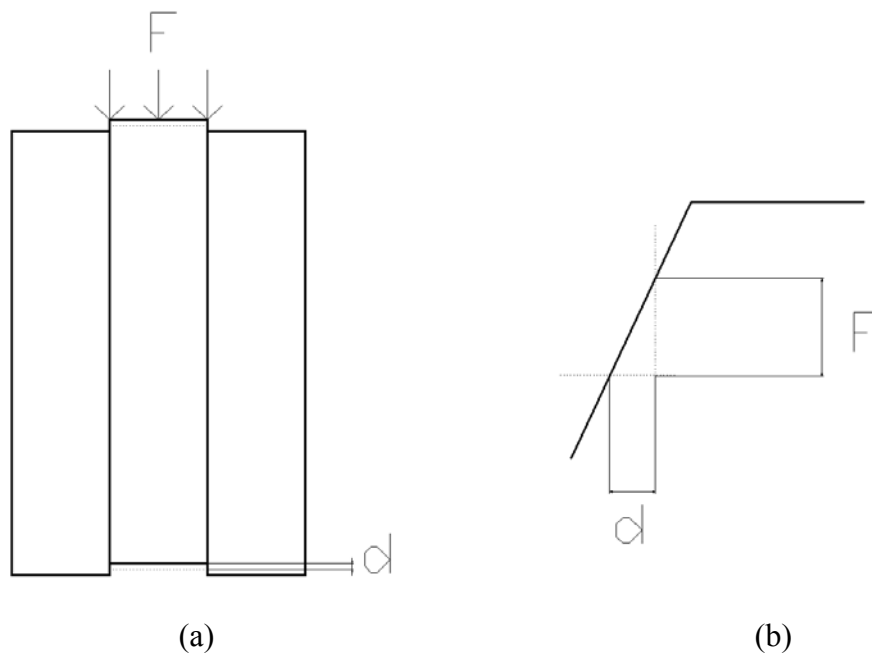


Figure 5.4 (a) The force applied results in a displacement (b) The force applied and the displacement can be seen in plots from laboratory

5.4 Effect of varied load level

To investigate what effect a variation of the normal force will have on the interaction behaviour between the boards a series of tests was made. In the previous chapter the test procedure used for testing the timber-to-timber friction was described. The same procedure was repeated again for this tests but this time after the first run with 4x100 N the horizontal load from the clamp load applier was increased according to Table 5.3

Table 5.3 Clamp loads used in the laboratory tests

Load number	1	2	3	4	5
Load level	4x50 N	4x100N	4x200N	4x300N	4x400N

The results from the tests can be seen in Figure 5.5.

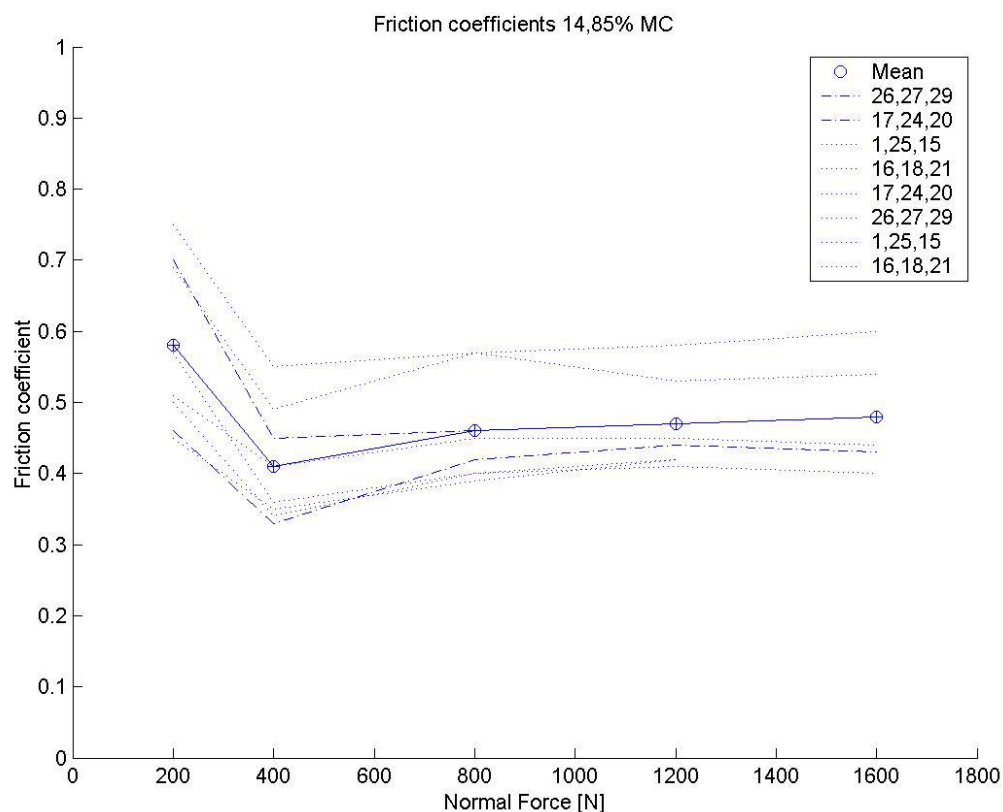


Figure 5.5 Friction coefficients varying with the normal force

The graphs plotted in Figure 5.5 are the Coulomb friction coefficient plotted against the load case (normal force). The results from Chapter 5.2 have been used to represent the first value (load case 1).

5.5 Effects of varied moisture content

Timber material properties are highly dependent on the moisture content. This can be seen among other places in Euro code which uses climate classes to calculate the design capacity of timber. In the literature (Baumberger, 1996) friction coefficients can be found for wet or dry timber varying from 0,2 for wet timber up to 0,6 for dry timber. It is therefore of interest for this Thesis to investigate what effect a variation of the moisture content in the boards will mean for the interacting friction.

The results from the first tests in Chapter 5.3 was used as reference values, having a moisture content in the board of 14,85%.

Four of the panels were picked out and stored in a normal indoor environment for 24 hours. The boards were once again weighted after the storing to control the moisture content. Mean moisture content in the boards of 11,25% was calculated.

The four panels, number 1 to 4 were tested with the same configuration as previous tests. The load cases used in the test are number 2 and 4. In the Figure 5.6 the friction coefficients are plotted against the load cases used in the tests.

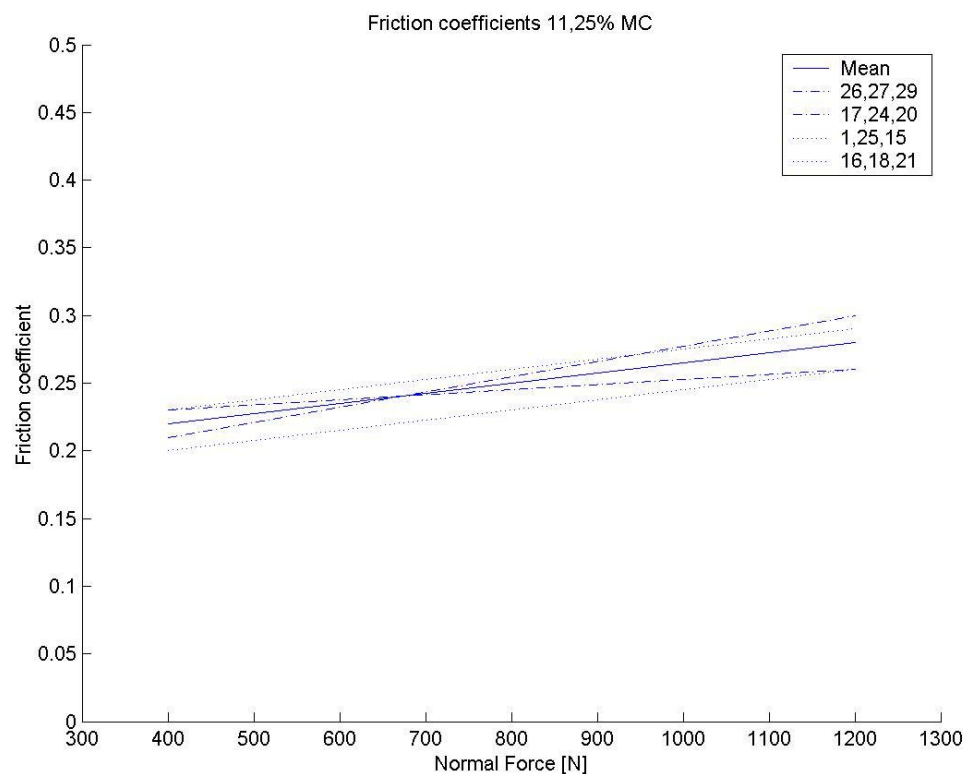


Figure 5.6 Friction coefficients moisture content 11,25%

The panels were unloaded after the test and stored another three days and nights in indoor climate. The moisture content in the boards after the second storage period could be determined to 9,76%. The panels were tested ones more according to the method described above and the results shown in Figure 5.7.

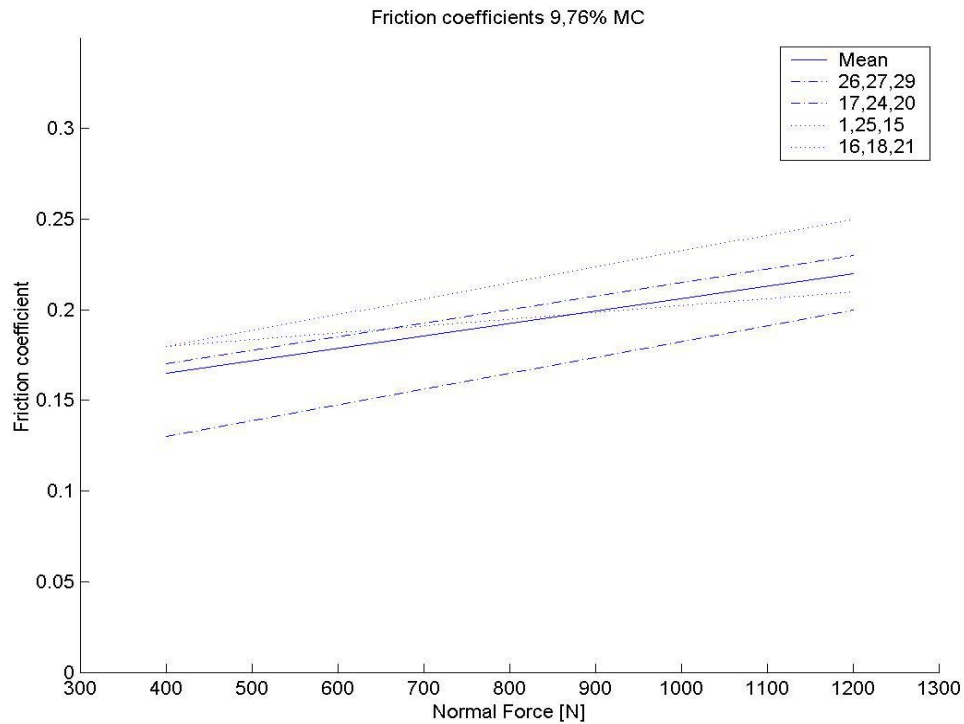


Figure 5.7 Friction coefficients at moisture content 9,76%

The following plots (Figures 5.8 ,5.9 and 5.10) describe the change of the friction coefficient for each individual panel.

Table 5.4 Friction coefficients, clamping force 400 N

Moisture content	14,85%	11,25%	10,5%	9,76%
Friction coefficient	0,39	0,22	0,19	0,17

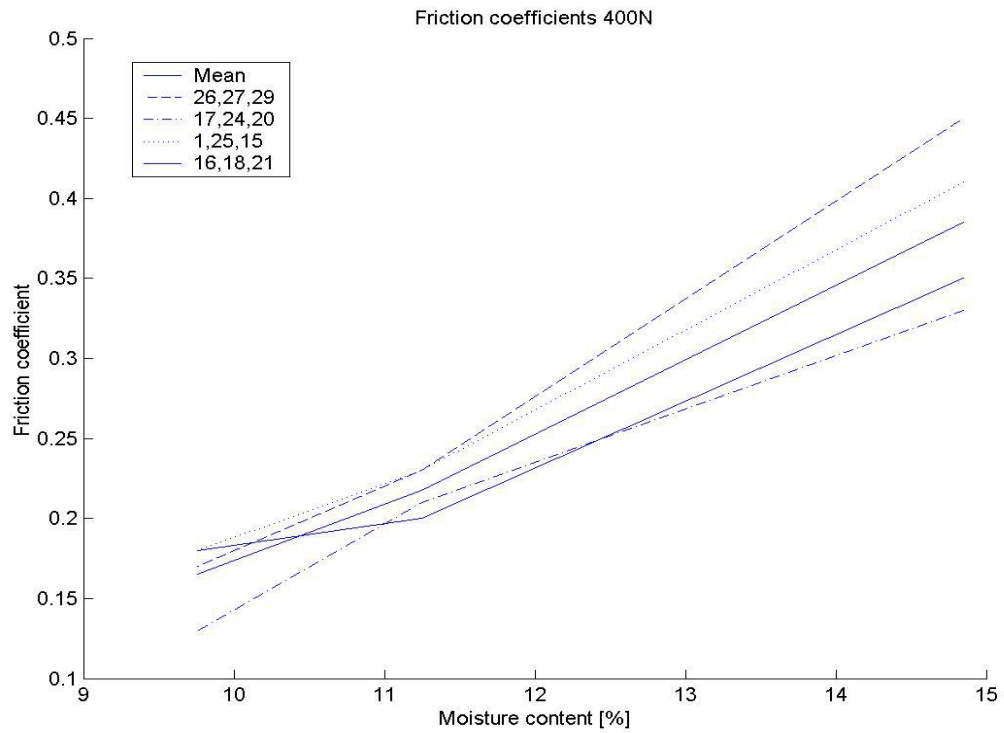


Figure 5.8 Friction coefficients vs. moisture content 400N

Table 5.5 Friction coefficients, clamping force 1200 N

Moisture content	14,85%	11,25%	10,5%	9,76%
Friction coefficient	0,45	0,28	0,25	0,22

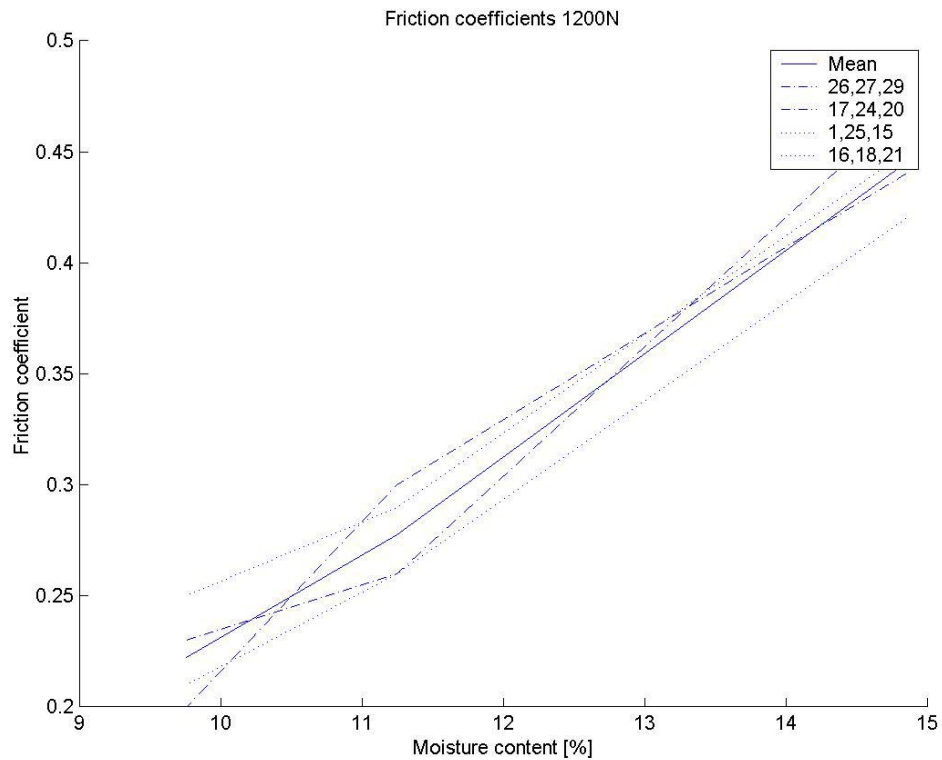


Figure 5.9 Friction coefficients vs. moisture content 1200N

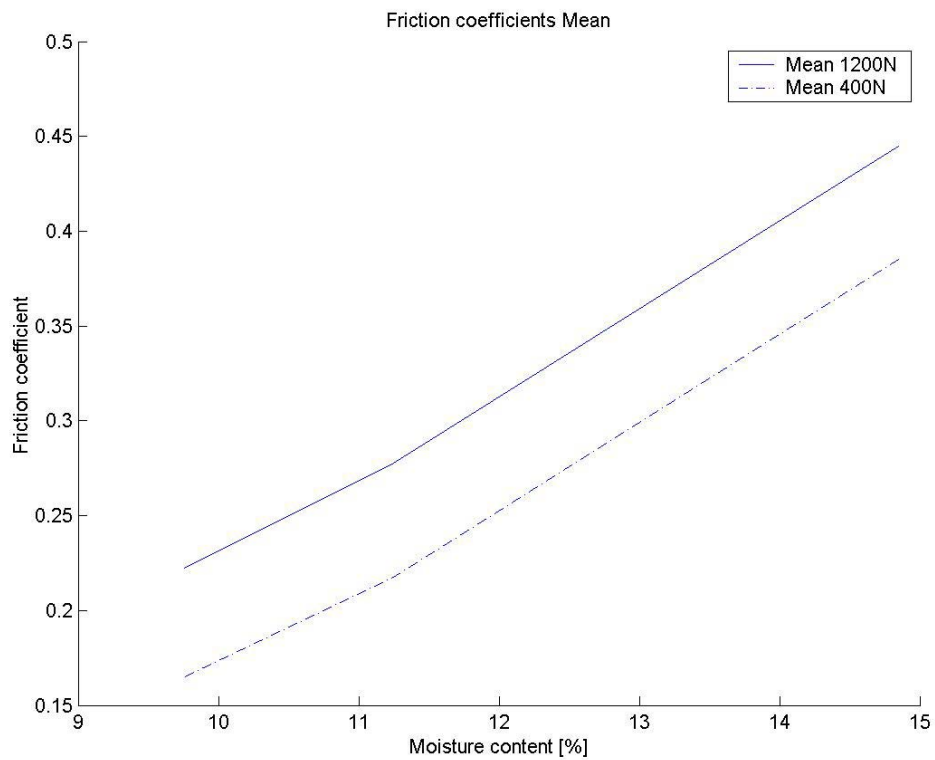


Figure 5.10 Mean friction coefficient vs. moisture content at two different clamping loads

5.6 Effects of repeated loading

According to the literature (Grahn and Jansson ,1997) the friction between to surfaces is the effect of microscopic irregularities of the surfaces connecting to each other. When repeated loading is made a smoothening effect can be assumed at the surface. This small test is to investigate the size of this smothering effect on the static friction between timber boards.

The testing of this phenomenon was included with the testing of varying load level described in Chapter 5.4. The testing was done in the same way as the other but instead of increasing the load to next load case after unloading the panel from vertical load the panel was once again loaded vertically with the same horizontal load case.

In the Table 5.6 the plot numbers representing the repeated tests is shown. The plots from the test can be seen in Appendix A.

Table 5.6 Repeated tests at predefined load case

Load [N]	Test number										
4x50	2.1	2.2	5.1	5.2	5.3	5.4	5.5				
4x100	1.1	1.2	5.6	5.7	9.1	9.2	10.1	10.2			
4x200	5.8	5.9									
4x300	9.3	9.4	10.3	10.4	10.5	11.3	11.4	11.5	11.5	12.3	12.4

The plots were interpreted according to the Figure 3.3 and the following results have been obtained. Se results in Table 5.7. The mean change from the tests was determined to 0,5%.

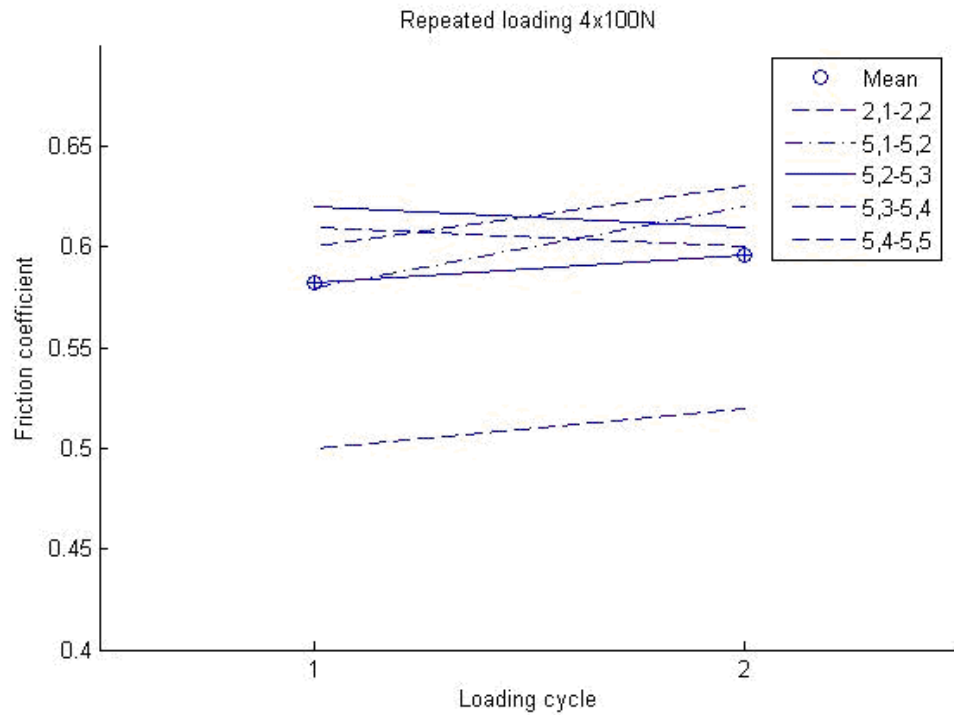


Figure 5.11 Result plot from repeated loading

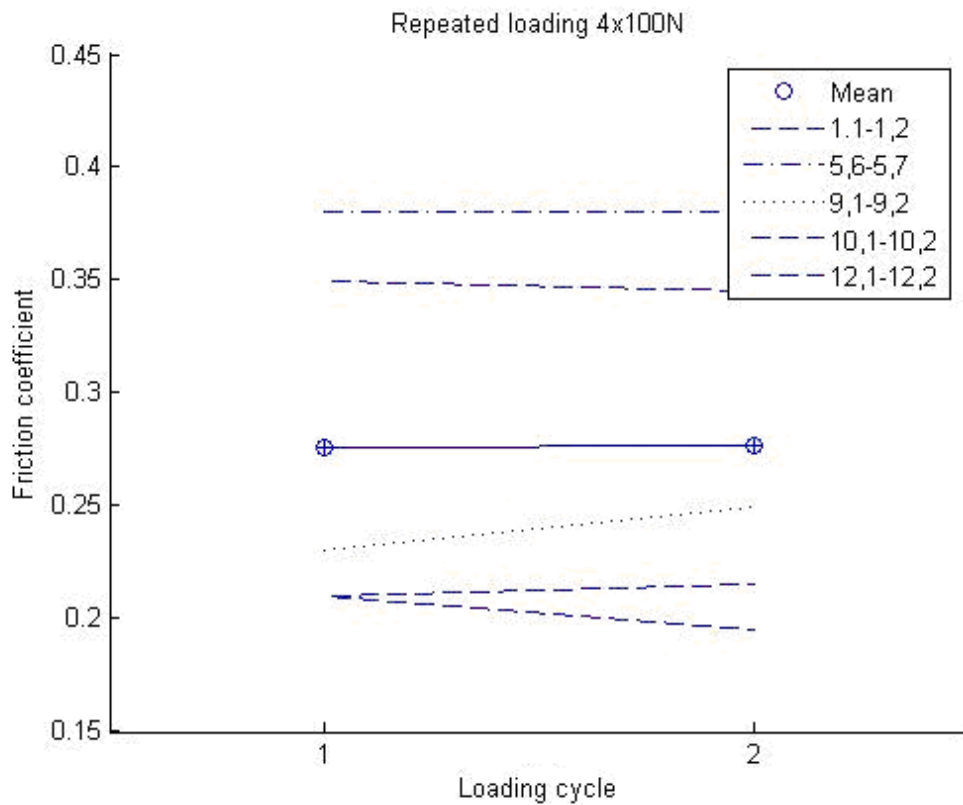


Figure 5.12 Result plot from repeated loading

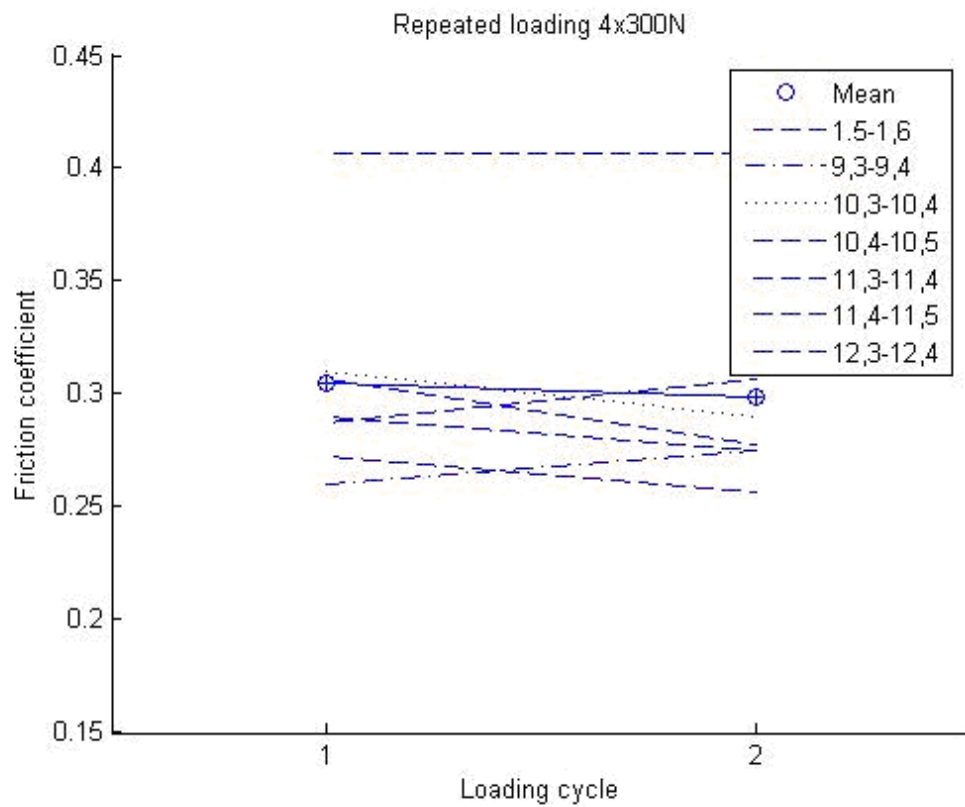


Figure 5.13 Result plot from repeated loading

Table 5.7 Results from tests with repeated loading

Test number	$\mu_{loading\ 1}$	$\mu_{loading\ 2}$	Load level	Difference
1.1-1.2	0,35	0,35	100	-1%
1.5-1.6	0,41	0,41	300	0%
2.1-2.2	0,50	0,52	50	4%
5.1-5.2	0,58	0,62	50	7%
5.2-5.3	0,62	0,61	50	-2%
5.3-5.4	0,61	0,6	50	-2%
5.4-5.5	0,6	0,63	50	5%
5.6-5.7	0,38	0,38	100	0%
5.8-5.9	0,40	0,43	200	8%
9.1-9.2	0,23	0,25	100	9%
9.3-9.4	0,26	0,28	300	6%
10.1-10.2	0,21	0,22	100	2%
10.3-10.4	0,31	0,29	300	-6%
10.4-10.5	0,29	0,28	300	-5%
11.3-11.4	0,29	0,31	300	7%
11.4-11.5	0,31	0,28	300	-9%
12.1-12.2	0,21	0,20	100	-7%
12.3-12.4	0,27	0,26	300	-6%

5.7 Effects of varying load rate

A small test series were performed to investigate what effect the vertical loading rate will have on the result of static friction. The horizontal load was kept at a constant level of 4x50N. The smallest horizontal load case was chosen in order to increase the sensitivity for vertical loading of the model. Three different loading rates were used for the test: 0,3 mm/min, 0,6mm/min and 2,4 mm/min. The choice of these rates is based on the standard rates of the Alpha machine and on work made by Johannesson (1979).

The following results were obtained (for full plots see Appendix A (5.1-5.5)).

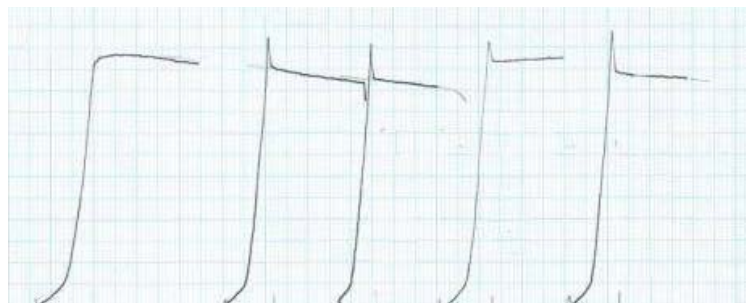


Figure 5.14 Result plots (Appendix A 5.1-5.5) from test with varied loading rate, clamp load 200N (x-axis displacement, y-axis load)

One test was also performed with a higher horizontal load, the load case used was number 3. The following plots were obtained (for full plots see Appendix A (7.5-7.7)).

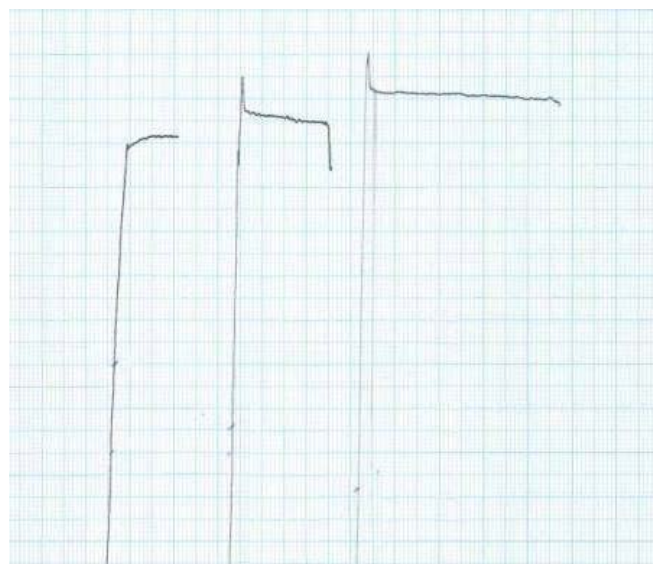


Figure 5.14 Result plots (Appendix A 7.5-7.7) from test with varied loading rate, clamp load 800N (x-axis displacement, y-axis load)

5.8 Effects of wallpaper attached to the panel

The final test made in laboratory is with the panel in interaction with glued wallpaper attached. Four of the panels used in initial laboratory tests were randomly picked for the test. The wallpaper used is a so-called non-moment wallpaper from producer. The wallpaper is created with extra high strength to make assembling on walls easier. Material properties received from the producer are as in Table 5.8. The E-modulus values are calculated according to theories of linear elastic materials.

Table 5.8 Material properties for wallpaper

Surface Weight (g/m ²)	280
Thickness (mm)	0,405
Dry tension strength in longitudinal direction (N/m)	6785
Dry tension strength in transversal direction (N/m)	3445
Wet tension strength in longitudinal direction (N/m)	6370
Wet tension strength in transversal direction (N/m)	2305
Max strain in longitudinal direction (%)	11,4
Max strain in transversal direction (%)	15
Calculated longitudinal E-modulus (MPa)	148,8
Calculated transversal E-modulus (MPa)	57,4

The values for the dry tension strength in Table 5.8 represents a value measured by the producer for the dry tension strength for one unit metre width of the wallpaper (Figure 5.16)

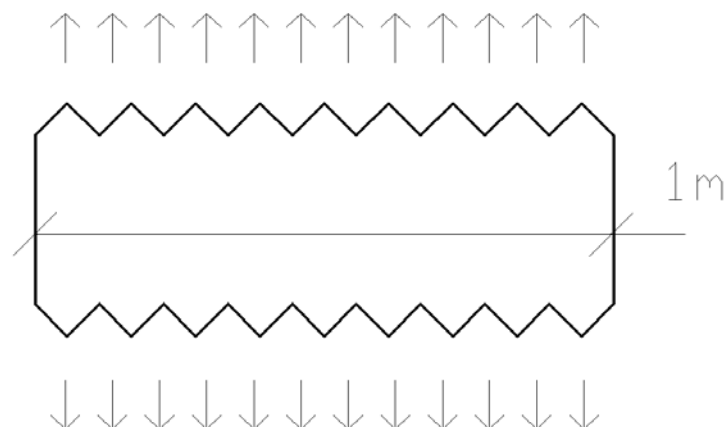


Figure 5.16 The ultimate tension strength of the attached wallpaper calculated per width of 1 m

The relationship between shear modulus and E-modulus according to Källsner (1984) in Equation (5.2) can be used to approximate the shear strength in our wallpaper. Assuming no bending resistance, the shear strength can be calculated to 2557,5 N/m - half the average value for tension strength.

$$G = \frac{E_{mean}}{2 \cdot (1 + \nu)} \quad (5.2)$$

The wallpaper is attached with the longitudinal direction in the vertical direction of the boards (Figure 5.17). Wallpaper glue used was “Tapetlim 1870” from the producer (Figure 5.18). The boards were placed on a table with PVC plastic on. The boards were forced together and held by a screw clamp to avoid glue between the boards (Figure 5.17). After assembling the wallpaper dried for 3 days before the tests were made.



Figure 5.17 Twelve boards with wallpaper attached in the vertical direction of the boards



Figure 5.18 Glue used for wallpaper

The test were made in the same manner as previous laboratory test (Figure 5.19), the vertical displacement of 10 mm on the board in the middle was placed before gluing. The increased effect was higher than expected and therefore the plots weren't accurate calibrated as seen in Appendix A, although, the capacity was easy to interpret on the digital display on the amplifier. Plots from panel 7 and 8 (Figure 5.20) are rather accurate and displays the behaviour of a board with wallpaper attached. By investigation of the plots from panel 7 and 8 the stiffness behaviour can be investigated in the same manner as it was without wallpaper in Chapter 5.3. The average value calculated from these diagrams reveals a value for the spring constant to 2,6 kN/mm.



Figure 5.19 Laboratory tests of panel with wallpaper

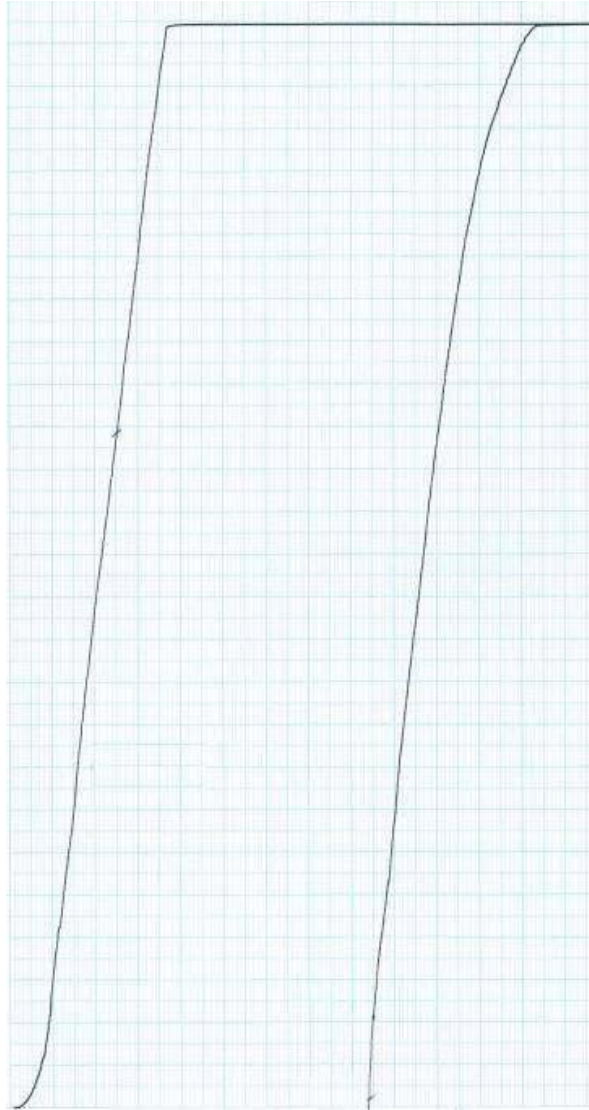


Figure 5.20 Graph of panel 7 and 8 (Appendix A 14.1-14.2), (x-axis displacement, y-axis load)

Two of the panels were tested with the clamp force of 400 N applied and the two other with 1200 N applied. By using the two different horizontal loads it is possible to see if the effect of the wallpaper in any way depends on the normal force applied. The moisture content in the boards before the wallpaper was attached was 11.25%. Compared with the boards without wallpaper attached the moisture content decrease slower because they where placed on a PVC plastic covering one of the surfaces and the wallpaper on the other (Figure 5.17). The moisture content after three days in the boards without wallpaper was 9,76%. The moisture content is somewhere between 11.25% and 9.76%, approximated to 10,5% and the friction constant μ is approximated to 0,18 for 400N normal force and 0,23 for 1200N normal force. Table 5.9 and 5.10 shows values for vertical load capacity for two different cases. One is measured in laboratory and one is calculated with an approximated friction constant. The last column shows the approximated difference in capacity with or without wallpaper.

Table 5.9 Difference of capacity with or without wallpaper with normal (clamping) force 400 N, average value for difference is 1966 N

	Measured max vertical load with wallpaper, 400N normal force, $\mu = 0,18$ and MC 10,5%	Calculated max vertical load without wallpaper, 400N normal force, $\mu = 0,18$ and MC 10,5%	Increased capacity due to wallpaper			
<div>Panel 7</div> <table><tr><td>14</td><td>7</td><td>9</td></tr></table> <div>Appendix A laboratory 7.2, 14.1</div>	14	7	9	1960N	144N	1816N
14	7	9				
<div>Panel 8</div> <table><tr><td>19</td><td>22</td><td>23</td></tr></table> <div>Appendix A laboratory 8.2, 14.2</div>	19	22	23	2260N	144N	2116N
19	22	23				

Table 5.10 Difference of capacity with or without wallpaper with normal (clamping) force 1200 N, average value for difference is 2333 N

	Measured max vertical load with wallpaper, 1200N normal force, $\mu = 0,23$ and MC 10,5%	Calculated max vertical load without wallpaper, 1200N normal force, $\mu = 0,23$ and MC 10,5%	Increased capacity due to wallpaper			
<div>Panel 6</div> <table><tr><td>13</td><td>12</td><td>10</td></tr></table> <div>Appendix A laboratory 6.4, 15.1</div>	13	12	10	3100N	552N	2548N
13	12	10				
<div>Panel 5</div> <table><tr><td>11</td><td>6</td><td>8</td></tr></table> <div>Appendix A laboratory 5.10,16.1</div>	11	6	8	2670N	552N	2118N
11	6	8				

6 Evaluation of laboratory tests

6.1 Test of timber friction coefficient

The results for the timber-to-timber friction coefficient obtained from the tests and displayed in Table 5.2 shows a good resemblance with values from literature (Baumberger, 1996). Compared with the values from literature the mean value of 0,54 might be high but it is within the expected region (0,3 to 0,6). One of the panels, number 7, differs from the others. The friction coefficient 0.69 can be considered too high but knowing from later tests made on the same panel with other load cases this panel shows slightly higher values all through the series. This is probably due to some larger irregularity on one of the interacting surfaces, however, not visible by ocular inspection.

6.2 Varied horizontal load level

Two interesting effects can be seen in the results from this test. The first one is that the initial values for the friction coefficient representing load case 1 (4x50N) is remarkably higher than the rest of the values. This might be explained by the theory that an unloaded surface has a more irregular microstructure than one loaded. This theory was tested in Chapter 5.6 to investigate these effects but with the result that no clear conclusion could be seen whether this effect was active or not. Another possibility to explain the higher friction value for this load case can be the performance of the tests. When comparing the calibration values for the spring a small deviation from the manufacturer's curve can be seen, Figure 4.19. If an error has been made during the calibration of the springs a higher horizontal load has been submitted to the panels during the tests than the calculated value of 200 N totally. This would lead to higher friction values than expected.

The second effect can be seen for the higher load cases. For load cases over 800N the friction constant can be assumed to be constant and only small variations occur if the horizontal load is increased. These results show a good agreement with the Coulumb friction theory and the conclusion that for normal forces higher than 800N /38 cm length t&g the friction coefficient can be assumed to be independent of the level of normal force.

The variation of friction coefficient for the panels can of course be explained by the individual variation of the properties of the interacting surfaces. It can be seen that even if the values of the friction coefficient agree more with tabular values if the horizontal load level is higher the individual variation is still very significant.

6.3 Varied moisture content

To start the evaluation of the moisture dependency the results friction coefficient was compared in Figure 5.6 and Figure 5.7. Although a larger variation can be seen for the lower load case at high moisture content, both the curves seem to follow the same pattern. One reason for this variation might be the combination of low load and high moisture content. The low load makes the result sensitive to individual variations among the interacting surfaces and the high moisture content can have a different

effect on the material properties of each board. As the moisture content in the boards decreases so does the friction coefficient. The relationship between the friction and the moisture content is surprisingly linear for both plots. An estimated value for the loss is 0,045 on the friction coefficient 1%-unit moisture content within the interval of 9,5%-15% moisture content. This linearity is used to approximate the friction coefficient between the boards used for the tests with wallpaper. This strong decreasing effect was a most unexpected result since the literature (Baumberger, 1996) recommends the opposite. In the literature wet timber has a lower friction coefficient than the dry timber. One explanation for this effect might be that in the literature the interacting surfaces tested are actually wet to compare with the ones tested in this thesis that has a high moisture content but can be considered dry on the surface. As can be seen in Figure 5.10 the mean behaviour for the two tested levels of load follows a very similar pattern. The results for the friction coefficient from the higher load is approximately 0,05 higher than the once from the lower load case. One reason for this effect might be what has been written above about the lower load having a higher sensitivity on individual differences. For further work in this thesis the effects of varied moisture content will be displayed on a FE model wall. This effect needs to be investigated further if more conclusions are to be made.

6.4 Repeated loading

If studying the behaviour of the static friction under repeated loading no clear effects can be seen in the laboratory results. The plots of test 1.5 and 1.6 or 5.6 and 5.7 in Appendix show no reduction of the static friction coefficient. The peak values for both loading cycles are the same. But if studying plots of test 1.2 and 1.3, 10.3-10.5 and 12.1 and 12.2 a decrease of capacity is shown, the decrease from 10.3 to 10.5 is almost 11%. This can be explained by the smothering theory described in Chapter 5.6 and can be considered as the expected result. However, this is only representing the behaviour of around 30% of all tested specimen. A much larger group, around 50% of the laboratory specimens (the once in Table 5.6 not mentioned before) shows an increasing friction coefficient after the first loading. The best example to display this effect can be seen in the plots of test number 9.1 and 9.2. The increase of load capacity is almost 9%. This phenomenon is difficult to explain and it also seems to occur independent of the clamping load level. A theory is that this is an effect either caused by inaccuracy of the laboratory equipment or that it is due to the large individual variation of timber surfaces. Since the timber surface is not homogenous the result may vary in a non-expected manner.

For further work in this thesis the static timber-to-timber friction coefficient is considered to be independent of effects of repeated loading, no long-term effects will either be studied. To draw any further conclusions concerning the effect of repeated loading on the timber-to-timber friction coefficient a more extensive research needs to be done.

Another reason for testing the repeated loading of the panels was to investigate why small peaks occurred on some of the plots and not on the others. According to theory (Baumberger 1996) this is the effect of micro structural irregularities on the interacting surfaces connecting to boards. These effects should however be reduced after loaded to failure. There are however no visible effects of any reduction of this

peak after repeated loading. For more information on how the peak values vary see Appendix B.

Under repeated loading a clear tendency according to the tests can be seen on the kinetic friction that follows after the peak value of the static friction. After the first loading cycle the kinetic friction constant slowly drops according to the Figure 6.1. When the second loading is made no clear reaction can be seen on the value for the static friction constant but the kinetic picks up where it has ended in the first loading cycle. This effect will however be of less interest since the kinetic friction coefficient only was used in this thesis to secure a non-brittle failure of the wall.

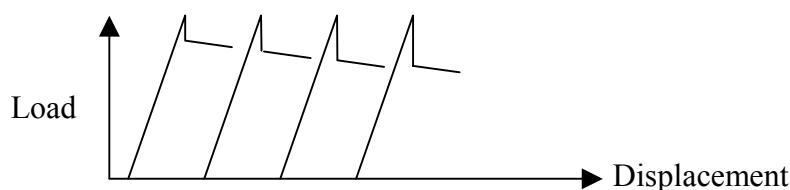


Figure 6.1 Behaviour of kinetic friction under repeated loading

6.5 Varied load rate

When an analysis of the results from test number 5.1 to 5.5 and 7.4 to 7.6 is made two different tendencies can be discovered. The result from panel 5 show a very small decrease of the friction force when the loading rate is increased. This behaviour is most unexpected but can maybe be explained by the theory of effects of repeated loading as shown in Chapter 6.4. The investigation of this effect concludes that no such behaviour could be proved. This effect is also the reason for varying the loading rate and not starting with the lowest. As can be seen in the result from the test the decrease of friction force is very small and the level of variations well within the borders of inaccuracy of the model.

For the next test performed on panel 7 with a higher horizontal load level (load case 3) the increase of the load capacity can be seen when increasing the loading rate. This time the loading is made in size order with the lowest loading rate (0,3 mm/min) first. The increase of friction force from the first loading to the second and the second to the last is 40 N in relation to the total medium load of the three tests of 950 N resulting in a variation of less than 5%. This increasing effect is larger than the first, but can be assumed to be within the interval of insecurity for the test procedure. Therefore the conclusion of this test is that no load rate dependency of the friction constant can be seen. However, there are some variations that might need more investigation for future work.

6.6 Wallpaper attached to panel

Before reading this evaluation of the effect with wallpaper attached is it important to remember that few tests were made and the results are not statistically proofed. The results are although very interesting both from the results in this thesis and for future studies.

As shown in Figure 5.19, buckling occurs on the wallpaper in two lines along the interaction between the boards. This buckling is a result of tension forces in the wallpaper. The tensions in the wallpaper are as in Figure 6.2.

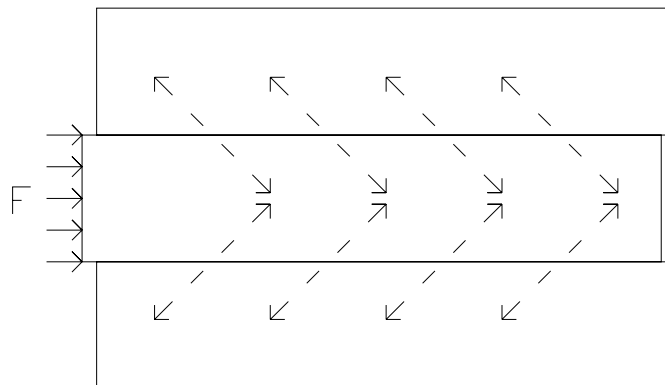


Figure 6.2 Tension in the wallpaper as dashed lines

Decisive for the capacity of the panel is the strength and the stiffness behaviour of the resultant forces in the wallpaper attached. The strength capacity and the stiffness behaviour is considered separately in this evaluation and summarised afterwards.

6.6.1 Strength Capacity

To see if the increased capacity due to the wallpaper can be verified, an approximated method is used to see if the increase in capacity is realistic. Reaction forces transferred to the boards is dimensioning for the increased capacity due to the wallpaper (Figure 6.3).

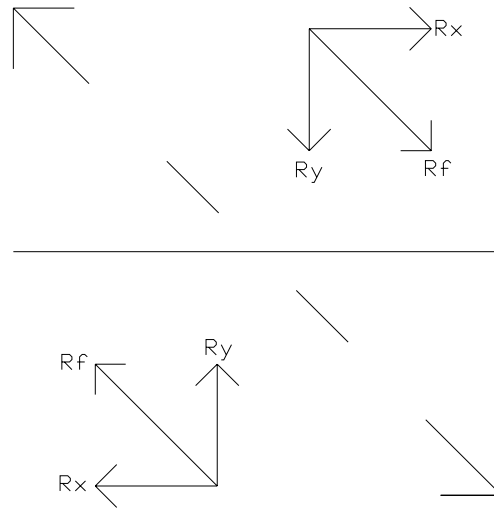


Figure 6.3 The upper right corner from Figure 6.2, Tensions (dashed line) in the wallpaper with the reaction forces transferred to the boards

The reaction force in vertical direction R_y increases the normal force decisive for the friction force. Reaction force R_x is increasing the resultant force. The total force in the horizontal direction as a resultant to the applied force F (Figure 6.2) can be calculated (Equation 6.1).

$$F = R_x + R_y \cdot \mu \quad (6.1)$$

The angle between the forces is depending on the material properties of the wallpaper but if 45 degrees angle can be assumed for the reaction force R_f , the size of R_x and R_y is.

$$R_x = R_f \cdot \frac{1}{\sqrt{2}} \quad (6.2)$$

$$R_y = R_f \cdot \frac{1}{\sqrt{2}} \quad (6.3)$$

With known reaction force from the wallpaper the capacity to resultant the applied force F can be calculated.

$$F = R_f \cdot \frac{1}{\sqrt{2}} + R_f \cdot \frac{1}{\sqrt{2}} \cdot \mu \quad (6.4)$$

According to Equation 6.4 the reaction force in the wallpaper before failure can be calculated. Our results from the laboratory reveal values of the increased capacity between 1816N to 2548N (Table 5.9 and 5.10). If the increased capacity is known the reaction forces for wallpaper based on 780 mm interaction length can be calculated. This capacity can be recalculated for 1m lengths in order to easy compare with known capacities for the wallpaper. In Table 6.1 and 6.2 values for the reaction forces are calculated for a friction interval 0,15 to 0,25. The reaction forces are calculated for the measured increased capacities with wallpaper for 1,8 kN (Table 6.1) and 2,6 kN (Table 6.2).

Table 6.1 Reaction forces in wallpaper calculated according to Equation 6.4 for the increased capacity $F = 1,8 \text{ kN}$

Friction coefficient	Reaction force (0,78m) [N]	Reaction force 1 m length [N]
0,15	2214	2838
0,16	2194	2813
0,17	2176	2789
0,18	2157	2766
0,19	2139	2742
0,2	2121	2720
0,21	2104	2697
0,22	2087	2675
0,23	2070	2653
0,24	2053	2632
0,25	2036	2611

Table 6.2 Reaction forces in wallpaper calculated according to Equation 6.4 for the increased capacity $F = 2.6 \text{ kN}$

Friction coefficient	Reaction force (0,78m) [N]	Reaction force 1 m length [N]
0,15	3197	4099
0,16	3170	4064
0,17	3143	4029
0,18	3116	3995
0,19	3090	3961
0,2	3064	3928
0,21	3039	3896
0,22	3014	3864
0,23	2989	3833
0,24	2965	3802
0,25	2942	3771

The reaction forces in the wallpaper for resultant forces 1,8 kN to 2,6 kN for the panel are between 2,6 kN and 4,1 kN for 1 m length. The resultant force is the shear capacity of the interacted panel. The shear strength 2557,5 N, the tension strength of 6785 N longitudinal and 3445 N transversal is the capacities known for 1 metre of the wallpaper. The capacity in the wallpaper in this case is probably an interaction between these capacities. The reaction forces are within the interval of the highest and lowest capacity of the wallpaper. If the glue is assumed very strong, a shear failure in the wallpaper occurs. An increased effect of transversal and longitudinal force can be assumed with more elastic glue, both for the capacity of failure and force affecting the increased friction between the boards, but with increased distance between. However, the major interest for this thesis is the increased capacity for the panel.

6.6.2 Stiffness behaviour

With the shear stiffness approximated to about 2600 N/mm in Chapter 5.8, the displacement between the boards in the panel for forces between 2000 and 2600 was up to 1 mm. As seen in Figure 6.4 the buckling of wallpaper is clearly seen and the buckles are measured to 10 mm. The failure mode is combined failure of both glue and wallpaper, with 10 mm buckles in the wallpaper before cracks occur. Diagonal

tension in 10 mm of the wallpaper corresponds to strain around 14% with known displacement of 1 mm in vertical direction (Figure 6.5). The strain capacity given by the producer is 11,4% transversal and 15% longitudinal. By studying the failure mode in detail it is an interaction between the glue and the wallpaper, with stronger glue a more brittle failure had been achieved. Even if the displacement of about 1 mm can be considered quite small it will be more critical in a wall with 27 boards with the same tension between all of them



Figure 6.4 Zoom in from Figure 5.19, buckling on the wallpaper, foreground 8 mm diameter threaded steel rod

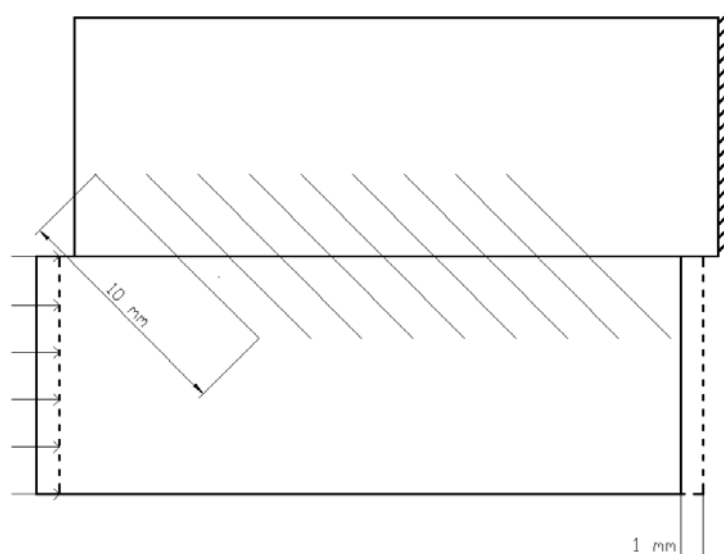


Figure 6.5 Buckles in wallpaper of 10 mm forced by the 1 mm displacement between the boards. Tension in buckles around 14%

6.6.3 Summary effects of wallpaper

The approximated method for calculating gives realistic values for the reaction forces in the wallpaper. By studying the buckles and the displacement of the boards the strain value in wallpaper corresponds well with values obtained from the producer. Stiffer glue gives a more stiff behaviour, a higher resistance and a more brittle failure of the panel, though it is probably decreasing the capacity. To find a good material that interacts so the shear resistance is stiff enough and the capacity is high enough will need more studies.

7 FE Modelling

7.1 Modeling the laboratory test of friction with t&g panel

As described in the introduction, this thesis includes both by laboratory tests and FE modeling. To investigate full scale t&g walls the FE program ABAQUS was used. The model building process is described in this chapter.

The first step to create the full model of the wall is to simulate the laboratory tests described in previous chapter. This first model is describing the pure interaction between the t&g timber boards and will later be used on the whole shear wall in Chapter 7.5.

As described above the laboratory tests was performed with three pieces of timber interacting by Columb friction and subjected to one horizontal and one vertical pressure force to simulate the shear load that was subjected to the wall unit.

7.1.1 Model of t&g board

The boards were modeled as solid elements (C3D8R) in order to model the interaction between the boards as accurate as possible. By doing this choice of element each interacting surface can be identified and be given specific properties.



Figure 7.1 Geometry of t&g timber board used in the ABAQUS model of the laboratory tests

7.1.2 Material properties

The material properties used in the model are based on the doctored thesis by Ormarsson (1999) and can be seen in Table 7.1 The t&g boards are modeled with anisotropic properties to represent a real board of spruce as close as possible.

Table 7.1 Anisotropic material properties for spruce [Pa]

E_L	E_T	E_R	G_{LT}	G_{LR}	G_{TR}
9.9E+009	4E+008	2.2E+008	4E+008	2.5E+008	2.5E+007

To assign the material properties to the solid element a homogenous section including the anisotropic material parameters was created and assigned to the element.

7.1.3 Time step

To obtain the model to respond as close as possible to the response of the elements in the laboratory tests three different time steps was created.

In the first time step (initial) all boundary conditions and interactions between the boards were introduced to lock the boards together in the model.

In the next step (contact) a horizontal pressure load is applied to the test model in order to get the friction between the pieces to become active.

Finally in step tree (load step) the vertical displacement of the middle board is applied to start the calculations.

All the steps created are of the type “static general” which means that they will follow each other in time creating a model time history in three steps and give the results from a static analysis.

7.1.4 Interactions

Since this model is built up by solid three-dimensional elements, the definition of the interacting surfaces is done manually in ABAQUS CAE window. The tongue and the groove are modeled with their actual dimensions as can be seen in Figure 7.2. When the boards are loaded they will interact only on the surfaces that come into contact with one another. The reason that both sides of the tongue are free from contact in the initial state is the fact that in reality the surfaces of the boards are fixed in the same level by the frame structure.

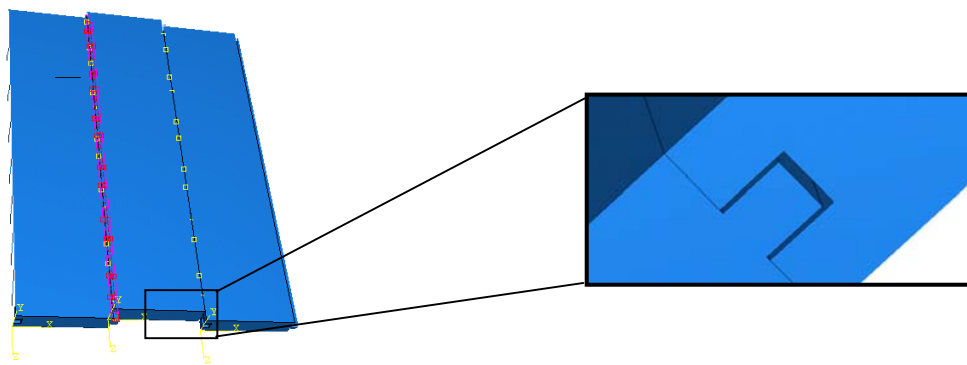


Figure 7.2 Interaction between the t&g timber boards in the ABAQUS model of the laboratory tests

7.1.4.1 Interaction properties

To define interaction between two surfaces in ABAQUS the interaction properties in both the transversal and the normal direction to the interaction plane needs to be assigned.

For the normal direction ABAQUS has four standard choices of the “pressure-over closure” relationship to describe the interaction.

For this model the type “hard contact” is used because it does not assume that the material is softening after contact. This type of contact also assumes that when there is no contact between the boards, forces will not be transferred between the interacting surfaces and when there is contact no upper limit for the level of the pressure force transmitted exists. The choice of “hard contact” between the boards was combined with the option to allow separation after contact so that the model will follow a “real” behavior. The way the interaction works is schematically shown in Figure 7.3.

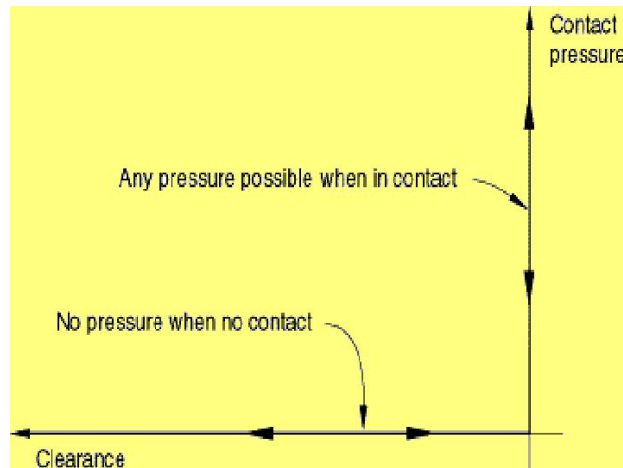


Figure 7.3 Interaction behaviour in the normal direction for the option "hard contact" (ABAQUS Manual)

For the choice of whether or not to use the option augmented Lagrangian method, this method was rejected in order to reduce the number of iterations. However, if used, this method allows the slave nodes to penetrate the master surface and it can provide an easier solution of the system. The master surface is the one deciding the normal direction in ABAQUS.

For the tangential properties in the model, a penalty friction formulation was used. This means that the frictional constraint is assigned an elastic stiffness; this is also the default choice in ABAQUS standard. The option to the penalty formulation is Lagrange multiplier method that enables an infinite sticking stiffness in which the elastic slip will be equal to zero. This method however is much more time consuming to compute.

Three different properties are needed to define a friction model when using ABAQUS, friction, shear stress and elastic slip. In friction sheet, the choice of isotropic or anisotropic friction is made. This option controls whether or not the friction is varying in different direction within the friction plane. For this model the choice of isotropic friction is made. The only thing defined more in this sheet is the static friction coefficient and it is varied according to Table 7.2. In the next sheet named "shear stress" the limit of the highest level of shear stress transmitted by the friction constraint is defined, for this model the option no limit is used. Finally in the third sheet called "elastic slip" the allowable elastic slip for the model is to be defined. There are two ways of defining this slip when using ABAQUS standard. Either it is done by defining the elastic slip by a relative distance to the slip surface dimensions or by a fixed distance. For this model the standard option in ABAQUS is used with a relative distance of 0,5% of the element length.

7.1.5 Loads and boundaries

The model was fixed in space by three different boundary conditions in the lower end of the boards. The two outer boards are fixed in the vertical and normal direction to the plane and free in the third horizontal direction, see Figure 7.4. The mid point on the middle board's lower edge is fixed in the horizontal direction. These boundary conditions make it possible to apply load to the outer edges, (see Figure 7.5), and investigate the interaction between the boards.

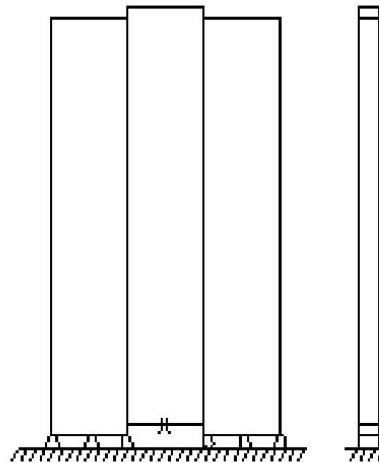


Figure 7.4 Static systems with boundary conditions of the tested ABAQUS model of the three t&g boards forming a small panel

In the next time step of the analysis, step (contact), a horizontal load is applied to the test model in order to activate the interaction between the boards. This horizontal load is applied according to Figure 7.5 because of the board geometry since the tongue is smaller than the groove.

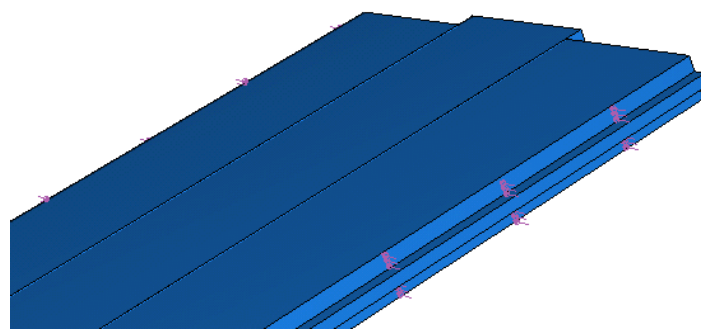


Figure 7.5 3D-model describing the clamp loading by showing the loaded surfaces

Finally to trigger the model an axial load is applied to the upper edge of the middle board, see Figure 7.6. This load is either a pressure load or a displacement. If the pressure load is used the model will work and describe the stress distribution until the critical level of the load is reached. When the board starts to slide then the model will fail as a result of the overloaded static capacity. If the load case with displacement of

the upper edge was used the model remains stabile during the whole analysis. Therefore the model controlled with displacement was used for further studies.

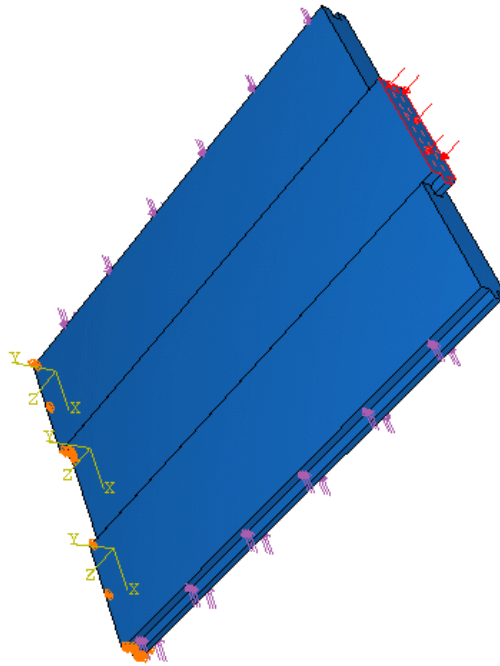


Figure 7.6 Description of all loading (clamp load and vertical load) of the ABAQUS model with boundary conditions

7.1.6 Mesh

To create a node pattern in ABAQUS the mesh module is used. Since the geometry of the parts is relatively simple the standard procedure to create a mesh over the elements of the model was used. This procedure starts with seeding the elements which means creating a pattern of markers on the element borders that was used of the ABAQUS mesh generator to create a cubic element pattern. To create the seed pattern an element size is chosen in this case 20x20x7,33 mm to create elements of representative size.

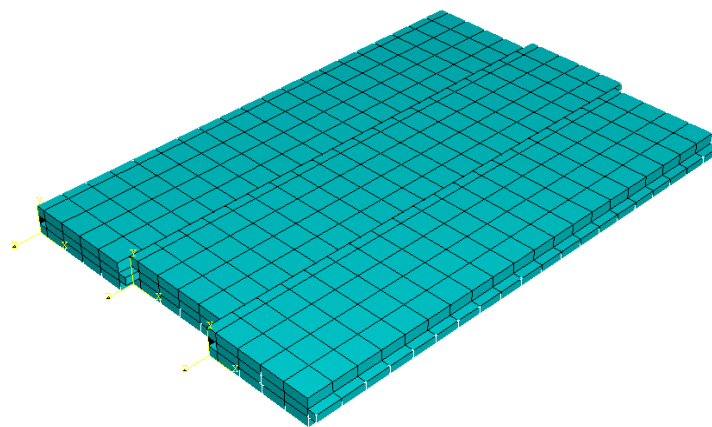


Figure 7.7 Description of mesh configuration for the panel

7.1.7 Results

To verify the results a hand-calculation was made using the Columb friction theory described in Chapter 3.1. Using the symmetry of the laboratory test a system similar to the one in Figure 4.7 can be established.

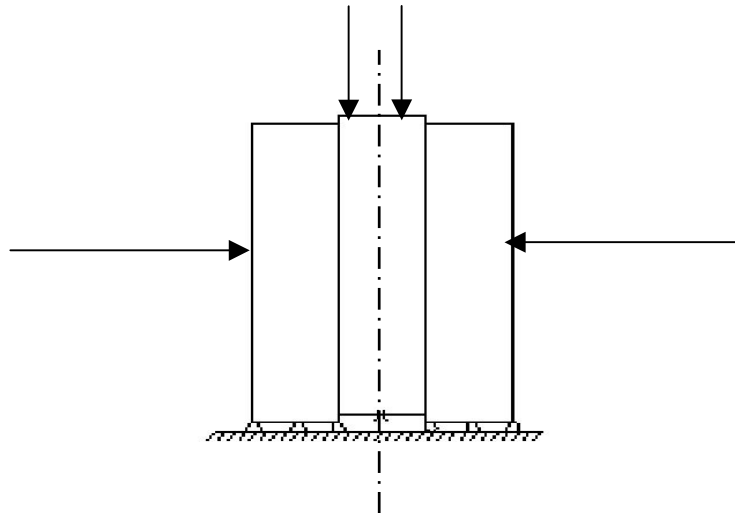


Figure 7.8 Principal sketch of laboratory model

Table 7.2 Table with friction forces from hand-calculation with Equation 3.1 [N]

Friction Coefficient	Clamp load 1 kN	Clamp load 10 kN	Clamp load 20 kN
0,1	100	1000	2000
0,3	300	3000	6000
0,5	500	5000	10000

The friction coefficient is varied in three steps from 0.1, 0.3, 0.5 and the normal force is varied from 1 kN to 20 kN. As can be seen if comparing the results shown in Table 7.2 and 7.3 a very good agreement with the theory is achieved. As shown in Figure 7.8 the model can be divided with a symmetry line and therefore to obtain the correct friction coefficient between the boards the pressure force on the upper edge of the middle board needs to be divided in two parts.

Table 7.3 Table with friction forces from ABAQUS [N]

Friction Coefficient	Clamp load 1 kN	Clamp load 10 kN	Clamp load 20 kN
0,1	99,999	999,813	2021,14
0,3	299,993	2999,47	5998,29
0,5	499,973	4997,89	9979,21

With this comparison the conclusion that the ABAQUS model is sufficiently accurate to represent the laboratory test can be made.

7.2 Simplified model of performed laboratory test

To reduce the computational time, the previous study of the laboratory model made with 3D solid elements and friction interaction behaviour was simplified. This was achieved using 3D shell elements instead and attempting to find a simpler way to model the friction.

7.2.1 Boards

The boards are modelled with a 3D shell element type S4R. This element is simplification of solid element with half the number of nodes (Figure 7.9). Anisotropic values are used for the timber, but also isotropic values are tested. This test was made to verify that change in element type and also variation between anisotropic and isotropic values doesn't affect the result. The aim is to be able to continue modelling with isotropic values to reduce computational time without increasing the errors. The E-modulus used in isotropic test is 9 GPa and shear modulus 3,3 GPa. The anisotropic values used are the same as in Chapter 7.1 according to Ormarsson (1999). The dimensions and the assembly of the boards differ from the lab with solid elements. Then using shell elements, the geometry of the tongue and the groove is neglected.

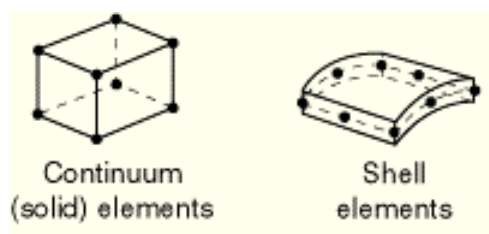


Figure 7.9 Schematic illustration of difference between solid element and shell element

7.2.2 Friction modelling with Slot+Align connectors

To simplify the interaction behaviour from the previous model where the friction was used, is it important to know that friction in ABAQUS is modelled as large number of springs. By using defined springs, the amount of springs can be customized, and therefore also the amount of calculations required in the analysis. The connector type “Slot” (Figure 7.10) in ABAQUS is a connector behaviour with a user-defined behaviour in tangential direction along the interaction and a lock in the normal directions.

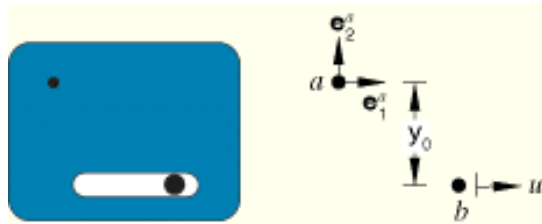


Figure 7.10 Schematic figure of the Slot connector behaviour (ABAQUS manual)

By using the rotational command align with the slot command a connection between two nodes that aligns their local directions is provided. (Figure 7.11)

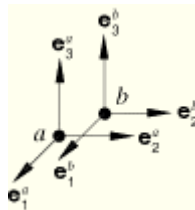


Figure 7.11 Schematic figure of the Align connector behaviour (ABAQUS manual)

By using a numerous (in this case 20 connectors on each side) of “slot+align” connectors along the interaction between the boards, the friction behaviour can be modelled (Figure 7.12).

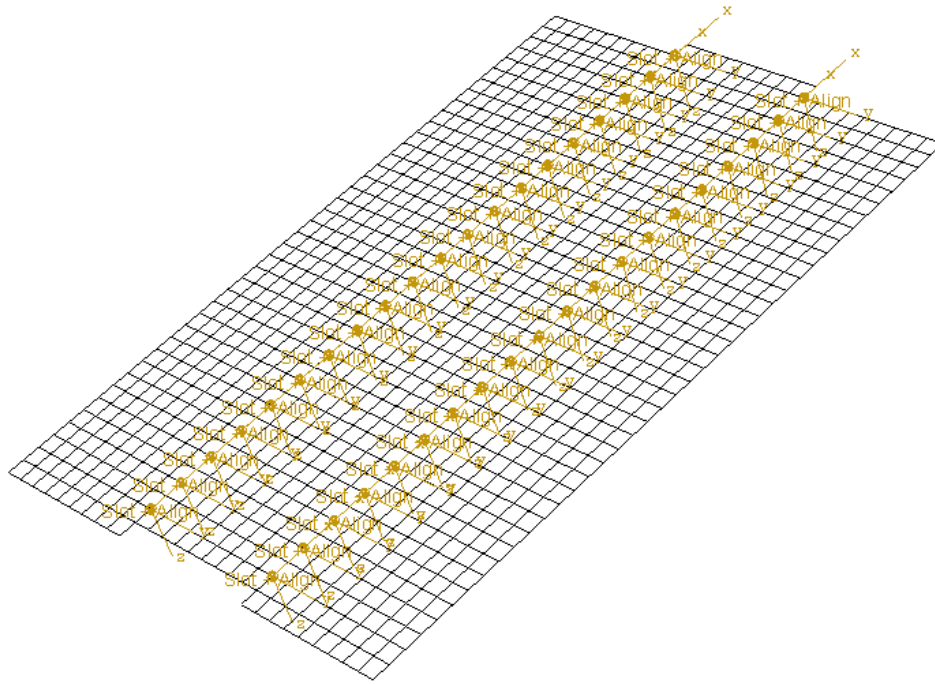


Figure 7.12 The panel with all the “slot+align” connectors along the interaction between the boards

The spring force has to correspond to a value for a specified friction constant with a specified normal force. The stiffness of the springs needs to correspond to the load-displacement values from the laboratory tests (Chapter 5.3). The load-displacement values was translated into spring stiffness, and in Table 7.4 and 7.5 values for original size (0,78 m), unit length (1m) and total wall length (2,4m) for the interaction used in modelling are shown. From these spring parameters the maximum elongations of the springs are calculated for two different maximum capacities. Chosen capacities of 2000 and 3000 Newton is selected to compare with values from the test with wallpaper shown on Table 7.7 and 7.8. The maximum capacity has to be divided equally on the number of “slot+align” connectors.

Table 7.4 Values used for “slot+align” connectors in simplified simulation of laboratory test at 0,28 mm elongation of the connector springs

Board length	Spring stiffness [kN/mm]	Max capacity [kN]
0,78 m	7,2	2,0
1,0 m	9,2	2,6
2,4 m	22,2	6,2

Table 7.5 Values used for “slot+align” connectors in simplified simulation of laboratory test at 0,42 mm elongation of the connector springs

Board length	Spring stiffness [kN/mm]	Max capacity [kN]
0,78 m	7,2	3,0
1,0 m	9,2	3,8
2,4 m	22,2	9,2

The linear values used before reaching maximum load for the “slot+align” connector in the models can be seen in Table 7.4 and Table 7.5 together with the maximum load. The behaviour is bilinear and the working curve for the “slot+align” connectors used can be seen schematically in Figure 7.13.

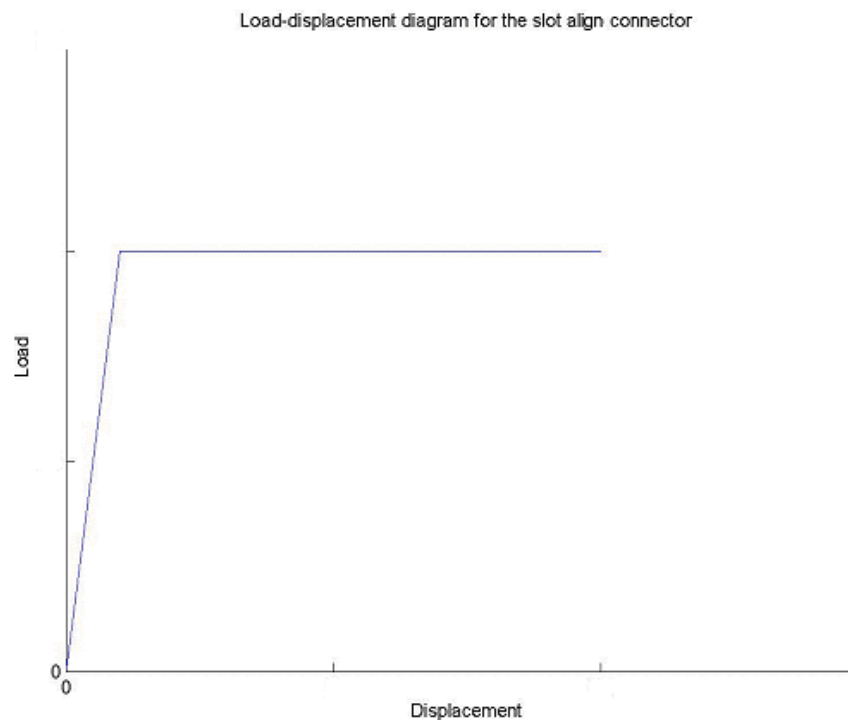


Figure 7.13 Load-displacement curve for slot align connectors. Dashed lines marks maximum capacities

7.2.3 Load and Boundary Conditions

The panels' boundary conditions are the same as the model with solid 3D elements (Chapter 7.1), it is locked for displacement in the bottom of board 1 and 3. Compared to the model with friction interaction no normal force has to be added because the behaviour in the spring between the t&g boards corresponds to the behaviour of a simulated normal force. Load applied on the top of board 2 is a displacement load of 10 mm.

7.2.4 Results from ABAQUS simulation

The result shows resultant forces in the upper nodes of the second board (Table 7.6). By comparing these results with the results from the model with solid homogenous 3D elements in Table 7.3 the simplification of the model can be accepted. The result was exactly the same for both isotropic and anisotropic values for the timber and therefore isotropic values are used in further studies.

Table 7.6 Results from ABAQUS simulation of laboratory model with 3D shell elements and “slot+align” connectors [N]

Friction coefficient	Clamp load 1 kN	Clamp load 10 kN	Clamp load 20 kN
0,1	99,9962	999,996	2000
0,3	299,996	3000	6000
0,5	499,996	5000	10000

7.3 Panel with wallpaper added

When modelling the effect that occurs when wallpaper is attached to the panel, the spring constant in slot align the “slot+align” connectors has to be modified. The behaviour of the spring has to correspond to the behaviour shown in Chapter 5.8 with the behaviour of the panel with wallpaper attached to the panel. The “slot+align” connectors were modelled to correspond to the behaviour of a panel with wallpaper with capacity of 2 kN and 3 kN, compared with laboratory test of panel number 5-8. Loads and boundary conditions are kept as in model without wallpaper.

Table 7.7 Values used for “slot+align” connectors in simplified simulation of laboratory test at 0,77 mm elongation of the connector springs

Board length	Spring stiffness [kN/mm]	Max capacity [kN]
0,78 m	2,6	2,0
1,0 m	3,3	2,6
2,4 m	8,0	6,2

Table 7.8 Values used for “slot+align” connectors in simplified simulation of laboratory test at 1,16 mm elongation of the connector springs

Board length	Spring stiffness [kN/mm]	Max capacity [kN]
0,78 m	7,2	3,0
1,0 m	9,2	3,8
2,4 m	22,2	9,2

7.3.1 Results from wallpaper simulation

The results from this study have to be investigated from two points of view, both the capacity and the stiffness behaviour have to be correct. The result from the test with max capacity of 2 and 3 kN corresponds exactly to the resultant force from all the nodes on the top of the second board. The strain behaviour for the test with 2000 kN is shown in Figure 7.14 corresponds well to the schematic behaviour shown in Figure 7.13. Figure 7.14 shows the nodal forces for the top nodes on the mid board. The maximum elongation of a connector according to Table 7.7 is 0,772 mm and in the value according to the Figure 7.14 is about 0,8. The small difference can be explained with some deformations in the board material. The model is considered accurate enough to continue with full-sized models.

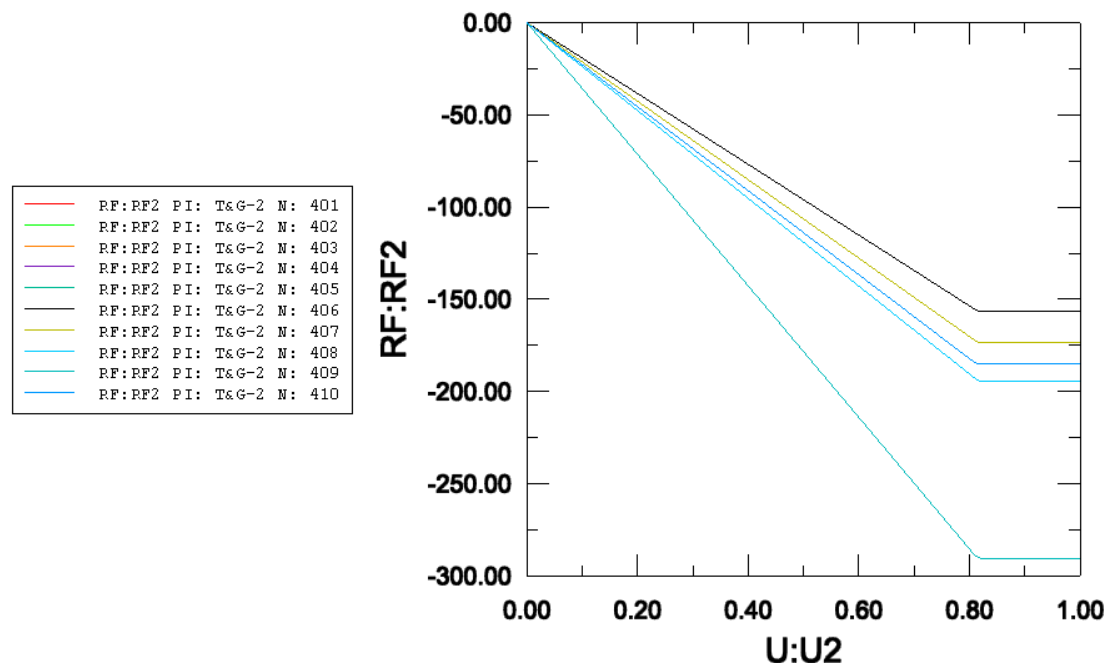


Figure 7.14 Displacement of the top nodes of the mid board with wallpaper. Results for each node plotted separately for a maximum load capacity of 2000N

7.4 Shear wall with plywood

The final aim for this thesis is to model a shear wall with t&g and with configuration according to tests standard EN594. The first step in the developing process of this model is to create a shear wall with plywood as the wood-based panel material. The configuration of this model was according to EN594, see Figure 7.15 and the loading according to Figure 7.16.

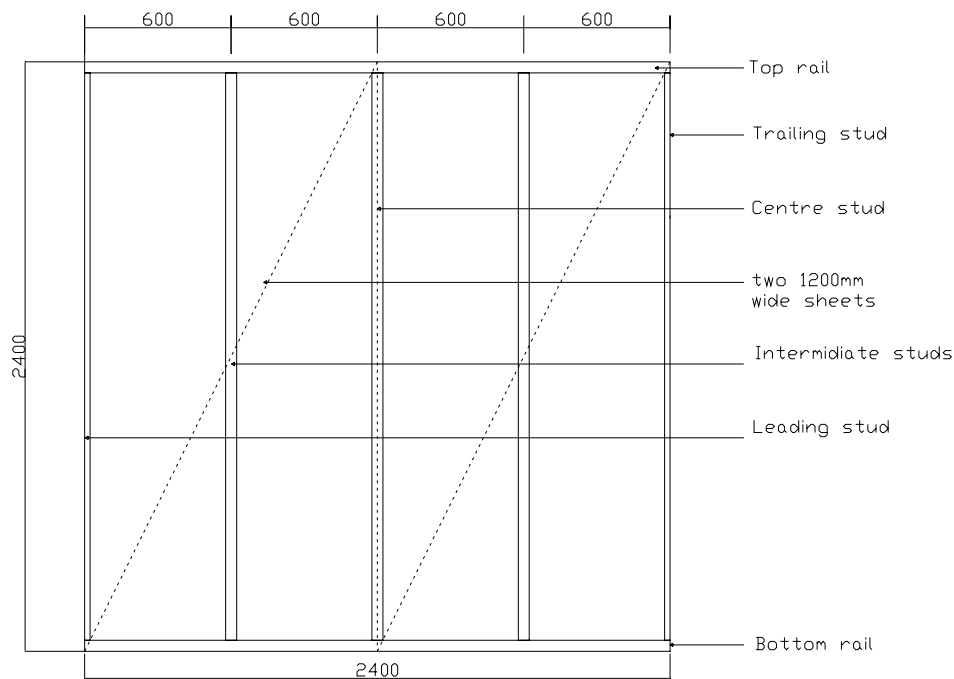


Figure 7.15 Configuration of test panel with plywood

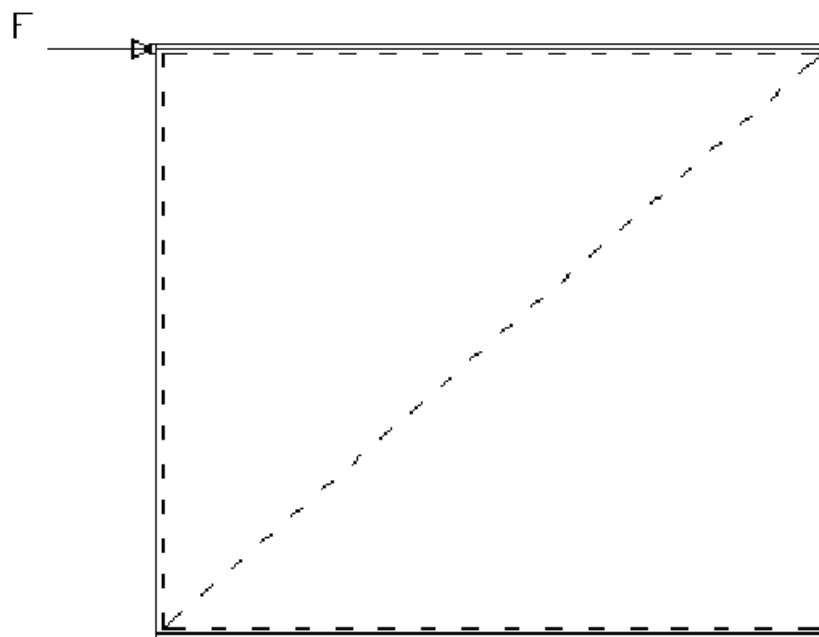


Figure 7.16 Load configuration of test panel with plywood

7.4.1 Frame

The timber frame structure is modeled with 3D beam element of the type B31. A section representing the cross section of a 95x45 mm stud was assigned to the beam. The beams are assumed to be isotropic linear elastic with a E-modulus of 9 GPa and a shear modulus of 3,3 GPa (Poisson ration 0,35). The beam members is created in the ABAQUS part module with a total length of 2.4 m and then divided into 16 elements each 150 mm long. The five vertical members are hinged to the top and the bottom rails with the connector type JOIN. The JOIN connector unites the position of the two connected nodes in the X,Y,Z-directions but allows free rotation in all three directions. This choice of connector allows comparison with the theoretical model for hand-calculation described in Chapter 3.1 but neglects the small contributions of stiffness that can be found in actual nailed-timber joints.

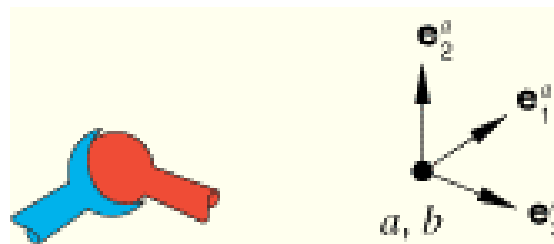


Figure 7.17 Principal behavior of JOIN connector, (ABAQUS Manual)

7.4.2 Plywood sheathing

The plywood sheathing is modeled with solid homogenous 3D elements type C3D8R, of the size 150x150x8 mm. The material is modeled as an isotropic material with an E-modulus of 6,41 GPa and a shear modulus of 592 MPa (Källsner, 1984).

7.4.3 Nails

The nails connecting the plywood sheathing is modeled by the connector type cartesian in ABAQUS. The cartesian connector type represents a 3 dimensional spring element. In order to get the connector to work in a correct way, it needed to be combined with the previously used rotational option Align. The spring stiffness of the Cartesian connectors was chosen to according to the Table 7.9. The values were obtained from Källsner (1984).

Table 7.9 Connector stiffness used for cartesian connector

Direction	X-direction	Y-direction	Z-direction
K-stiffness [N/m]	500000	500000	500000

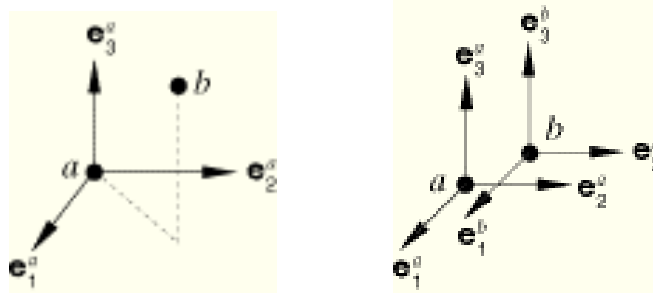


Figure 7.18 Principal behaviour of Cartesian connector, right figure with Align, (ABAQUS Manual)

7.4.4 Boundary conditions

The bottom rail is fully fixed along its full length according to EN594. The top rail is prevented from displacement in the out of plane direction in order to secure stability. As described above the frame members are hinged together and separation is prevented.

7.4.5 Load acting on shear wall

A racking load is applied in the top right corner and has a magnitude of 12 kN. This load was chosen after studying laboratory results obtained by Källsner (1984) studying different shear walls.

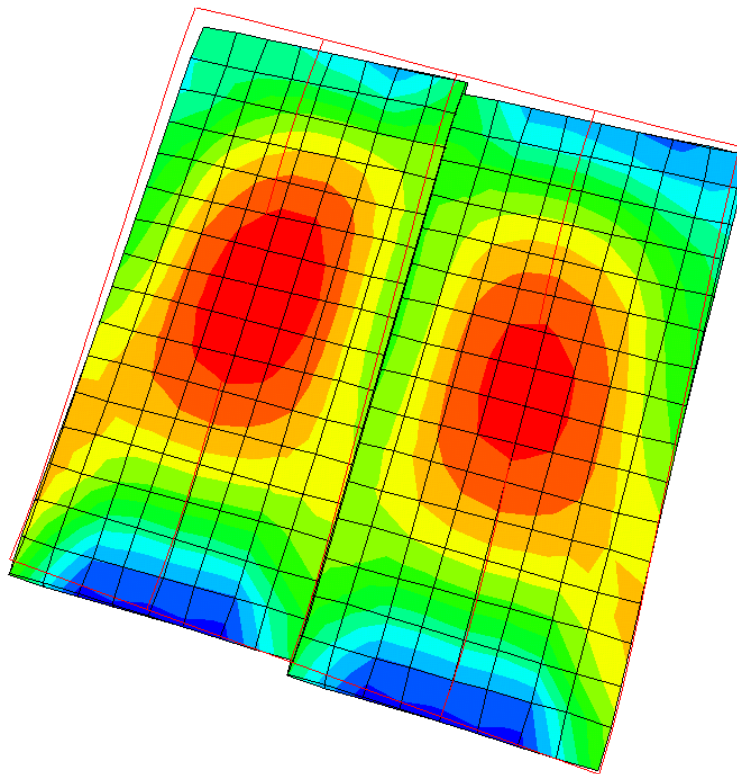


Figure 7.19 Principal stresses and deformations in shear wall with plywood loaded with racking load

7.4.6 Results

After the FE analysis the values of the horizontal displacement can be seen in the report file created by ABAQUS, see Table 7.10. The marked cell in the bottom left corner represents the displacement of the loaded corner in meters and was used to calibrate the model.

Table 7.10 Displacements of top rail of the shear wall with plywood [m] The loaded corner is in node no. 17 and the opposite corner is node no. 1. The nodes are evenly distributed over the top rail with a spacing of 150 mm

Node no.	Displacement
1	9,0656E-03
2	9,07015E-03
3	9,07663E-03
4	9,08476E-03
5	9,09485E-03
6	9,10745E-03
7	9,12206E-03
8	9,13837E-03
9	9,15676E-03
10	9,18371E-03
11	9,2126E-03
12	9,24314E-03
13	9,2757E-03
14	9,31084E-03
15	9,3481E-03
16	9,38719E-03
17	9,42851E-03

7.4.7 Verification of model

To verify the FE model of the shear wall described in the previous chapter a hand-calculation of the displacement of the loaded top corner of the frame has been performed according to the method recommended by Källsner (1984), also described in Chapter 3.2 The hand-calculation model is designed to work for a single shear panel according to Figure 3.4. To use the hand-calculation model the racking force of 12 kN applied in the ABAQUS model above was divided in two equal loads of 6 kN.

The displacement of the loaded top corner is calculated according to:

$$u_{frame} = (1/k)Hh^2 \left[\left(1 / \sum_{i=1}^n x_i'^2 \right) + \left(1 / \sum_{i=1}^n y_i'^2 \right) \right] + \gamma_s h \quad (7.1)$$

Where the different parameters are:

Table 7.11 Shear wall parameters for hand-calculation

k	500000	Slip modulus of nail	N/m
H	12000/2	External Force at top corner	N
b	1,2	Width of panel	m
t	0,008	Thickness of panel	m
h	2,4	Height of the panel	m
$\sum x_i'^2$	13,5	Sum of square distance fastener X-direction	m ²
$\sum y_i'^2$	44,82	Sum of square distance fastener Y-direction	m ²

$$\gamma = \frac{H}{G_{mod} \times b \times t} = \frac{6000}{592E9 \times 1,2 \times 0,008} = 0,0691 \quad (7.2)$$

$$u_{frame} = \frac{1}{500000} \times 6000 \times 2,4^2 \times \left(\frac{1}{44,82} + \frac{1}{13,5} \right) + 0,0691 \times 2,4 \quad (7.3)$$

$$u_{frame} = 0,0094m \quad (7.4)$$

The FE model is considered accurate enough. The difference is less than 1% and therefore no further investigation of this model is considered.

7.5 Modelling of full scale shear wall with t&g

In this Chapter the final ABAQUS model will be presented. A 2,4x2,4 metre shear wall with t&g boards attached to a frame structure with elastic nails.

7.5.1 Frame

In this model the same frame as in Chapter 7.4 will be used. The same material properties with $E = 9 \text{ GPa}$ and $G = 3,3 \text{ GPa}$ will also be used. The element size will however be change to a size of 44 mm resulting in 55 elements per stud and rail.

7.5.2 T&g sheathing

The t&g boards were modeled with solid homogenous 3D elements type C3D8R, of the size 44x44x22 mm. Each board was modeled with 110 elements and 27 horizontal boards built up the wall. The material properties of the t&g boars was assumed to be linear elastic with the E modulus of 9 GPa and a shear modulus of 3,3 GPa. The configuration of the wall can be seen in the Figure 7.20.

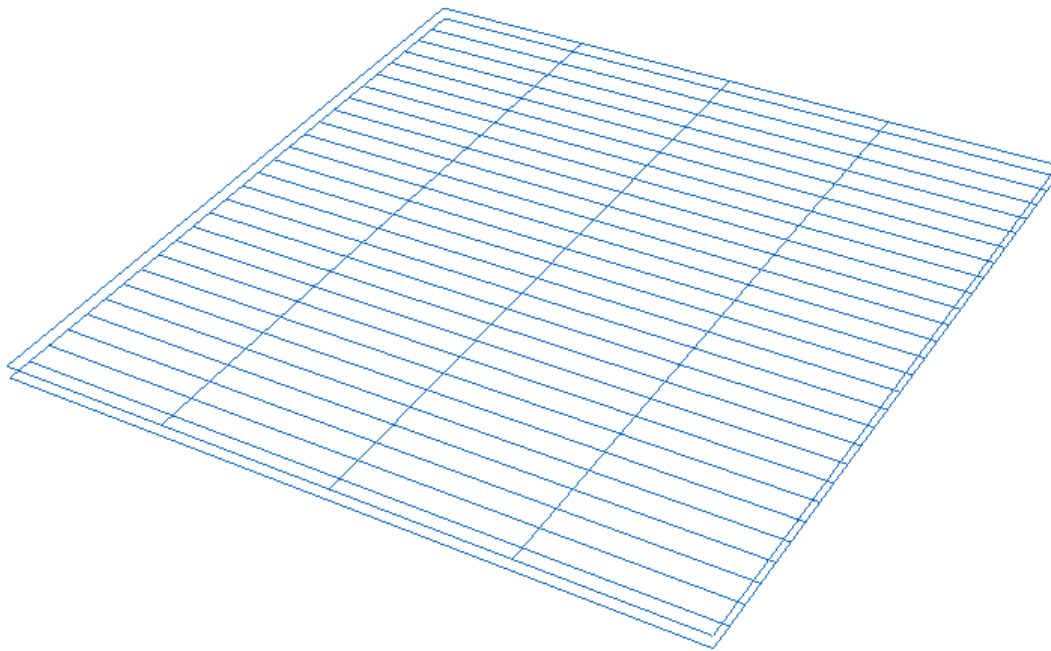


Figure 7.20 ABAQUS model of wall with t&g

7.5.3 Nails

The nails connecting the frame and the t&g boards were model in the same way as the in Chapter 7.4. Each board was attached to the frame according to Figure 7.21. The elastic properties for the Cartesian connectors can be seen in Table 7.9.

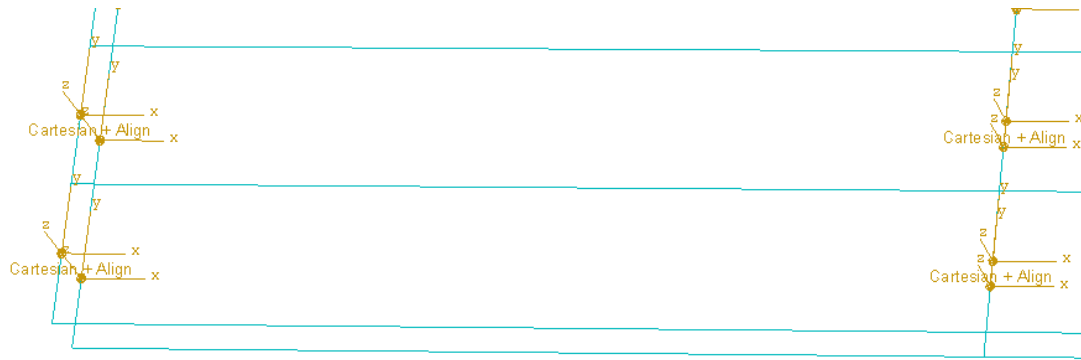


Figure 7.21 Positioning of Cartesian connector representing the nails connecting the t&g boards to frame

7.5.4 Interaction properties

The interacting friction between the t&g boards has been modelled according to the method described in Chapter 7.2. The connector type “slot connector” has been used in combination with the rotational connector option “align” to model the friction.

Each board was assigned with 15 slot align connectors on each side according to Figure 7.22. The “slot+align” connectors was distributed evenly over the board length in order to get a shear force transformation over the whole length. How the friction that was calculated from the laboratory tests was translated to a spring constant can be seen in Chapter 5.3. The linear values used before reaching maximum load for the “slot+align” connector in the models can be seen in Table 7.12 and the maximum load can be seen in the Table 7.13.

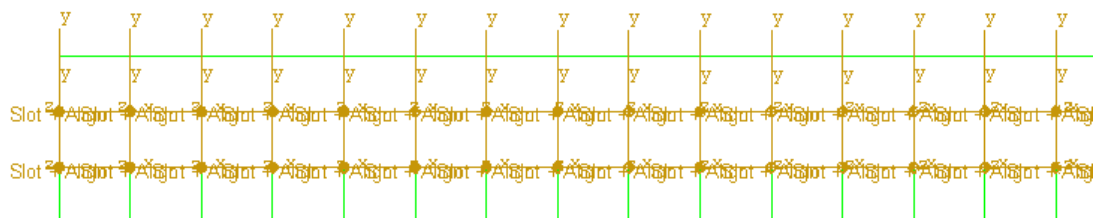


Figure 7.22 Distribution of the “slot+align” connectors over the 2,4 m t&g boards

12 load cases have been used to investigate the behaviour of the wall. The choice of load levels is made with background of Chapter 4. The three load cases used represents a vertical load on the t&g panel of 500N/m, 1000N/m and 3000N/m. Note that these loads are not the total vertical load on the wall seen in Figure 4.8.

Table 7.12 Spring constants [kN/mm] used for slot+ align connectors

Clamp load [N]	MC. 14,85%	MC. 11,25%	MC. 9,76%	Wallpaper
4x50 / 40cm	22,1	22,1	22,1	
4x100 / 40cm	22,1	22,1	22,1	8,0
4x300 / 40cm	22,1	22,1	22,1	8,0

Table 7.13 Maximum friction load [N] on a 2400 mm board

Clamp load [N]	MC. 14,85%	MC. 11,25%	MC. 9,76%	Wallpaper
4x50 / 40cm	696	492	564	
4x100 / 40cm	924	528	408	12660
4x300 / 40cm	3240	2016	1584	17310

Table 7.14 Maximum load [N] on each connector

Clamp load [N]	MC. 14,85%	MC. 11,25%	MC. 9,76%	Wallpaper
4x50 / 40cm	46,40	32,80	37,60	
4x100 / 40cm	61,60	35,20	27,20	844,00
4x300 / 40cm	216,00	134,40	105,60	1154,00

Table 7.15 Elongation of each connector [mm] at maximum load

Clamp load [N]	MC. 14,85%	MC. 11,25%	MC. 9,76%	Wallpaper
4x50 / 40cm	0,031	0,022	0,025	
4x100 / 40cm	0,042	0,024	0,018	1,589
4x300 / 40cm	0,146	0,091	0,072	2,173

7.5.5 Boundary conditions and loads

The same loads and boundaries as in Chapter 7.4 were used in this model. The reason for using the same boundaries and loads is that the values from this model with t&g will be compared in the evaluation with the results from the model with plywood. The racking load on the panel was chosen to a displacement of the top corner of 9,4 mm. The reason for this choice of load is that the results will be comparable to the results from Chapter 7.4. The bottom rail was fixed in all direction assuming sufficient anchorage and the top rail was fixed in the normal direction to secure stability.

7.5.6 Results from ABAQUS

Table 7.16 Obtained racking load [N] of panel with 9,4 mm displacement

Vertical load on 2,4 m t&g [N]	MC. 14,85%	MC. 11,25%	MC. 9,76%	Wallpaper
1200	696	492	564	
2400	924	528	408	2513
7200	3240	2016	1584	2513

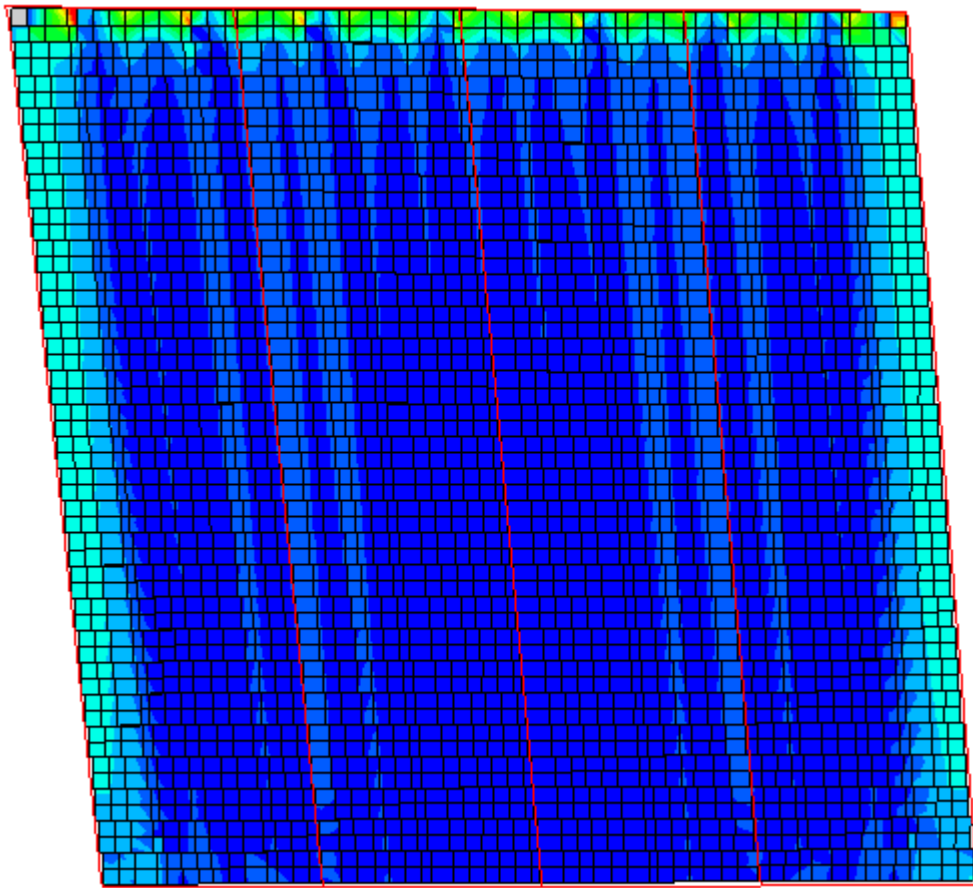


Figure 7.23 Principal stresses in shear wall with t&g boards and wallpaper 9.4 mm horizontal displacement of left frame corner

7.5.7 Evaluation

The result (Table 7.16) from the ABAQUS model corresponds very well for the tests made for pure friction. However the vertical loads on the wall needs to be very high in order to obtain sufficient racking capacity of the wall in order to utilize it as a shear wall. Therefore the option to use pure friction is abandoned and the option to use wallpaper attached to the panel will be further studied. The difference between the models can be explained by the fact that the value for spring constant used in the slot+align connectors for panels with wallpaper is around 8000 N/mm compared with the one for pure friction that is around 22000 N/mm. The spring force in the connectors with wallpaper will not reach maximum due to the small displacement of the top corner. A small parametric study was made to investigate the effect of stiffer wallpaper that is stiffening the connectors but not increasing the ultimate strength.

7.5.8 Parametric study

As shown in Chapter 7.5 the full capacity of the attached wallpaper could not be used because of the small displacement. If a stiffer connection is used in the wall more of the wallpaper capacity can be used and the vertical load can be kept at lower levels.

In this parameter study the spring constant k of the connector is varied from 8000 N/mm to 25000 N/mm according to Table 7.17.

Table 7.17 Spring constants used for slot+ align connector [N/mm] and obtained racking loads [kN]

Spring constant [N/mm]	8000	16000	20000	25000
Racking load	2,5	4,5	5,3	6,2

To obtain verification of the values and of the way the wall works, a simplified hand-calculation can be made. The assumptions are made that the frame is totally rigid and assembled with hinges. The nails connecting the boards with the frame are assumed to be fixing the frame and the boards together in the horizontal direction but not in the vertical. The following expressions can then be established. The total racking force is the displacement multiplied by the “spring stiffness” of the connectors. The total elongation of all the connector is the same as the displacement of the top loaded corner of the frame. The maximum displacement of the top corner is the maximum displacement of 1 board multiplied by 26. If performing this on the values shown in Table 7.17 the values for displacement at maximum load in Table 7.18 is obtained.

Table 7.18 Maximum displacement of the top loaded frame corner [mm]

Spring constant [N/mm]	8000	16000	20000	25000
Displacement	41,1	20,6	16,5	13,2

The values for the racking load in Table 7.17 is based on a displacement of 9,4 mm. The amount of capacity used in the 4 cases can be calculated by dividing 9,4 mm with the maximum displacement, see results in Table 7.19.

Table 7.19 Utilisation factor [%] of the load capacity of wallpaper

Spring constant [N/mm]	8000	16000	20000	25000
Utilisation factor [%]	22,8	45,7	57,1	71,4

The utilisation factor times the ultimate capacity is the approximated racking load, see Table 7.20.

Table 7.20 Calculated racking load [kN]

Spring constant [N/mm]	8000	16000	20000	25000
Racking load	2,9	5,8	7,2	9,0

7.5.8.1 Evaluation of parametric study

The parametric study shows that it might be possible to obtain a racing load equal or higher than for a wall with plywood if the stiffness of the panel is increased. It can also be seen that if the stiffness of the panel is increased a larger deformation occurs in the nails instead of the panel.

8 Conclusion

The interaction behaviour between the t&g boards was studied in the laboratory to investigate if the friction can be assumed as a contribute to the shear capacity of a panel of t&g boards. The conclusion that can be made from the laboratory tests is that the boards show a very similar response to a homogenous timber-based panel material if the clamping force is large enough to secure friction behaviour. The clamping force is required to be the shear force divided with the friction coefficient to secure that the boards act as a homogenous panel and transferring shear force.

It was interesting to observe that the configuration of the wall had an effect on the magnitude of the vertical load transfer in the wall. If timber with high modulus of elasticity was used in the t&g boards, which is common, and timber with low modulus of elasticity was used in the studs, almost 1/6 of the vertical load was transferred by the t&g boards. If the timber used in the t&g and the studs was of same quality or if the t&g was of a lower stiffness than the studs, a very small part of the vertical load was transferred by the t&g boards. This resulted in negligible shear strength. If future work in the field of t&g shear walls is to be performed, an area that needs to be tested more carefully is the vertical load transfer.

A very clear, but unexpected result was discovered in the tests investigating the effects on friction between the boards with a varying moisture content in the boards. An introductory literature studies recommended a lower friction constant for wet timber than for dried timber but the tests performed in this study showed the opposite results. A clear tendency could be shown as the moisture content was decreasing in the boards so was the friction between the boards. Attempts to produce explanations for this effect and why it differs from the literature were made. More precise figures and values of the size of the moisture dependent friction can be found in the thesis.

Some of the most valuable results in this thesis are the results from the panels tested with wallpaper attached to the t&g panel. At relatively low clamping forces the wallpaper produces a clear increase of the shear capacity of the panel. Results show that this increase could be seen as almost independent of the clamping load on the panel. However, the results are dependent on the interaction between the boards and the wallpaper. Only one test series of 4 panels was made in this thesis and the conclusions are not secured. The result values only represent a likely behaviour for the tested models. The area of t&g boards in interaction with wallpaper or other fabrics is highly recommended for further studies.

The modelling part of this thesis was performed using the commercial FE program ABAQUS. This program was chosen for its relatively user-friendly interface. The first model in ABAQUS was created to obtain as good agreement as possible with laboratory tests. In this model the choice of predefined friction in ABAQUS was used and the results was very close to the hand-calculated reference values. A disadvantage with this method to model friction was that it required very long computational time. The friction with user-defined springs was introduced to the model and a major reduction could be made in computational time. It is therefore recommended for future work to model the friction between t&g boards using defined springs.

The effect of isotropic and anisotropic material values was investigated when studying the frictional behaviour. It was concluded that no visible effects could be seen on the frictional behaviour if isotropic material data was used instead of the anisotropic. A small decrease of computational time could be noticed if the option with isotropic material data was used. A note shall be made that the material data will have large effect on the normal force in the t&g boards as described earlier.

In the final model the racking resistance of a 2,4 x 2,4 m wall was investigated. The results showed that for tested magnitudes of the vertical load on the wall the racking values as a result of pure friction was very small compared to a wall with plywood. Therefore the recommendation that can be made from these tests is that additional shear resistance needed to be added. From the results of the tested wall with wallpaper attached, the racking load was also very small compared to tests with plywood. The reason for this was that the stiffness of the wallpaper connection was too low. Only a small part of the capacity was utilized before reaching the predefined displacement. The conclusion is therefore that a stiffer wallpaper or fabric needs to be used. A small parametric study was made to see how stiff the connection must be to reach the same capacity as for plywood panel. The result showed approximately three times the wallpaper connector stiffness or the same as the connections for pure friction will be needed.

A final remark is that if a stiff and cheap fabric can be found, t&g panels can replace plywood and other wood-based panel materials. The cost of t&g boards has a square metre cost of about 1/3 of plywood. A problem that needs to be solved is the fire resistance of the t&g boards. If a fire resistant fabric is attached to the wall no additional gypsum needs to be added and the costs could be reduced further.

9 References

- Anon. 1992 Tongued-and-grooved boards. Dimensions SIS 232813
- Anon. 1995, Timber structures – Test methods – Racking Strength and stiffness of timber frame panels, (EN 594) CEN/TC 124 Brussels
- Anon. 2003, Träkonstruktioner - konstruktions virke – hållfasthetsklasser ,(Timber Construction – Construction timber - design classes) EN 338 SIS förlag AB Stockholm Sweden
- Anon. 2004, Eurocode 5, Design of timber structures, (EN 1995-1-1:2004)
- Anon. 2004 SMHI 2004 webpage www.smhi.se
- Baumberger T. 1996 Physics of sliding friction, Dordrecht 1996
- Engström B 1994 Beräkning av betong och murverkskonstruktioner (Design in concrete, in Swedish) Göteborg 2001
- Grahn R., Jansson P. 1997 Mekanik Statik och Dynamik (Mechanics, Static and dynamics) Lund, Sweden, 1997
- Hoffmeyer P. ,1995 Step lecture A4-Timber engineering Step 1, First edition Centrum Hout the Netherlands 1995.
- Johannesson, B 1979. Skjuvprovning av trä och plywood (Tests in shear of timber and plywood) Publ S 79:2, Dept of Structural Engineering Chalmers University of Technology Göteborg Sweden (in Swedish)
- Johannesson B and Johansson G 1979. Tuve landslide 1977. Investigation of damage propensity of frames in single family houses (In Swedish) Byggforskningen R137:1979 BFR Stockholm Sverige
- Kliger R, Perstorper M, Johansson G. 1997. Bending properties of Norway spruce timber. Comparison between fast- and slow-grown stands and influence of radial position of sawn timber. Ann. Sci. For. 55 (1998) 349-358 Paris
- Källsner B. 1984 Skivor som vindstabiliserande element vid träregelväggar (Panels as Wind-Bracing Elements in Timber-framed Walls Wood tecnology report no. 56
- Nordling C. Österman J. 1999 Physics Handbook for science and engineering. Studentlitteratur, 6th edition, Lund, Sweden,1999
- Ormarsson, S. 1999, Nummerical Analysis of Moisture-Related Distortions in Sawn Timber Publ 99:7 Department of Structural Mechanics Chalmers Univerity of Technology, Göteborg, Sweden
- Polverini E. 2000, Finite Element Analysis of the Racking Resistens of Timber Shear Walls Publ. 00:1 Department of Structural Engineering Chalmers university of technology, Göteborg, Sverige

von Platen, F. 2004. Mer trä i byggandet – Underlag för en nationell strategi att främja användningen av trä i byggandet. (More timber in the construction process – A national strategy to promote the use of timber in the construction process) Regeringskansliet Näringsdepartementet (Swedish ministry of industry, employment and communications) Rapport Ds 2004:1. (In Swedish)

10 Appendix A - Diagrams and Values from laboratory

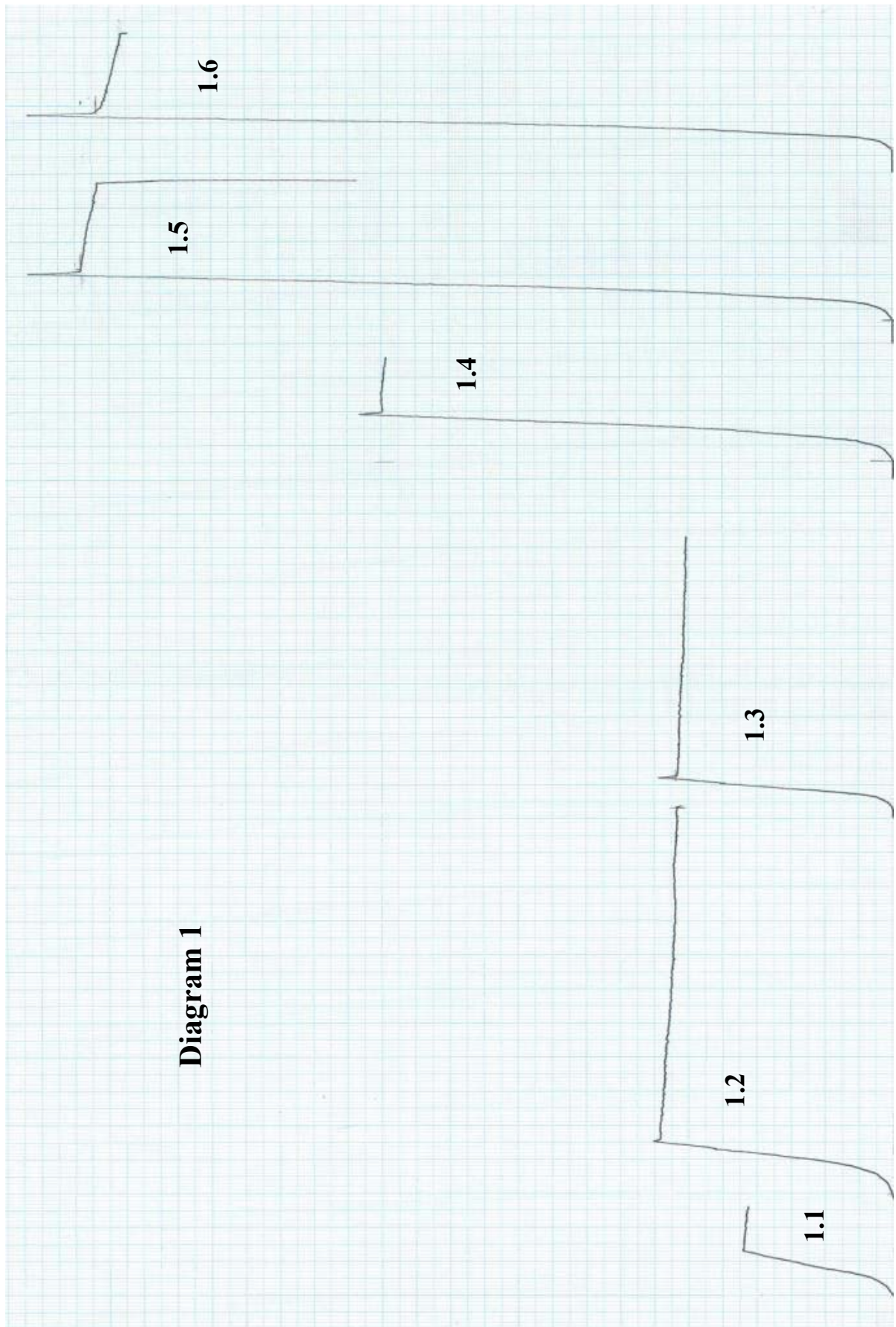
Notes for Appendix A

The produced moisture contents are the mean values for the test series.

The standard loading rate in the tests are 0,3mm/min. For tests with other loading rate is defined separately in the appendix.

X-axis in diagrams is the displacement. The scale factor is 2,5 mm = 20 cm in original size, where each square in the diagram represents 1 cm².

Y-axis in diagrams is the load. The scale factor is 1 kN = 25 cm in original size, where each square in the diagram represents 1 cm².



1.1

		Weight (g)
Board	16	336,2
Board	18	372,4
Board	21	349,7

Moisture Content (%): 14,85

Horsontal Load (N): 200

Max Vertical Load, Vmax (N): 180

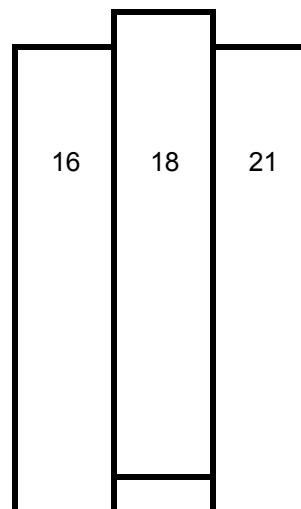
Static Friction Coefficient (μ): 0,45

Displacement at Vmax, d (mm): 0,1625

Load rate (mm/min): 0,3

Previously loaded (digram number): none

Remarks: none



1.2

		Weight (g)
Board	16	336,2
Board	18	372,4
Board	21	349,7

Moisture Content (%): 14,85

Horsontal Load (N): 400

Max Vertical Load, Vmax (N): 280

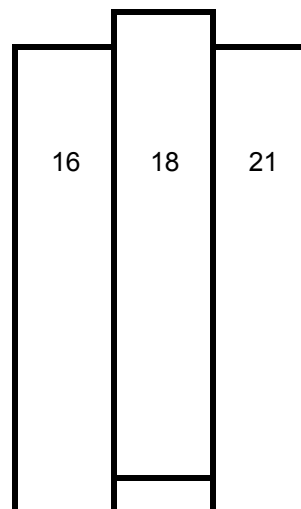
Static Friction Coefficient (μ): 0,35

Displacement at Vmax, d (mm): 0,2

Load rate (mm/min): 0,3

Previously loaded (digram number): 1.1

Remarks: none



1.3

		Weight (g)
Board	16	336,2
Board	18	372,4
Board	21	349,7

Moisture Content (%): 14,85

Horsontal Load (N): 400

Max Vertical Load, Vmax (N): 276

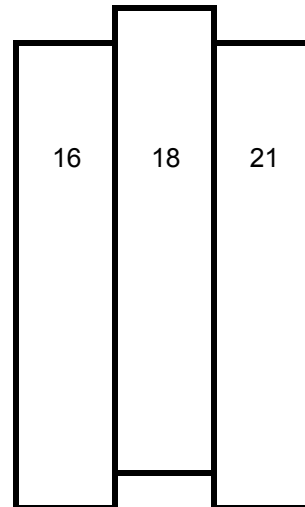
Static Friction Coefficient (μ): 0,345

Displacement at Vmax, d (mm): 0,125

Load rate (mm/min): 0,3

Previously loaded (digram number): 1.1, 1.2

Remarks: none



1.4

		Weight (g)
Board	16	336,2
Board	18	372,4
Board	21	349,7

Moisture Content (%): 14,85

Horsontal Load (N): 800

Max Vertical Load, Vmax (N): 624

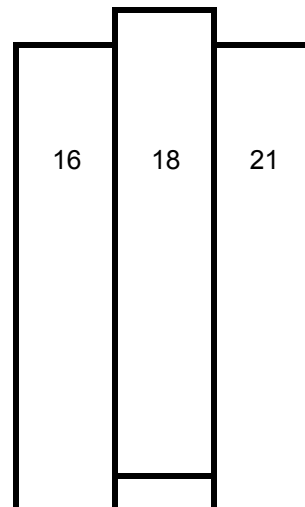
Static Friction Coefficient (μ): 0,39

Displacement at Vmax, d (mm): 0,1875

Load rate (mm/min): 0,3

Previously loaded (digram number): 1.1, 1.2, 1.3

Remarks: none



1.5

		Weight (g)
Board	16	336,2
Board	18	372,4
Board	21	349,7

Moisture Content (%): 14,85

Horsontal Load (N): 1200

Max Vertical Load, Vmax (N): 1008

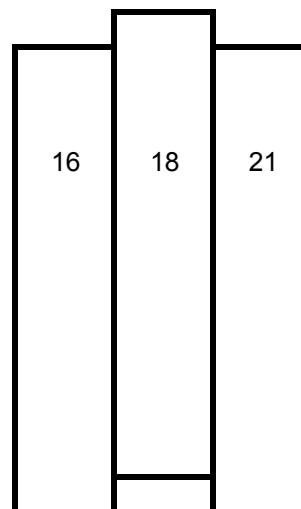
Static Friction Coefficient (μ): 0,42

Displacement at Vmax, d (mm): 0,175

Load rate (mm/min): 0,3

Previously loaded (digram number): 1.1, 1.2, 1.3, 1.4

Remarks: none

**1.6**

		Weight (g)
Board	16	336,2
Board	18	372,4
Board	21	349,7

Moisture Content (%): 14,85

Horsontal Load (N): 1200

Max Vertical Load, Vmax (N): 1008

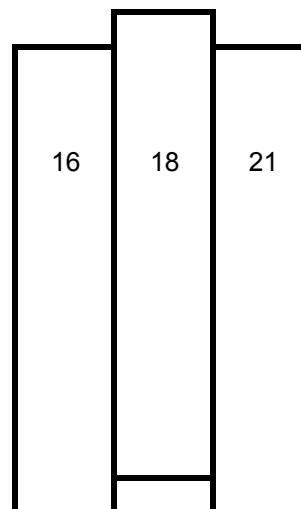
Static Friction Coefficient (μ): 0,42

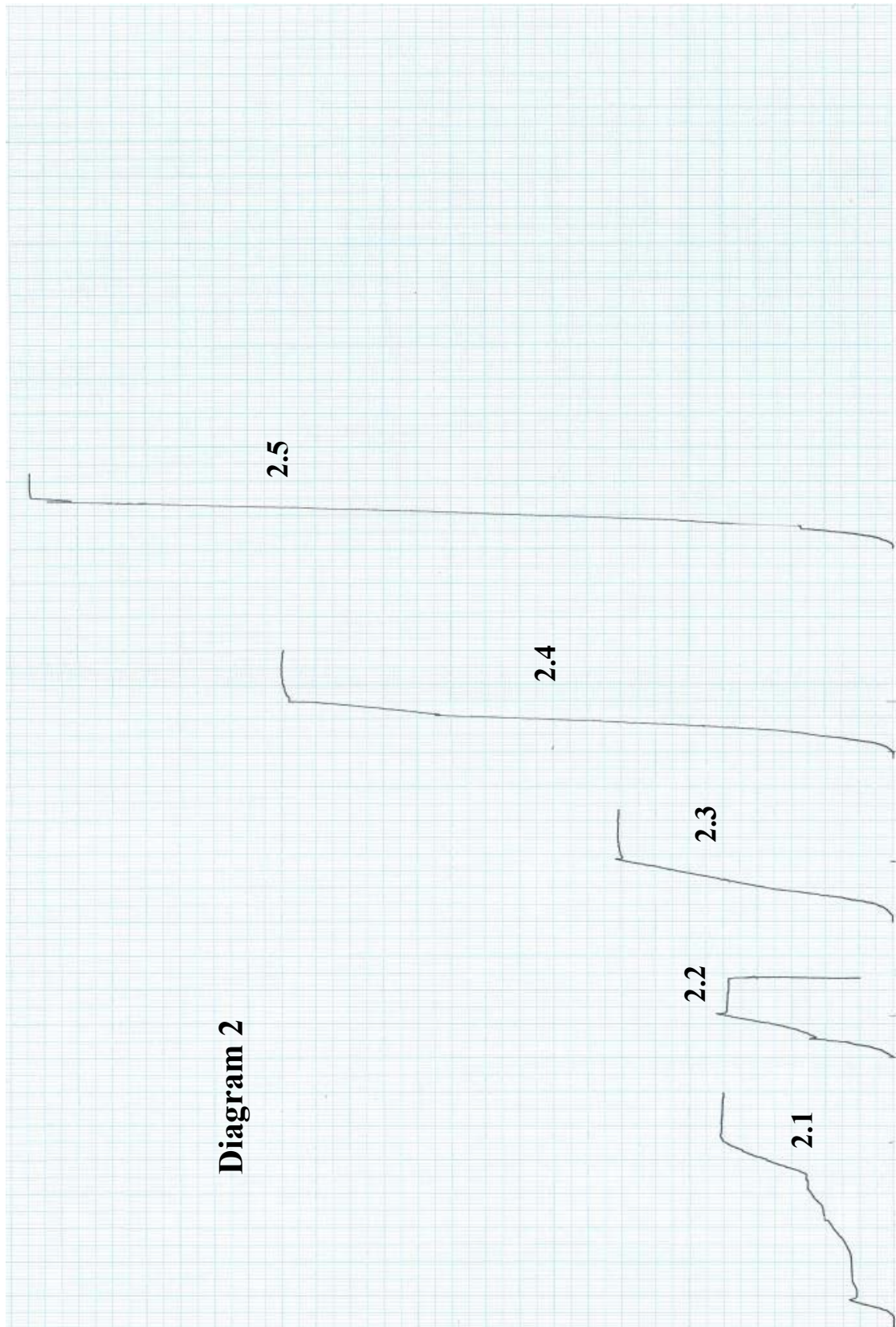
Displacement at Vmax, d (mm): 0,1375

Load rate (mm/min): 0,3

Previously loaded (digram number): 1.1, 1.2, 1.3, 1.4, 1.5

Remarks: none





2.1

		Weight (g)
Board	1	338,1
Board	25	351,5
Board	15	410,7

Moisture Content (%): 14,85

Horsontal Load (N): 200

Max Vertical Load, Vmax (N): 204

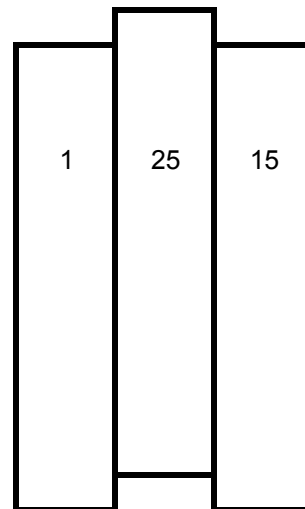
Static Friction Coefficient (μ): 0,51

Displacement at Vmax, d (mm): 0,625

Load rate (mm/min): 0,3

Previously loaded (digram number): none

Remarks: none



2.2

		Weight (g)
Board	1	338,1
Board	25	351,5
Board	15	410,7

Moisture Content (%): 14,85

Horsontal Load (N): 200

Max Vertical Load, Vmax (N): 208

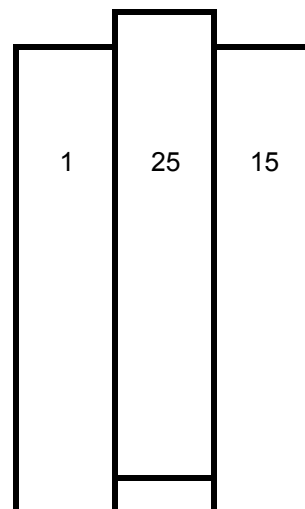
Static Friction Coefficient (μ): 0,52

Displacement at Vmax, d (mm): 0,15

Load rate (mm/min): 0,3

Previously loaded (digram number): 2.1

Remarks: none



2.3

		Weight (g)
Board	1	338,1
Board	25	351,5
Board	15	410,7

Moisture Content (%): 14,85

Horsontal Load (N): 400

Max Vertical Load, Vmax (N): 328

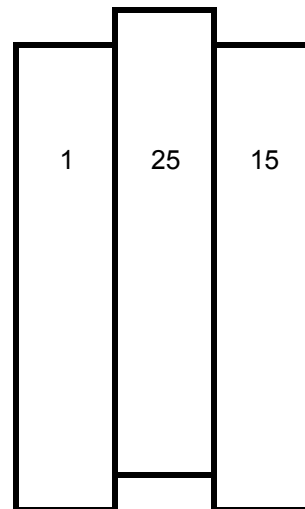
Static Friction Coefficient (μ): 0,41

Displacement at Vmax, d (mm): 0,2

Load rate (mm/min): 0,3

Previously loaded (digram number): 2.1, 2.2

Remarks: none



2.4

		Weight (g)
Board	1	338,1
Board	25	351,5
Board	15	410,7

Moisture Content (%): 14,85

Horsontal Load (N): 800

Max Vertical Load, Vmax (N): 708

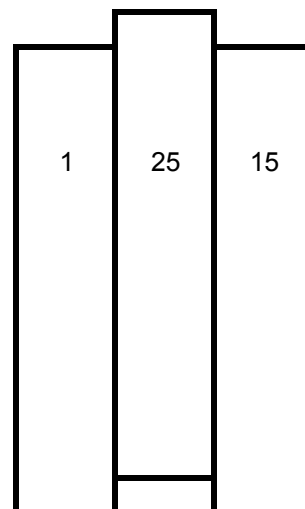
Static Friction Coefficient (μ): 0,4425

Displacement at Vmax, d (mm): 0,1875

Load rate (mm/min): 0,3

Previously loaded (digram number): 2.1, 2.2, 2.3

Remarks: none



2.5

		Weight (g)
Board	1	338,1
Board	25	351,5
Board	15	410,7

Moisture Content (%): 14,85

Horsontal Load (N): 1200

Max Vertical Load, Vmax (N): 1080

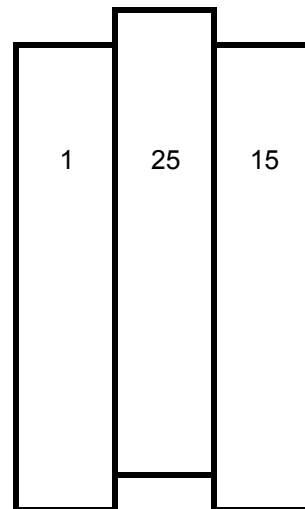
Static Friction Coefficient (μ): 0,45

Displacement at Vmax, d (mm): unknown

Load rate (mm/min): 0,3

Previously loaded (digram number): 2.1, 2.2, 2.3, 2.4

Remarks: none



2.6

		Weight (g)
Board	1	338,1
Board	25	351,5
Board	15	410,7

Moisture Content (%): 14,85

Horsontal Load (N): 1600

Max Vertical Load, Vmax (N): 1410

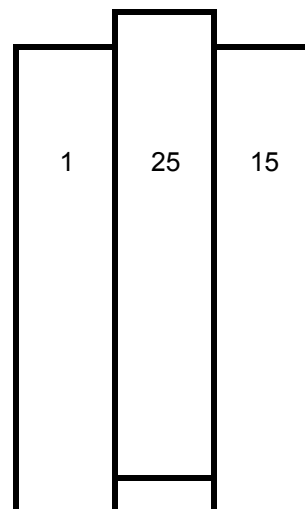
Static Friction Coefficient (μ): 0,440625

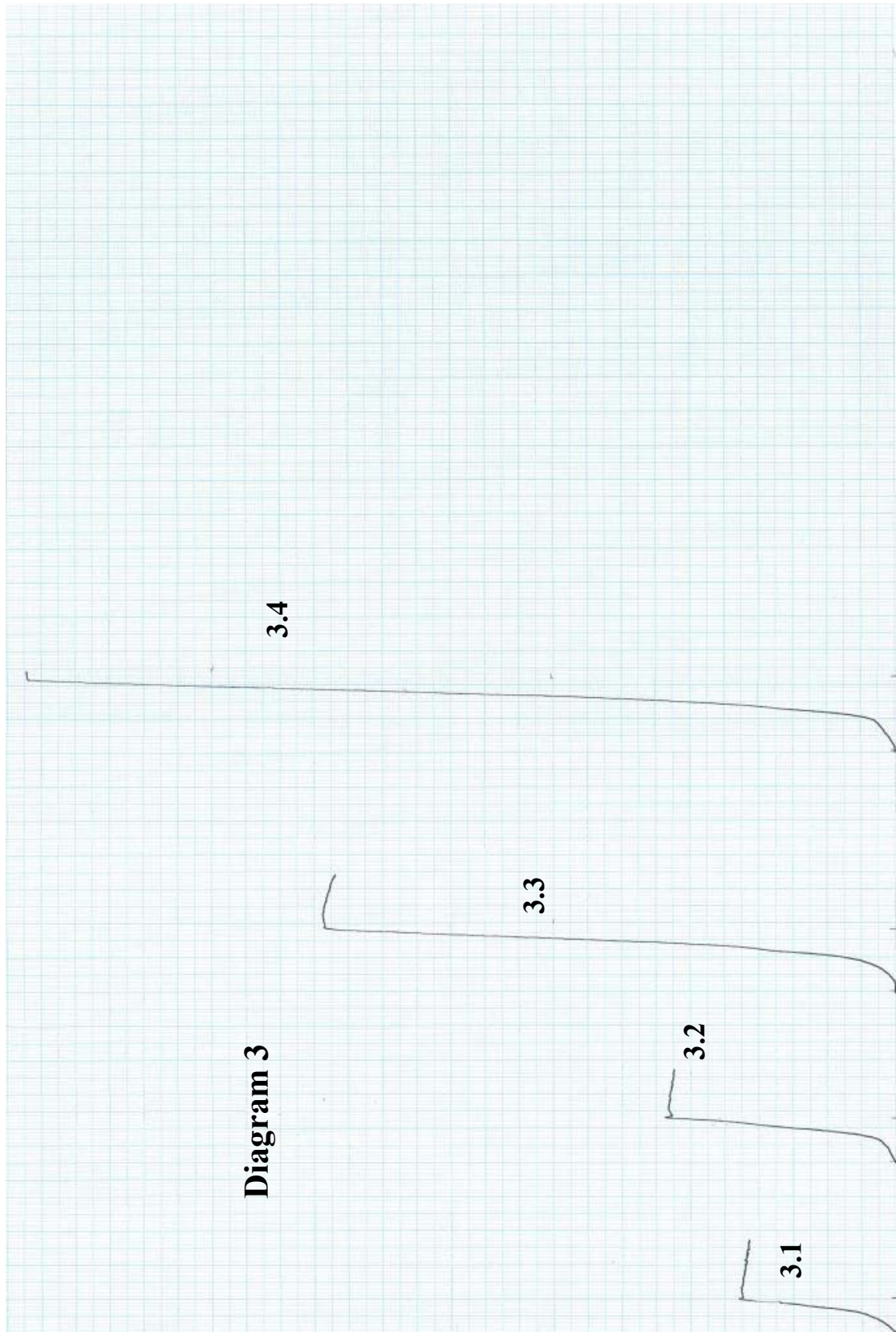
Displacement at Vmax, d (mm): unknown

Load rate (mm/min): 0,3

Previously loaded (digram number): 2.1, 2.2, 2.3, 2.4, 2.5

Remarks: none





3.1

		Weight (g)
Board	17	343,9
Board	24	405,7
Board	20	355

Moisture Content (%): 14,85

Horsontal Load (N): 200

Max Vertical Load, Vmax (N): 184

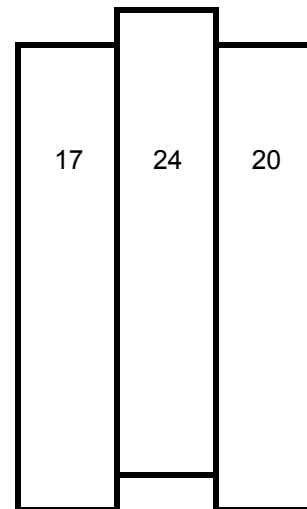
Static Friction Coefficient (μ): 0,46

Displacement at Vmax, d (mm): 0,125

Load rate (mm/min): 0,3

Previously loaded (digram number): none

Remarks: none



3.2

		Weight (g)
Board	17	343,9
Board	24	405,7
Board	20	355

Moisture Content (%): 14,85

Horsontal Load (N): 400

Max Vertical Load, Vmax (N): 268

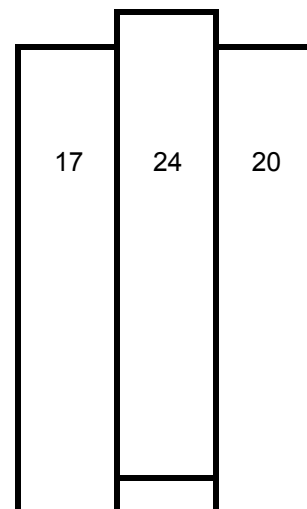
Static Friction Coefficient (μ): 0,335

Displacement at Vmax, d (mm): 0,1625

Load rate (mm/min): 0,3

Previously loaded (digram number): 3.1

Remarks: none



3.3

		Weight (g)
Board	17	343,9
Board	24	405,7
Board	20	355

Moisture Content (%): 14,85

Horsontal Load (N): 800

Max Vertical Load, Vmax (N): 668

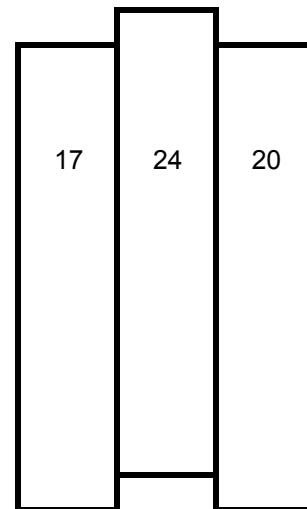
Static Friction Coefficient (μ): 0,4175

Displacement at Vmax, d (mm): 0,225

Load rate (mm/min): 0,3

Previously loaded (digram number): 3.1, 3.2

Remarks: none



3.4

		Weight (g)
Board	17	343,9
Board	24	405,7
Board	20	355

Moisture Content (%): 14,85

Horsontal Load (N): 1200

Max Vertical Load, Vmax (N): 1060

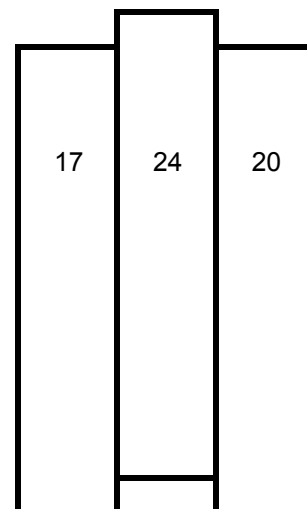
Static Friction Coefficient (μ): 0,441666667

Displacement at Vmax, d (mm): unknown

Load rate (mm/min): 0,3

Previously loaded (digram number): 3.1, 3.2, 3.3

Remarks: none



3.5

		Weight (g)
Board	17	343,9
Board	24	405,7
Board	20	355

Moisture Content (%): 14,85

Horsontal Load (N): 1600

Max Vertical Load, Vmax (N): 1360

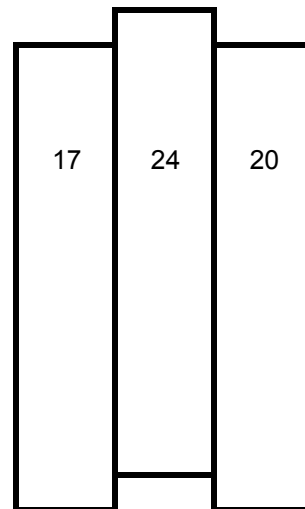
Static Friction Coefficient (μ): 0,425

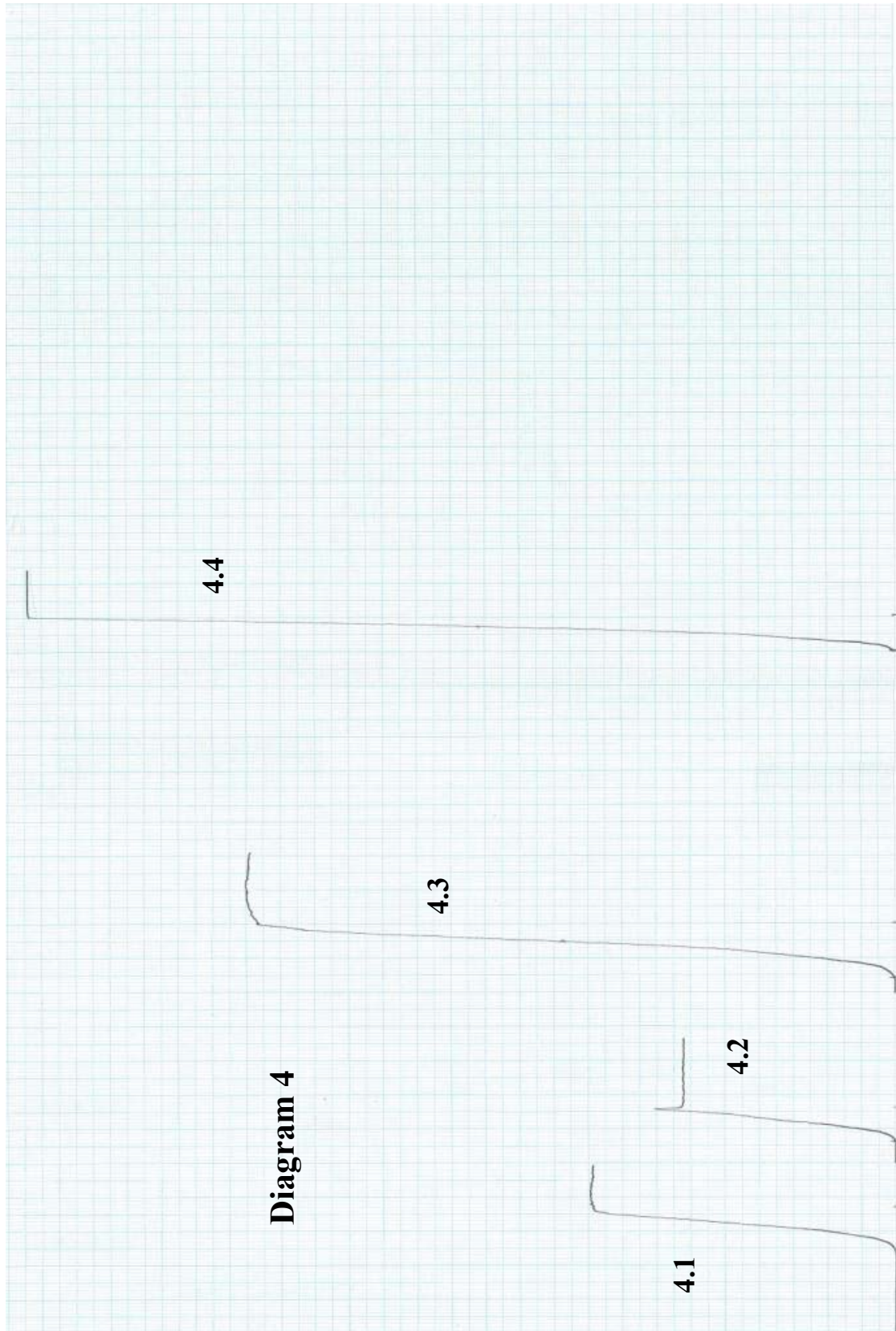
Displacement at Vmax, d (mm): unknown

Load rate (mm/min): 0,3

Previously loaded (digram number): 3.1, 3.2, 3.3, 3.4

Remarks: none





4.1

		Weight (g)
Board	26	389,9
Board	27	347,7
Board	29	364

Moisture Content (%): 14,85

Horsontal Load (N): 400

Max Vertical Load, Vmax (N): 356

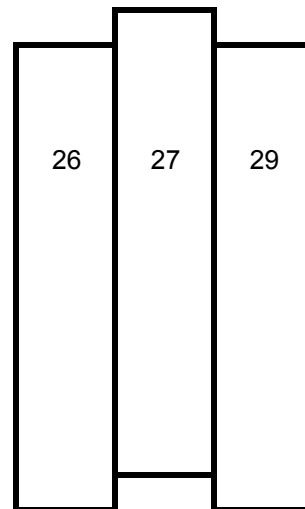
Static Friction Coefficient (μ): 0,445

Displacement at Vmax, d (mm): 0,1625

Load rate (mm/min): 0,6

Previously loaded (digram number):

Remarks: none



4.2

		Weight (g)
Board	26	389,9
Board	27	347,7
Board	29	364

Moisture Content (%): 14,85

Horsontal Load (N): 200

Max Vertical Load, Vmax (N): 280

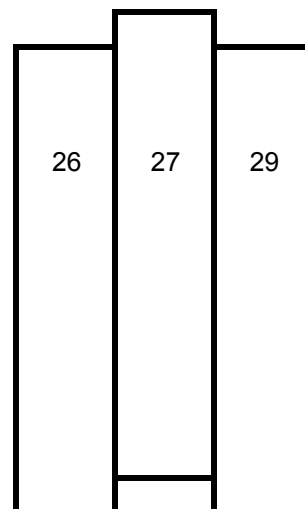
Static Friction Coefficient (μ): 0,7

Displacement at Vmax, d (mm): 0,125

Load rate (mm/min): 0,6

Previously loaded (digram number): 4.1

Remarks: none



4.3

		Weight (g)
Board	26	389,9
Board	27	347,7
Board	29	364

Moisture Content (%): 14,85

Horsontal Load (N): 800

Max Vertical Load, Vmax (N): 744

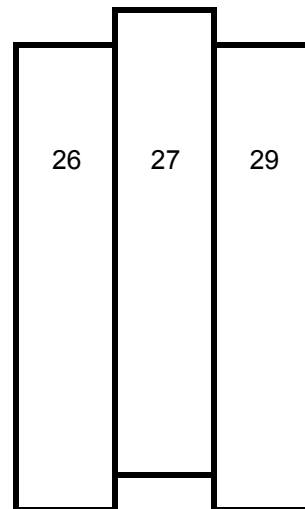
Static Friction Coefficient (μ): 0,465

Displacement at Vmax, d (mm): 0,2

Load rate (mm/min): 0,6

Previously loaded (digram number): 4.1, 4.2

Remarks: none



4.4

		Weight (g)
Board	26	389,9
Board	27	347,7
Board	29	364

Moisture Content (%): 14,85

Horsontal Load (N): 1200

Max Vertical Load, Vmax (N): 1121

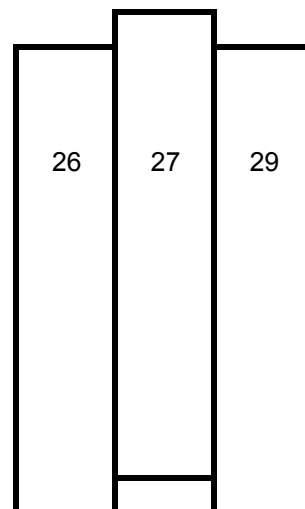
Static Friction Coefficient (μ): 0,467083333

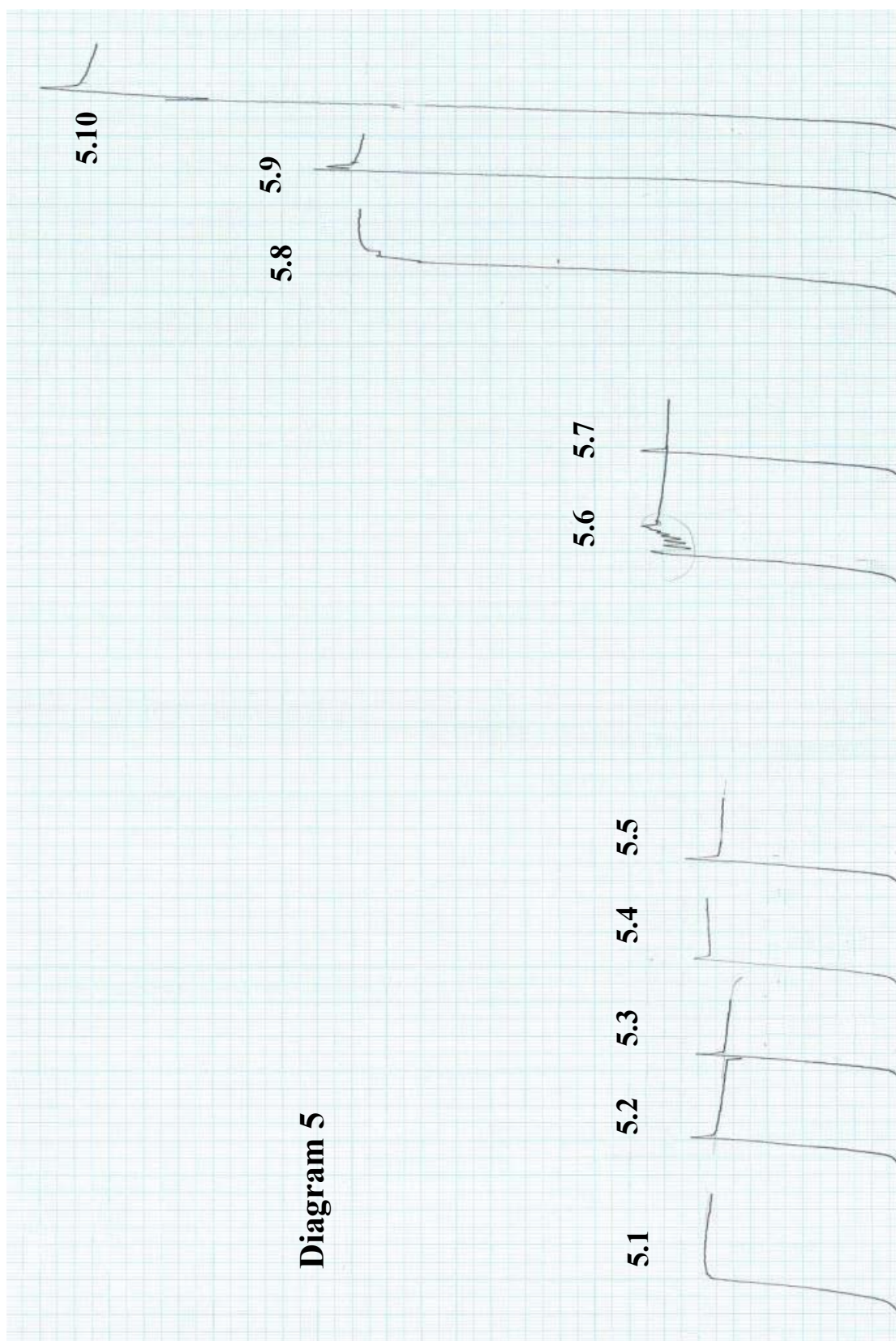
Displacement at Vmax, d (mm): unknown

Load rate (mm/min): 0.6

Previously loaded (digram number): 4.1, 4.2, 4.3

Remarks: none





5.1

		Weight (g)
Board	11	347,6
Board	6	345,2
Board	8	354,8

Moisture Content (%): 14,85

Horsontal Load (N): 200

Max Vertical Load, Vmax (N): 228

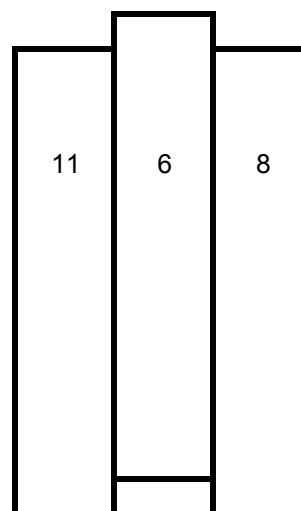
Static Friction Coefficient (μ): 0,57

Displacement at Vmax, d (mm): 0,1625

Load rate (mm/min): 0,6

Previously loaded (digram number):

Remarks: none



5.2

		Weight (g)
Board	11	347,6
Board	6	345,2
Board	8	354,8

Moisture Content (%): 14,85

Horsontal Load (N): 200

Max Vertical Load, Vmax (N): 248

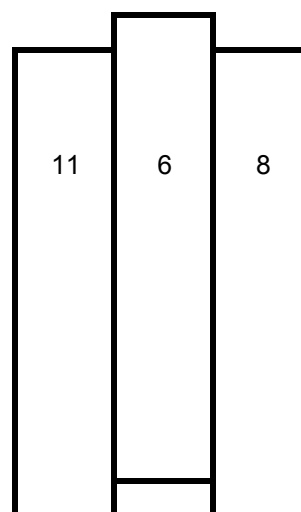
Static Friction Coefficient (μ): 0,62

Displacement at Vmax, d (mm): 0,1375

Load rate (mm/min): 0,3

Previously loaded (digram number): 5.1

Remarks: none



5.3

		Weight (g)
Board	11	347,6
Board	6	345,2
Board	8	354,8

Moisture Content (%): 14,85

Horsontal Load (N): 200

Max Vertical Load, Vmax (N): 244

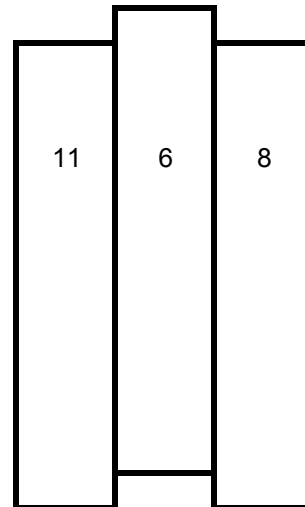
Static Friction Coefficient (μ): 0,61

Displacement at Vmax, d (mm): 0,1

Load rate (mm/min): 0,3

Previously loaded (digram number): 5.1, 5.2

Remarks: none



5.4

		Weight (g)
Board	11	347,6
Board	6	345,2
Board	8	354,8

Moisture Content (%): 14,85

Horsontal Load (N): 200

Max Vertical Load, Vmax (N): 244

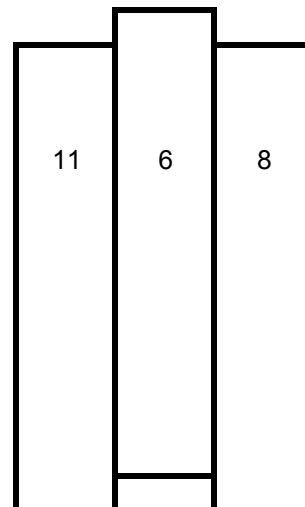
Static Friction Coefficient (μ): 0,61

Displacement at Vmax, d (mm): 0,1625

Load rate (mm/min): 2,4

Previously loaded (digram number): 5.1, 5.2, 5.3

Remarks: none



5.5

		Weight (g)
Board	11	347,6
Board	6	345,2
Board	8	354,8

Moisture Content (%): 14,85

Horsontal Load (N): 200

Max Vertical Load, Vmax (N): 256

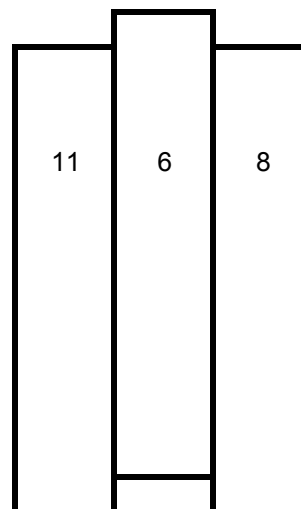
Static Friction Coefficient (μ): 0,64

Displacement at Vmax, d (mm): 0,15

Load rate (mm/min): 0,6

Previously loaded (digram number): 5.1, 5.2, 5.3, 5.4

Remarks: none



5.6

		Weight (g)
Board	11	347,6
Board	6	345,2
Board	8	354,8

Moisture Content (%): 14,85

Horsontal Load (N): 400

Max Vertical Load, Vmax (N): 292

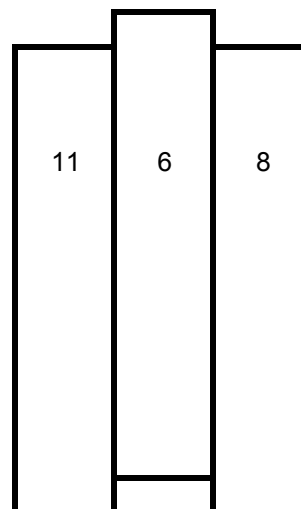
Static Friction Coefficient (μ): 0,365

Displacement at Vmax, d (mm): 0,2625

Load rate (mm/min): 0,3

Previously loaded (digram number): 5.1, 5.2, 5.3, 5.4, 5.5

Remarks: none



5.7

		Weight (g)
Board	11	347,6
Board	6	345,2
Board	8	354,8

Moisture Content (%): 14,85

Horsontal Load (N): 400

Max Vertical Load, Vmax (N): 304

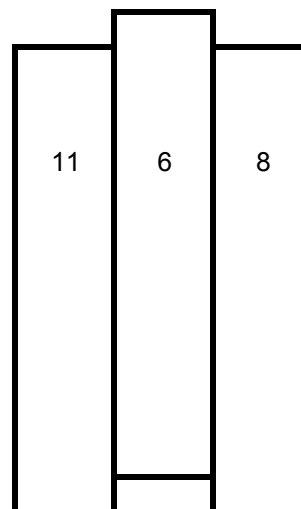
Static Friction Coefficient (μ): 0,38

Displacement at Vmax, d (mm): 0,1375

Load rate (mm/min): 0,3

Previously loaded (digram number): 5.1 - 5.6

Remarks: none



5.8

		Weight (g)
Board	11	347,6
Board	6	345,2
Board	8	354,8

Moisture Content (%): 14,85

Horsontal Load (N): 800

Max Vertical Load, Vmax (N): 624

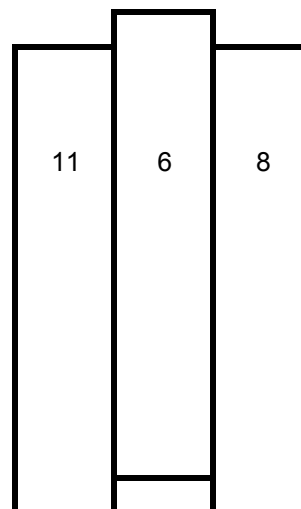
Static Friction Coefficient (μ): 0,39

Displacement at Vmax, d (mm): 0,15

Load rate (mm/min): 0,3

Previously loaded (digram number): 5.1 - 5.7

Remarks: none



5.9

		Weight (g)
Board	11	347,6
Board	6	345,2
Board	8	354,8

Moisture Content (%): 14,85

Horsontal Load (N): 800

Max Vertical Load, Vmax (N): 680

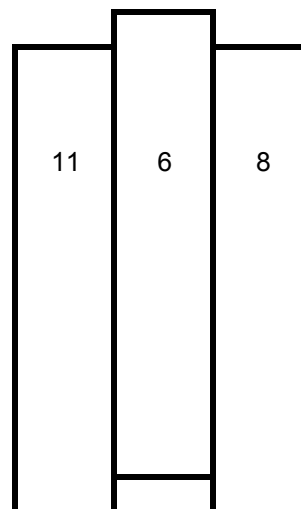
Static Friction Coefficient (μ): 0,425

Displacement at Vmax, d (mm): 0,125

Load rate (mm/min): 0,3

Previously loaded (digram number): 5.1 - 5.8

Remarks: none



5.10

		Weight (g)
Board	11	347,6
Board	6	345,2
Board	8	354,8

Moisture Content (%): 14,85

Horsontal Load (N): 1200

Max Vertical Load, Vmax (N): 992

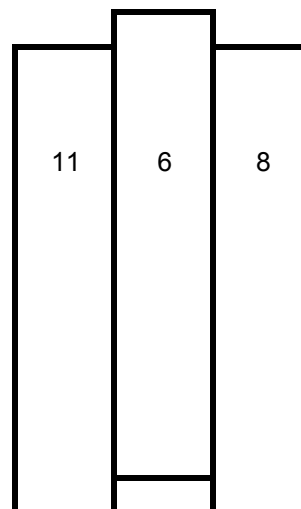
Static Friction Coefficient (μ): 0,413333333

Displacement at Vmax, d (mm): 0,2

Load rate (mm/min): 0,3

Previously loaded (digram number): 5.1 - 5.9

Remarks: none



5.11

Weight (g)		
Board	11	347,6
Board	6	345,2
Board	8	354,8

Moisture Content (%): 14,85

Horsontal Load (N): 1600

Max Vertical Load, Vmax (N): 1277

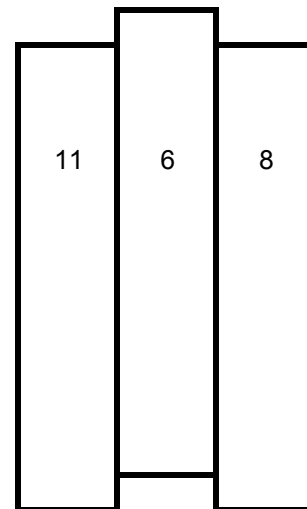
Static Friction Coefficient (μ): 0,3990625

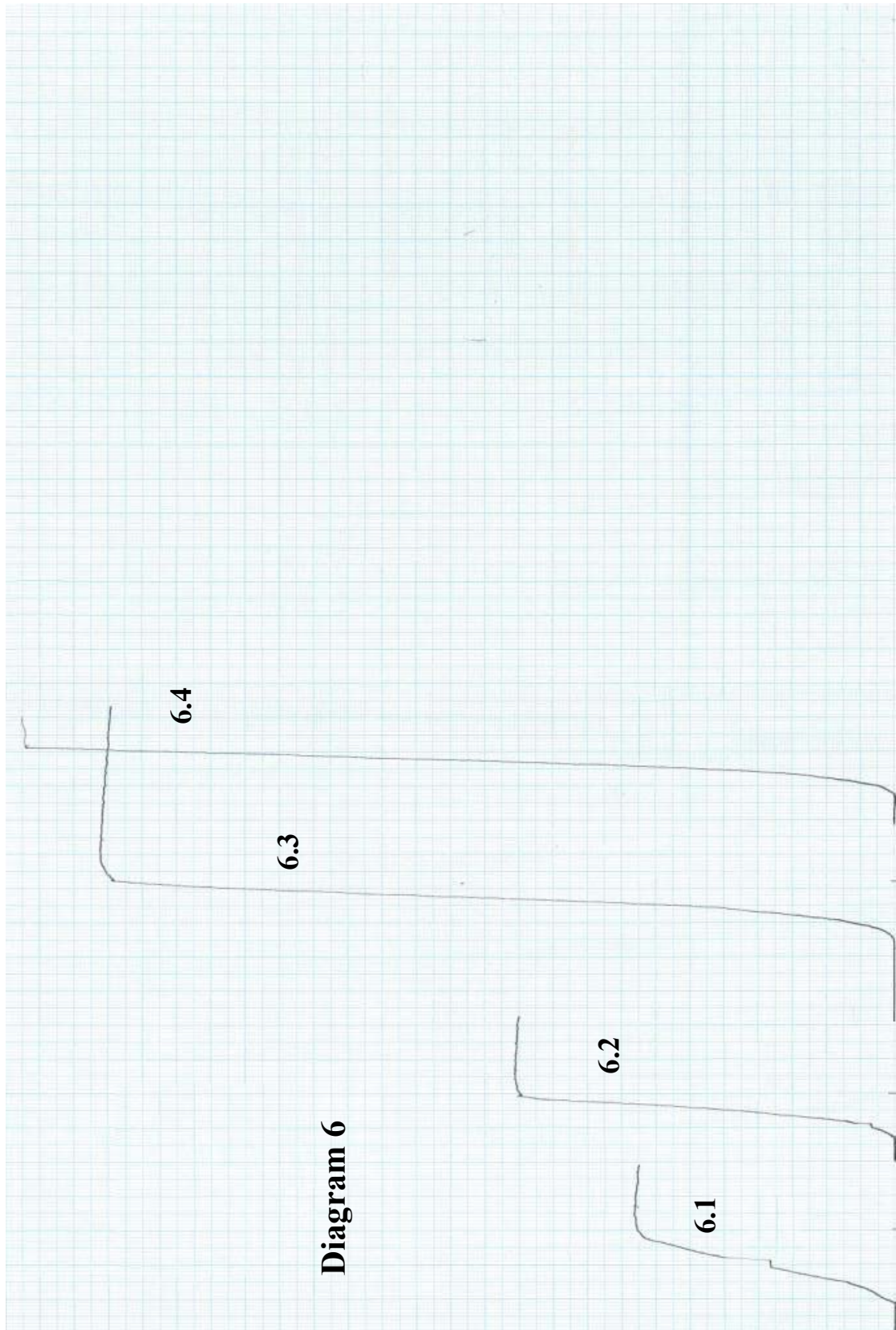
Displacement at Vmax, d (mm): unknown

Load rate (mm/min): 0,3

Previously loaded (digram number): 5.1-5.10

Remarks: none





6.1

		Weight (g)
Board	13	353,6
Board	12	350,2
Board	10	345,3

Moisture Content (%): 14,85

Horsontal Load (N): 200

Max Vertical Load, Vmax (N): 300

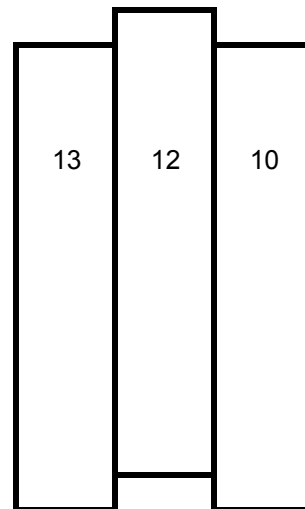
Static Friction Coefficient (μ): 0,75

Displacement at Vmax, d (mm): 0,275

Load rate (mm/min): 0.6

Previously loaded (digram number): none

Remarks: none



6.2

		Weight (g)
Board	13	353,6
Board	12	350,2
Board	10	345,3

Moisture Content (%): 14,85

Horsontal Load (N): 400

Max Vertical Load, Vmax (N): 440

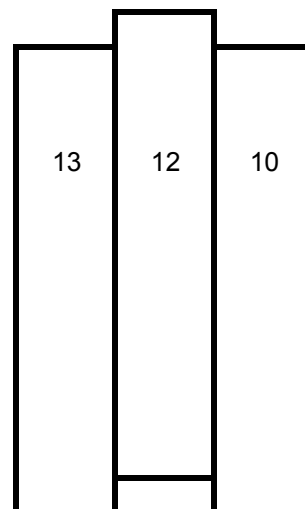
Static Friction Coefficient (μ): 0,55

Displacement at Vmax, d (mm): 0,1625

Load rate (mm/min): 0,6

Previously loaded (digram number): 6.1

Remarks: none



6.3

		Weight (g)
Board	13	353,6
Board	12	350,2
Board	10	345,3

Moisture Content (%): 14,85

Horsontal Load (N): 800

Max Vertical Load, Vmax (N): 912

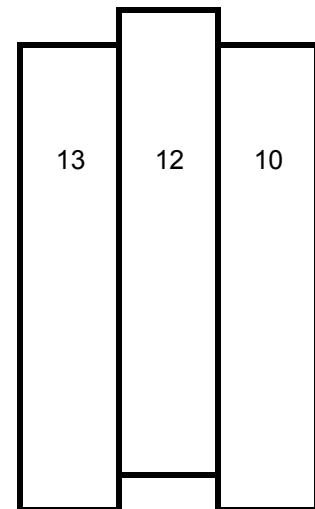
Static Friction Coefficient (μ): 0,57

Displacement at Vmax, d (mm): 0,2125

Load rate (mm/min): 0,6

Previously loaded (digram number): 6.1, 6.2

Remarks: none



6.4

		Weight (g)
Board	13	353,6
Board	12	350,2
Board	10	345,3

Moisture Content (%): 14,85

Horsontal Load (N): 1200

Max Vertical Load, Vmax (N): 1275

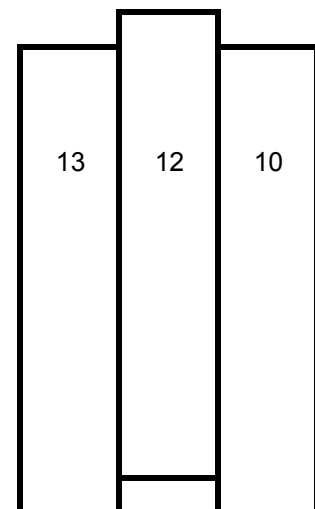
Static Friction Coefficient (μ): 0,53125

Displacement at Vmax, d (mm): unknown

Load rate (mm/min): 0,6

Previously loaded (digram number): 6.1- 6.3

Remarks: none



6.5

		Weight (g)
Board	13	353,6
Board	12	350,2
Board	10	345,3

Moisture Content (%): 14,85

Horsonal Load (N): 1600

Max Vertical Load, Vmax (N): 1730

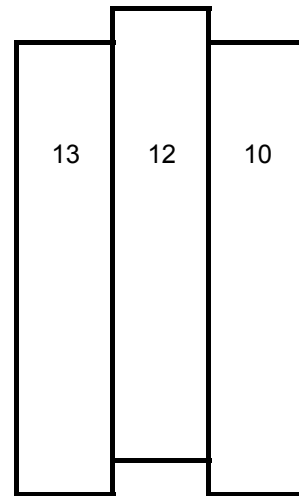
Static Friction Coefficient (μ): 0,540625

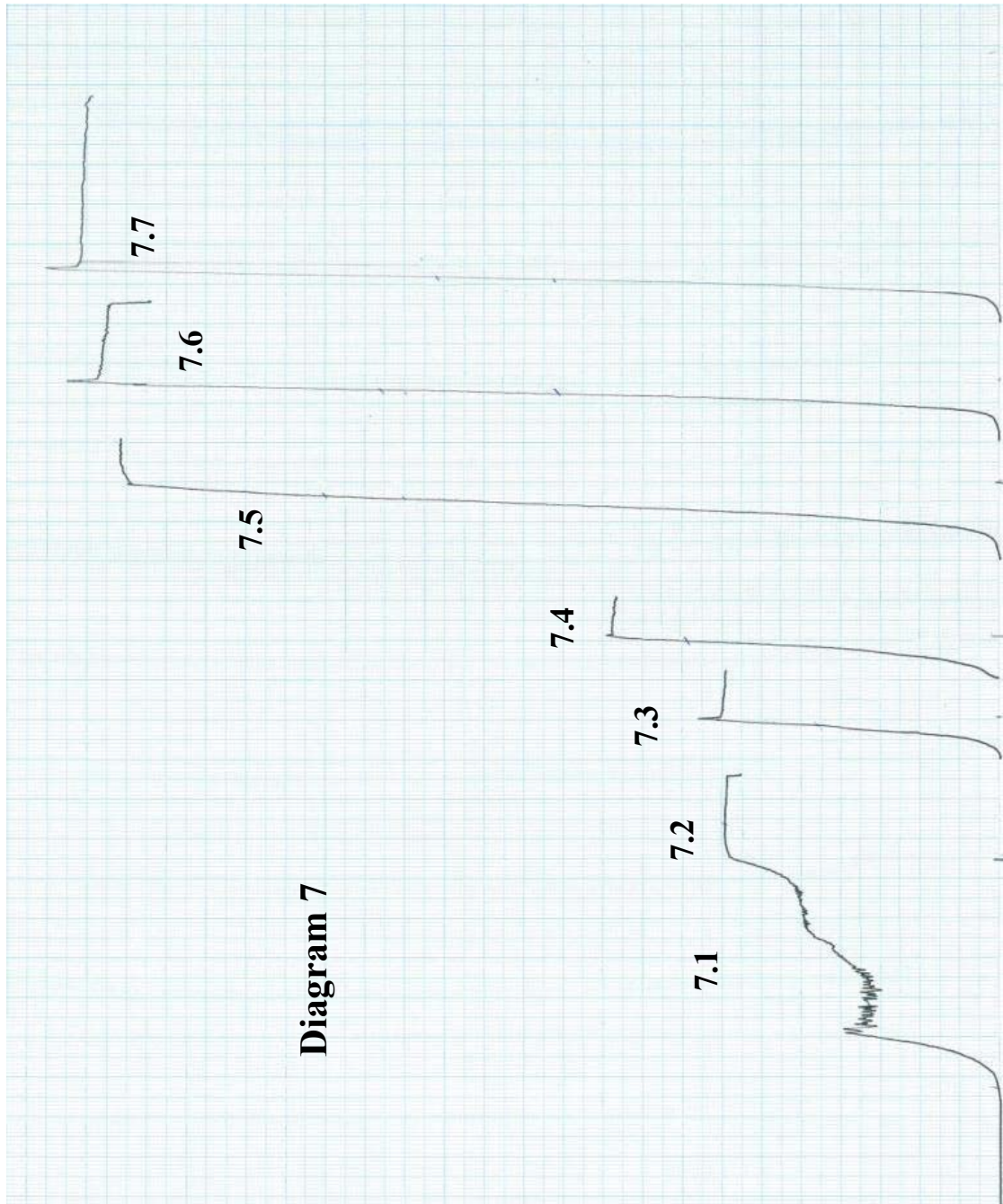
Displacement at Vmax, d (mm): unknown

Load rate (mm/min): 0,6

Previously loaded (digram number): 6.1 - 6.4

Remarks: none





7.1

		Weight (g)
Board	14	367,6
Board	7	379,6
Board	9	366,5

Moisture Content (%): 14,85

Horsontal Load (N): 200

Max Vertical Load, Vmax (N): 276

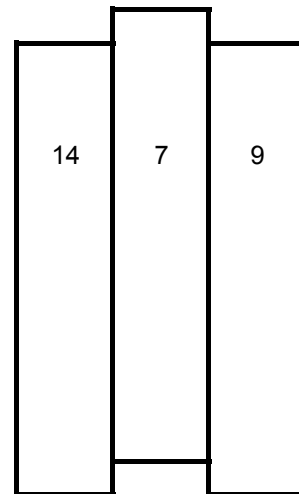
Static Friction Coefficient (μ): 0,69

Displacement at Vmax, d (mm): 0,7125

Load rate (mm/min): 0,3

Previously loaded (digram number): none

Remarks: none



7.2

		Weight (g)
Board	14	367,6
Board	7	379,6
Board	9	366,5

Moisture Content (%): 14,85

Horsontal Load (N): 200

Max Vertical Load, Vmax (N): 304

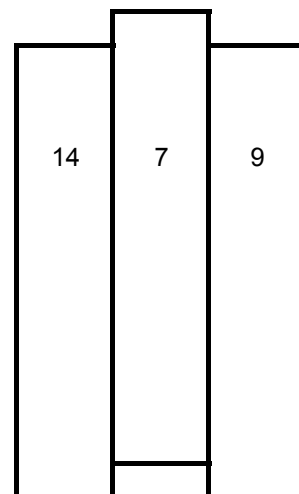
Static Friction Coefficient (μ): 0,76

Displacement at Vmax, d (mm): 0,125

Load rate (mm/min): 0,3

Previously loaded (digram number): 7.1

Remarks: none



7.3

		Weight (g)
Board	14	367,6
Board	7	379,6
Board	9	366,5

Moisture Content (%): 14,85

Horsontal Load (N): 400

Max Vertical Load, Vmax (N): 396

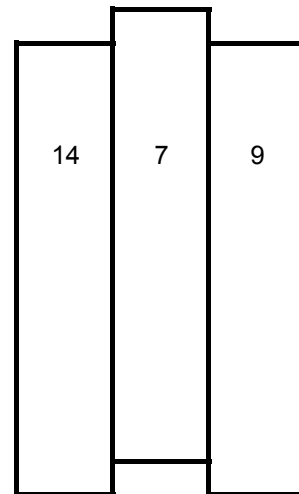
Static Friction Coefficient (μ): 0,495

Displacement at Vmax, d (mm): 0,1375

Load rate (mm/min): 0,3

Previously loaded (digram number): 7.1 - 7.2

Remarks: none



7.4

		Weight (g)
Board	14	367,6
Board	7	379,6
Board	9	366,5

Moisture Content (%): 14,85

Horsontal Load (N): 800

Max Vertical Load, Vmax (N): 884

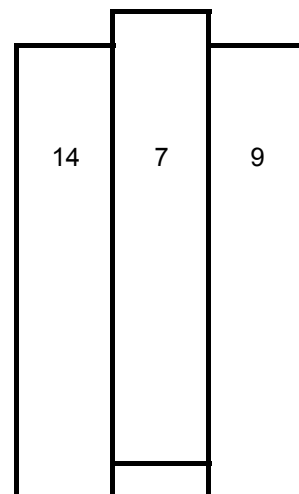
Static Friction Coefficient (μ): 0,5525

Displacement at Vmax, d (mm): 0,2375

Load rate (mm/min): 0,3

Previously loaded (digram number): 7.1 - 7.3

Remarks: none



7.5

		Weight (g)
Board	14	367,6
Board	7	379,6
Board	9	366,5

Moisture Content (%): 14,85

Horsontal Load (N): 800

Max Vertical Load, Vmax (N): 936

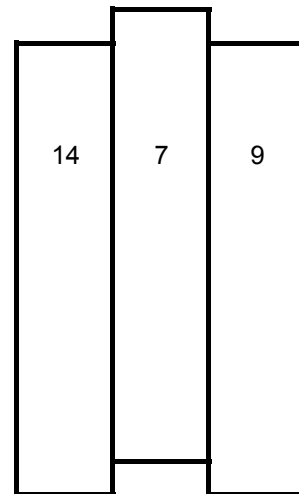
Static Friction Coefficient (μ): 0,585

Displacement at Vmax, d (mm): 0,1875

Load rate (mm/min): 0,6

Previously loaded (digram number): 7.1-7.4

Remarks: none



7.6

		Weight (g)
Board	14	367,6
Board	7	379,6
Board	9	366,5

Moisture Content (%): 14,85

Horsontal Load (N): 800

Max Vertical Load, Vmax (N): 956

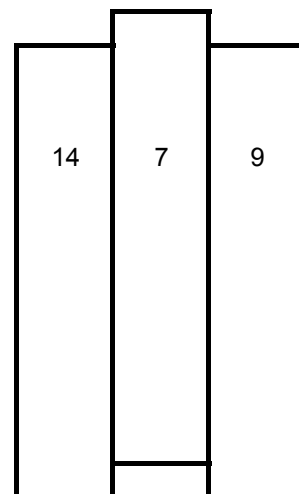
Static Friction Coefficient (μ): 0,5975

Displacement at Vmax, d (mm): 0,2

Load rate (mm/min): 0,3

Previously loaded (digram number): 7.1-7.5

Remarks: none



7.7

		Weight (g)
Board	14	367,6
Board	7	379,6
Board	9	366,5

Moisture Content (%): 14,85

Horsontal Load (N): 1200

Max Vertical Load, Vmax (N): 1405

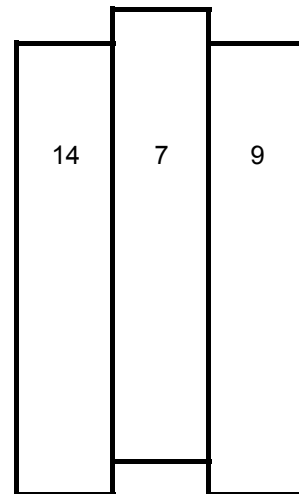
Static Friction Coefficient (μ): 0,585416667

Displacement at Vmax, d (mm): unknown

Load rate (mm/min): 0,3

Previously loaded (digram number): 7.1-7.6

Remarks: none



7.8

		Weight (g)
Board	14	367,6
Board	7	379,6
Board	9	366,5

Moisture Content (%): 14,85

Horsontal Load (N): 1600

Max Vertical Load, Vmax (N): 1930

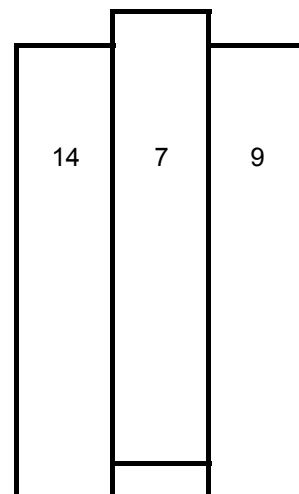
Static Friction Coefficient (μ): 0,603125

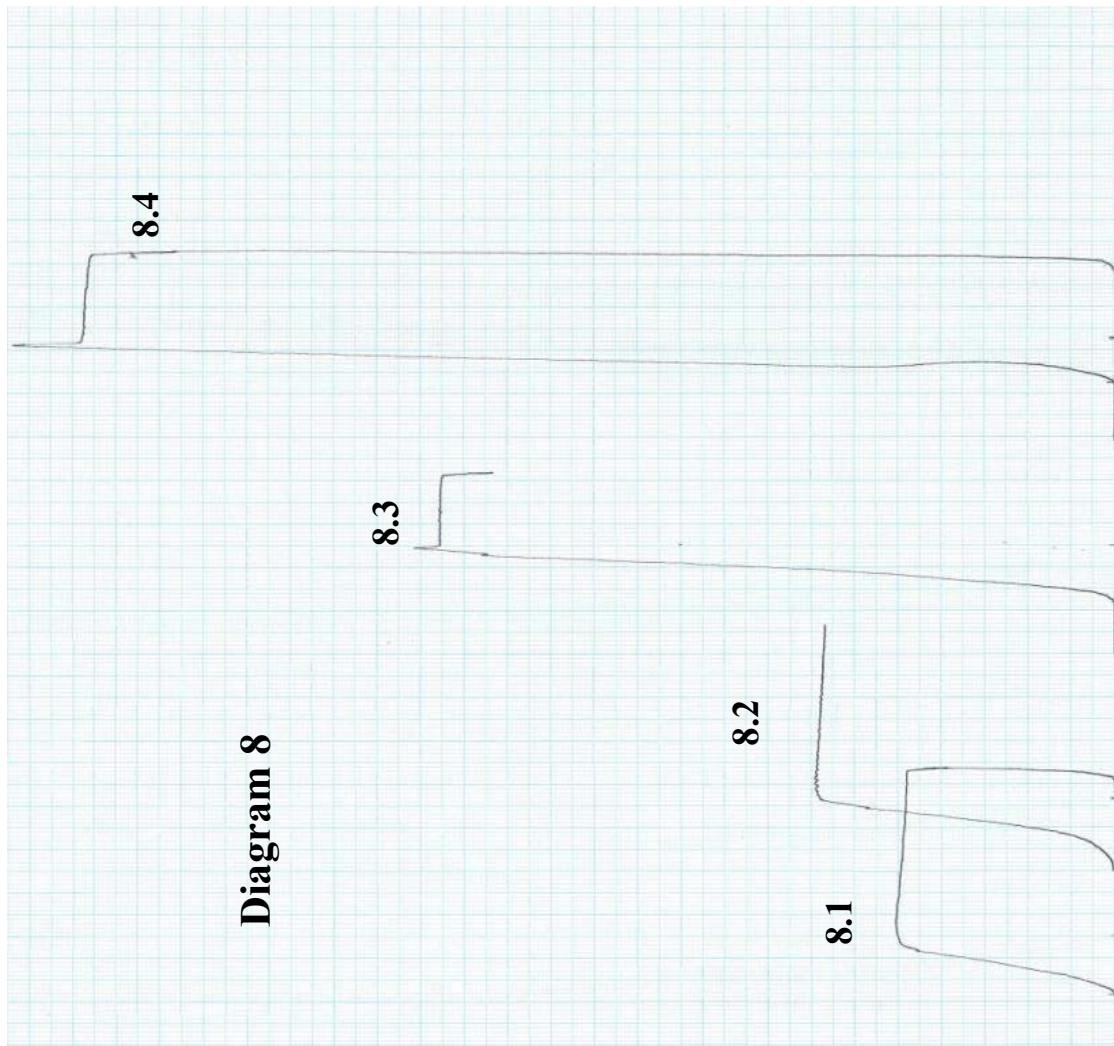
Displacement at Vmax, d (mm): 0,1875

Load rate (mm/min): 0,3

Previously loaded (digram number): 7.1-7.7

Remarks: none





8.1

		Weight (g)
Board	19	360,1
Board	22	396,5
Board	23	378,2

Moisture Content (%): 14,85

Horsontal Load (N): 200

Max Vertical Load, Vmax (N): 200

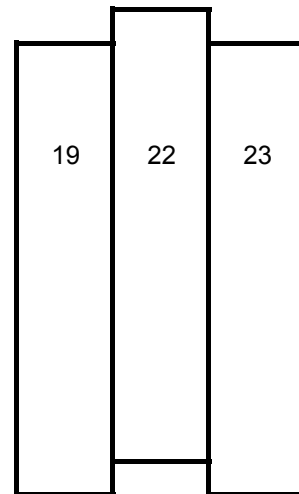
Static Friction Coefficient (μ): 0,5

Displacement at Vmax, d (mm): 0,1625

Load rate (mm/min): 0,6

Previously loaded (digram number): none

Remarks: none



8.2

		Weight (g)
Board	19	360,1
Board	22	396,5
Board	23	378,2

Moisture Content (%): 14,85

Horsontal Load (N): 400

Max Vertical Load, Vmax (N): 272

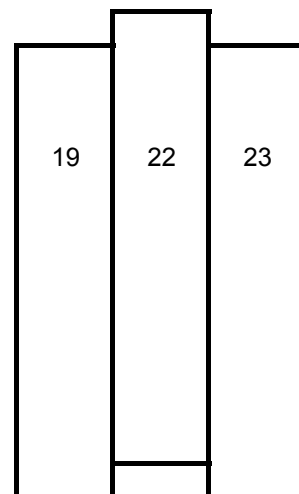
Static Friction Coefficient (μ): 0,34

Displacement at Vmax, d (mm): 0,2125

Load rate (mm/min): 0,6

Previously loaded (digram number): 8.1

Remarks: none



8.3

		Weight (g)
Board	19	360,1
Board	22	396,5
Board	23	378,2

Moisture Content (%): 14,85

Horsontal Load (N): 800

Max Vertical Load, Vmax (N): 644

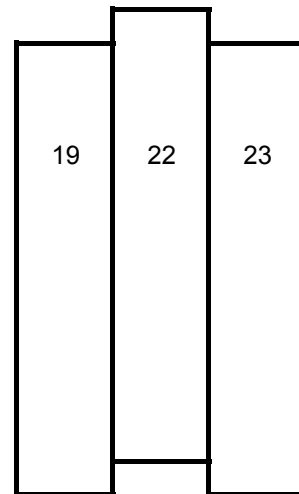
Static Friction Coefficient (μ): 0,4025

Displacement at Vmax, d (mm): 0,1625

Load rate (mm/min): 0,6

Previously loaded (digram number): 8,1-8,2

Remarks: none



8.4

		Weight (g)
Board	19	360,1
Board	22	396,5
Board	23	378,2

Moisture Content (%): 14,85

Horsontal Load (N): 1200

Max Vertical Load, Vmax (N): 1012

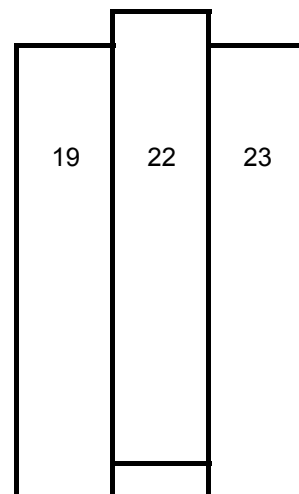
Static Friction Coefficient (μ): 0,421666667

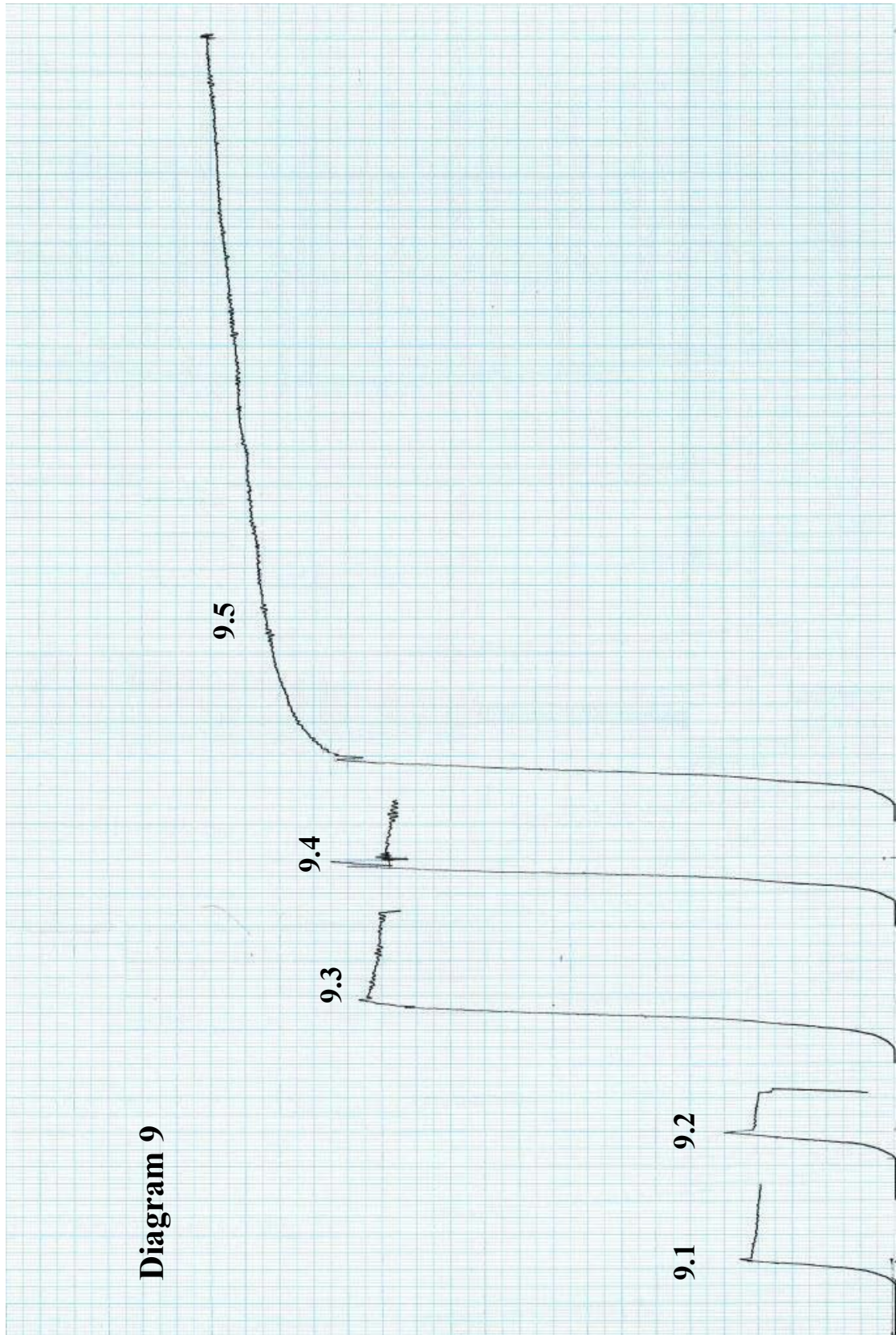
Displacement at Vmax, d (mm): 0,125

Load rate (mm/min): 0,6

Previously loaded (digram number): 8.1-8.3

Remarks: none





9.1

		Weight (g)
Board	26	380,2
Board	27	337,7
Board	29	356,6

Moisture Content (%): 11,25

Horsontal Load (N): 400

Max Vertical Load, Vmax (N): 180

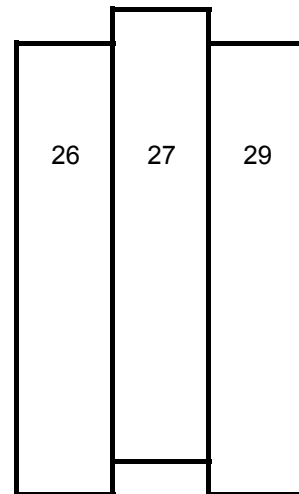
Static Friction Coefficient (μ): 0,225

Displacement at Vmax, d (mm): 0,1

Load rate (mm/min): 0,6

Previously loaded (digram number): 4.1 - 4.4

Remarks: none



9.2

		Weight (g)
Board	26	380,2
Board	27	337,7
Board	29	356,6

Moisture Content (%): 11,25

Horsontal Load (N): 400

Max Vertical Load, Vmax (N): 200

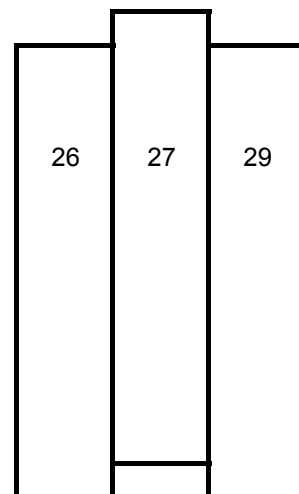
Static Friction Coefficient (μ): 0,25

Displacement at Vmax, d (mm): 0,1

Load rate (mm/min): 0,6

Previously loaded (digram number): 4.1 - 4.4, 9.1

Remarks: none



9.3

		Weight (g)
Board	26	380,2
Board	27	337,7
Board	29	356,6

Moisture Content (%): 11,25

Horsontal Load (N): 1200

Max Vertical Load, Vmax (N): 628

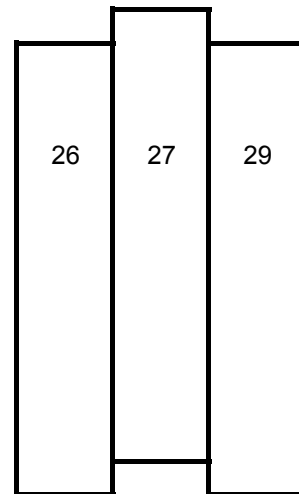
Static Friction Coefficient (μ): 0,261666667

Displacement at Vmax, d (mm): 0,1625

Load rate (mm/min): 0,6

Previously loaded (digram number): 4.1 - 4.4, 9.1 - 9.2

Remarks: none



9.4

		Weight (g)
Board	26	380,2
Board	27	337,7
Board	29	356,6

Moisture Content (%): 11,25

Horsontal Load (N): 1200

Max Vertical Load, Vmax (N): 656

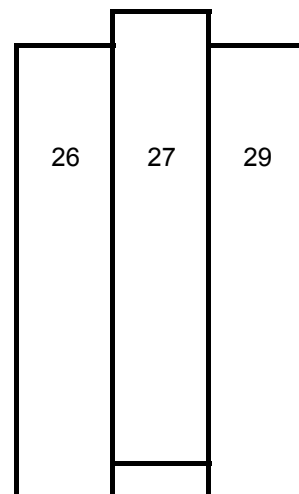
Static Friction Coefficient (μ): 0,273333333

Displacement at Vmax, d (mm): 0,1625

Load rate (mm/min): 0,6

Previously loaded (digram number): 4.1 - 4.4 9.1-9.3

Remarks: none



9.5

		Weight (g)
Board	26	380,2
Board	27	337,7
Board	29	356,6

Moisture Content (%): 11,25

Horizontal Load (N): 1200

Max Vertical Load, V_{max} (N): unknown

Static Friction Coefficient (μ):

Displacement at V_{max} , d (mm): unknown

Load rate (mm/min): 0,6

Previously loaded (diagram number): 4.1 - 4.4 9.1-9.4

Remarks: Two pins/tacks added according to picture in next page

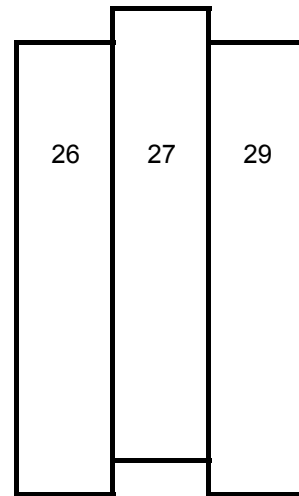
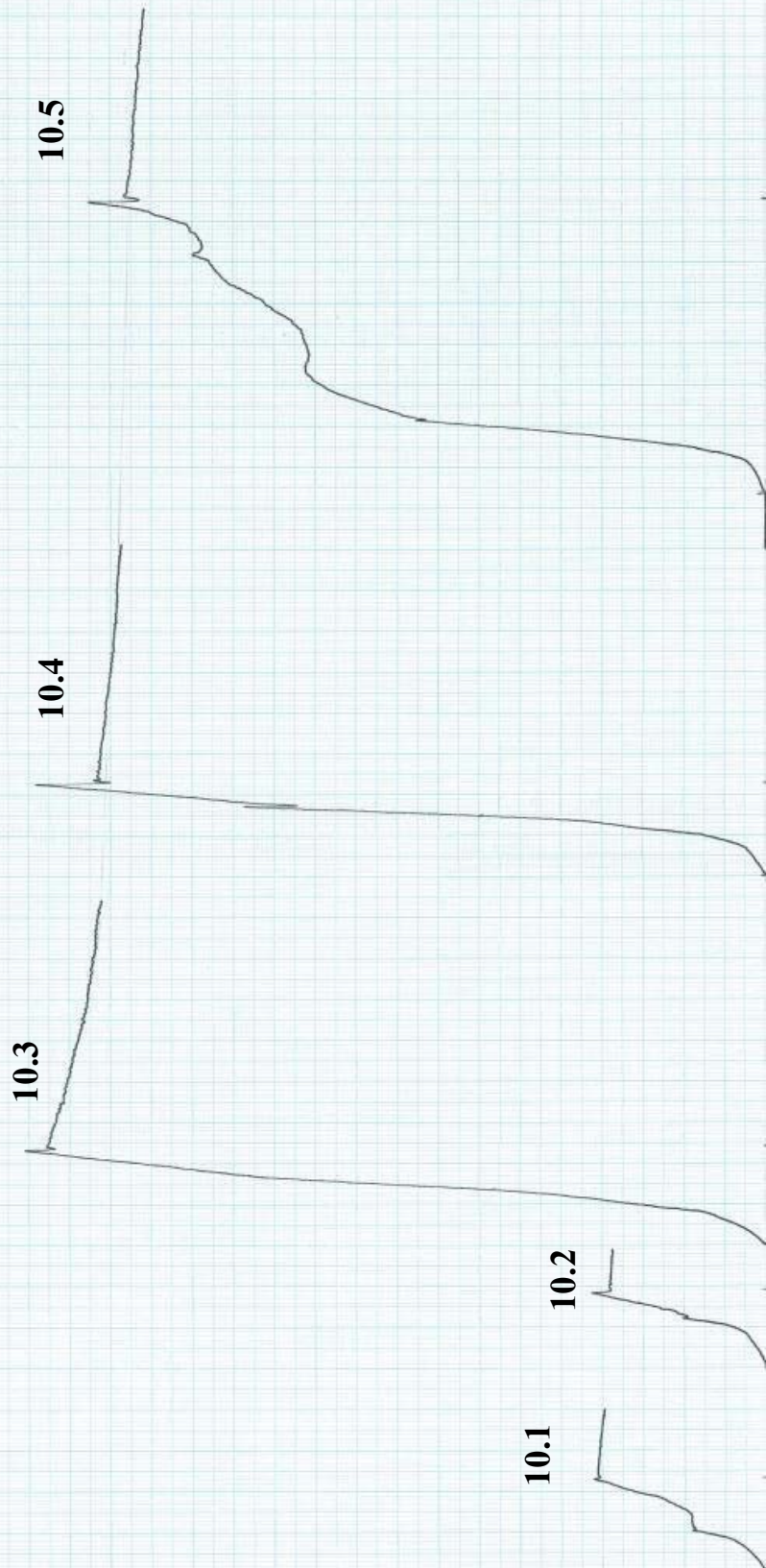


Diagram 10



10.1

		Weight (g)
Board	17	335,9
Board	24	401,6
Board	20	349

Moisture Content (%): 11,25

Horsontal Load (N): 400

Max Vertical Load, Vmax (N): 168

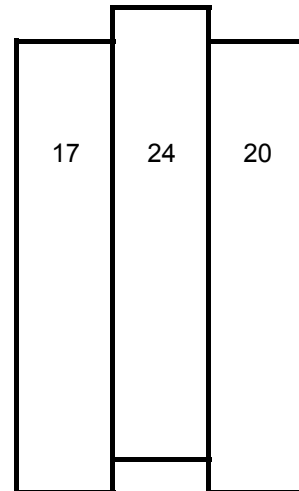
Static Friction Coefficient (μ): 0,21

Displacement at Vmax, d (mm): 0,2875

Load rate (mm/min): 0,3

Previously loaded (digram number): 3.1-3.5

Remarks: none

**10.2**

		Weight (g)
Board	17	335,9
Board	24	401,6
Board	20	349

Moisture Content (%): 11,25

Horsontal Load (N): 400

Max Vertical Load, Vmax (N): 172

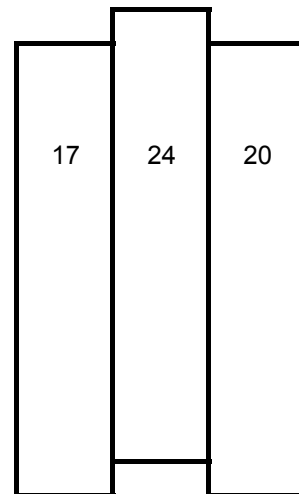
Static Friction Coefficient (μ): 0,215

Displacement at Vmax, d (mm): 0,2375

Load rate (mm/min): 0,3

Previously loaded (digram number): 3.1-3.5 10.1

Remarks: none



10.3

		Weight (g)
Board	17	335,9
Board	24	401,6
Board	20	349

Moisture Content (%): 11,25

Horsontal Load (N): 1200

Max Vertical Load, Vmax (N): 724

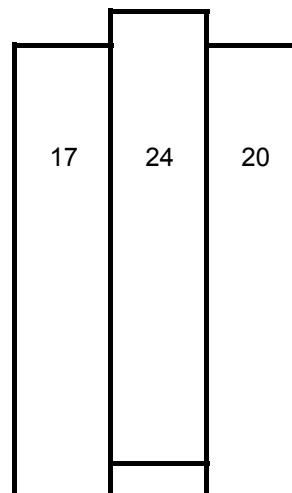
Static Friction Coefficient (μ): 0,301666667

Displacement at Vmax, d (mm): 0,3125

Load rate (mm/min): 0,3

Previously loaded (digram number): 3.1-3.5 10.1-10.2

Remarks: none



10.4

		Weight (g)
Board	17	335,9
Board	24	401,6
Board	20	349

Moisture Content (%): 11,25

Horsontal Load (N): 1200

Max Vertical Load, Vmax (N): 712

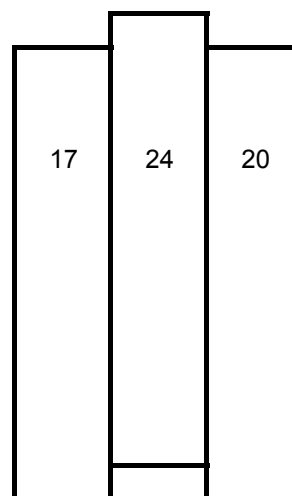
Static Friction Coefficient (μ): 0,296666667

Displacement at Vmax, d (mm): 0,2875

Load rate (mm/min): 0,3

Previously loaded (digram number): 3.1-3.5 10.1-10.3

Remarks: none



10.5

		Weight (g)
Board	17	335,9
Board	24	401,6
Board	20	349

Moisture Content (%): 11,25

Horsonal Load (N): 1200

Max Vertical Load, Vmax (N): 660

Static Friction Coefficient (μ): 0,275

Displacement at Vmax, d (mm): 0,9

Load rate (mm/min): 0,3

Previously loaded (digram number): 3.1-3.5 10.1-10.4

Remarks: Unloaded after 10.4, and then loaded up to 1200 N again.

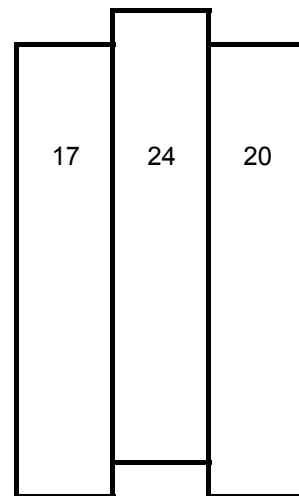
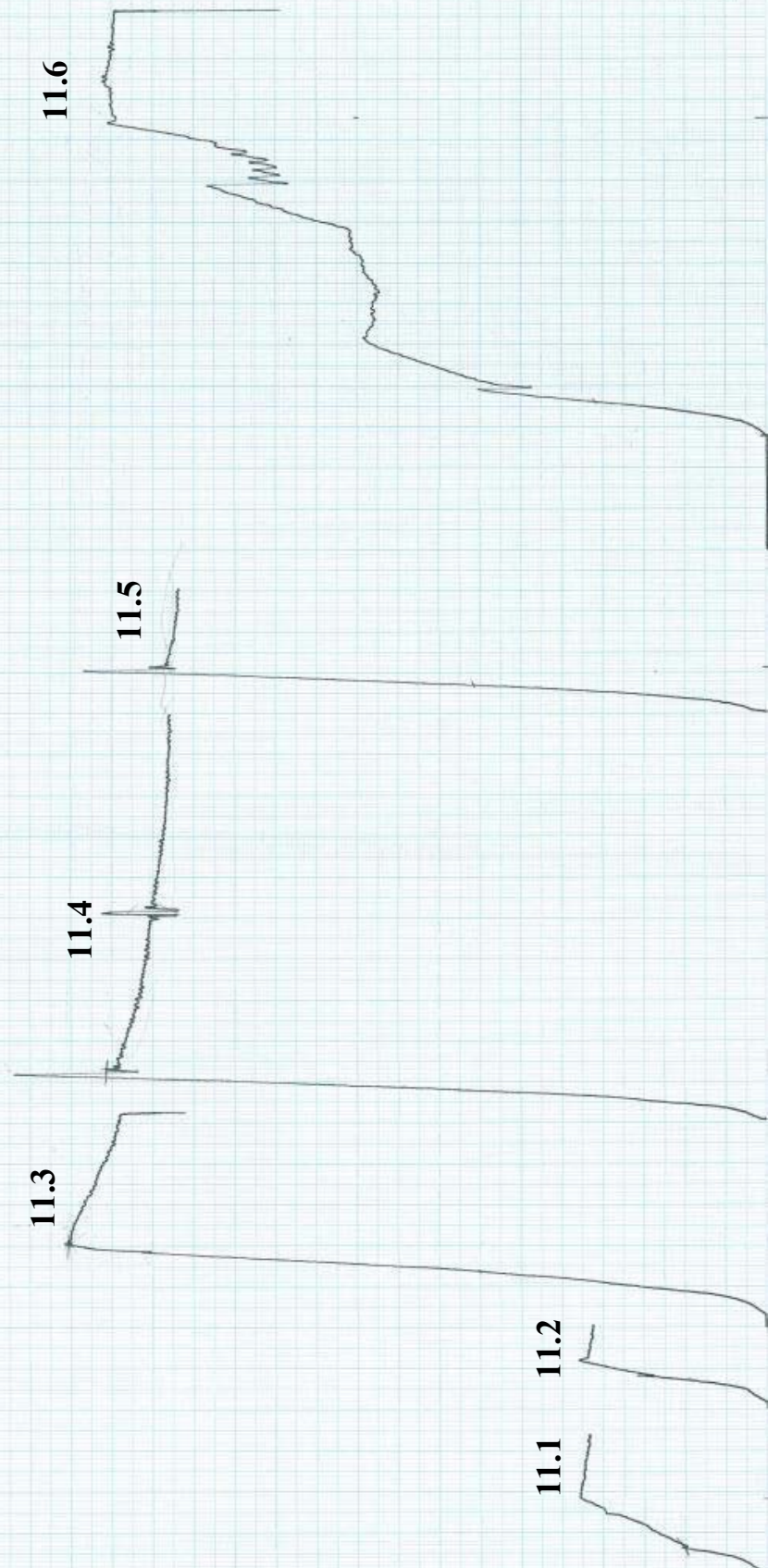


Diagram 11



11.1

		Weight (g)
Board	1	331,9
Board	25	346,9
Board	15	406,9

Moisture Content (%): 11,25

Horsontal Load (N): 400

Max Vertical Load, Vmax (N): 184

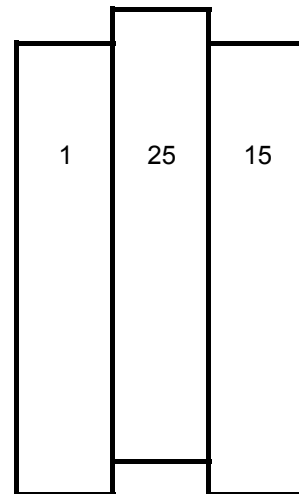
Static Friction Coefficient (μ): 0,23

Displacement at Vmax, d (mm): 0,225

Load rate (mm/min): 0,6

Previously loaded (digram number): 2.1-2.6

Remarks: none



11.2

		Weight (g)
Board	1	331,9
Board	25	346,9
Board	15	406,9

Moisture Content (%): 11,25

Horsontal Load (N): 400

Max Vertical Load, Vmax (N): 184

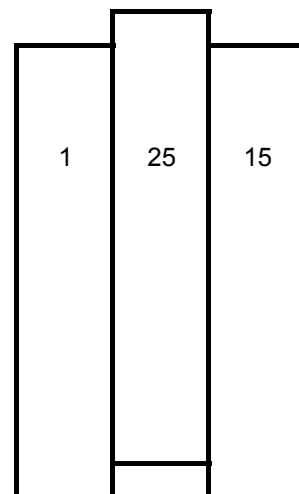
Static Friction Coefficient (μ): 0,23

Displacement at Vmax, d (mm): 0,15

Load rate (mm/min): 0,6

Previously loaded (digram number): 2.1-2.6 11.1

Remarks: none



11.3

		Weight (g)
Board	1	331,9
Board	25	346,9
Board	15	406,9

Moisture Content (%): 11,25

Horsontal Load (N): 1200

Max Vertical Load, Vmax (N): 684

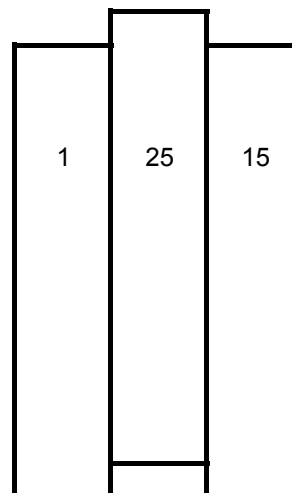
Static Friction Coefficient (μ): 0,285

Displacement at Vmax, d (mm): 0,2125

Load rate (mm/min): 0,6

Previously loaded (digram number): 2.1-2.6 11.1-11.2

Remarks: none



11.4

		Weight (g)
Board	1	331,9
Board	25	346,9
Board	15	406,9

Moisture Content (%): 11,25

Horsontal Load (N): 1200

Max Vertical Load, Vmax (N): 732

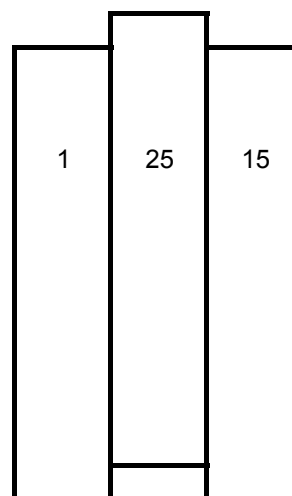
Static Friction Coefficient (μ): 0,305

Displacement at Vmax, d (mm): 0,1375

Load rate (mm/min): 0,6

Previously loaded (digram number): 2.1-2.6 11.1-11.3

Remarks: none



11.5

		Weight (g)
Board	1	331,9
Board	25	346,9
Board	15	406,9

Moisture Content (%): 11,25

Horsontal Load (N): 1200

Max Vertical Load, Vmax (N): 668

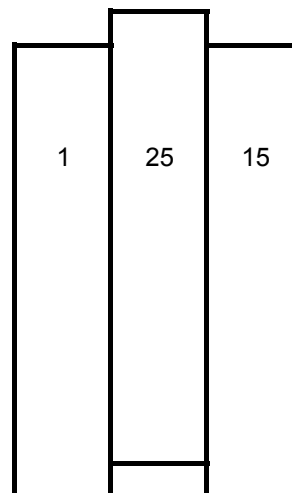
Static Friction Coefficient (μ): 0,278333333

Displacement at Vmax, d (mm): 0,1375

Load rate (mm/min): 0,6

Previously loaded (digram number): 2.1-2.6 11.1-11.4

Remarks: none

**11.6**

		Weight (g)
Board	1	331,9
Board	25	346,9
Board	15	406,9

Moisture Content (%): 11,25

Horsontal Load (N): 1200

Max Vertical Load, Vmax (N): 644

Static Friction Coefficient (μ): 0,268333333

Displacement at Vmax, d (mm): 0,9625

Load rate (mm/min): 0,6

Previously loaded (digram number): 2.1-2.6 11.1-11.5

Remarks: Unloaded after 11.5, and then loaded up to 1200 N again.

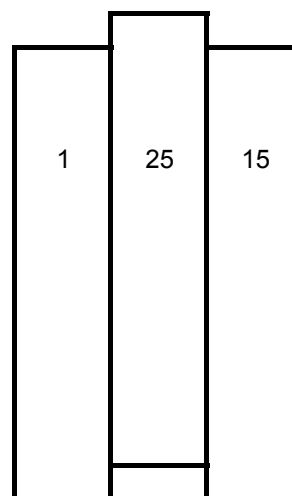
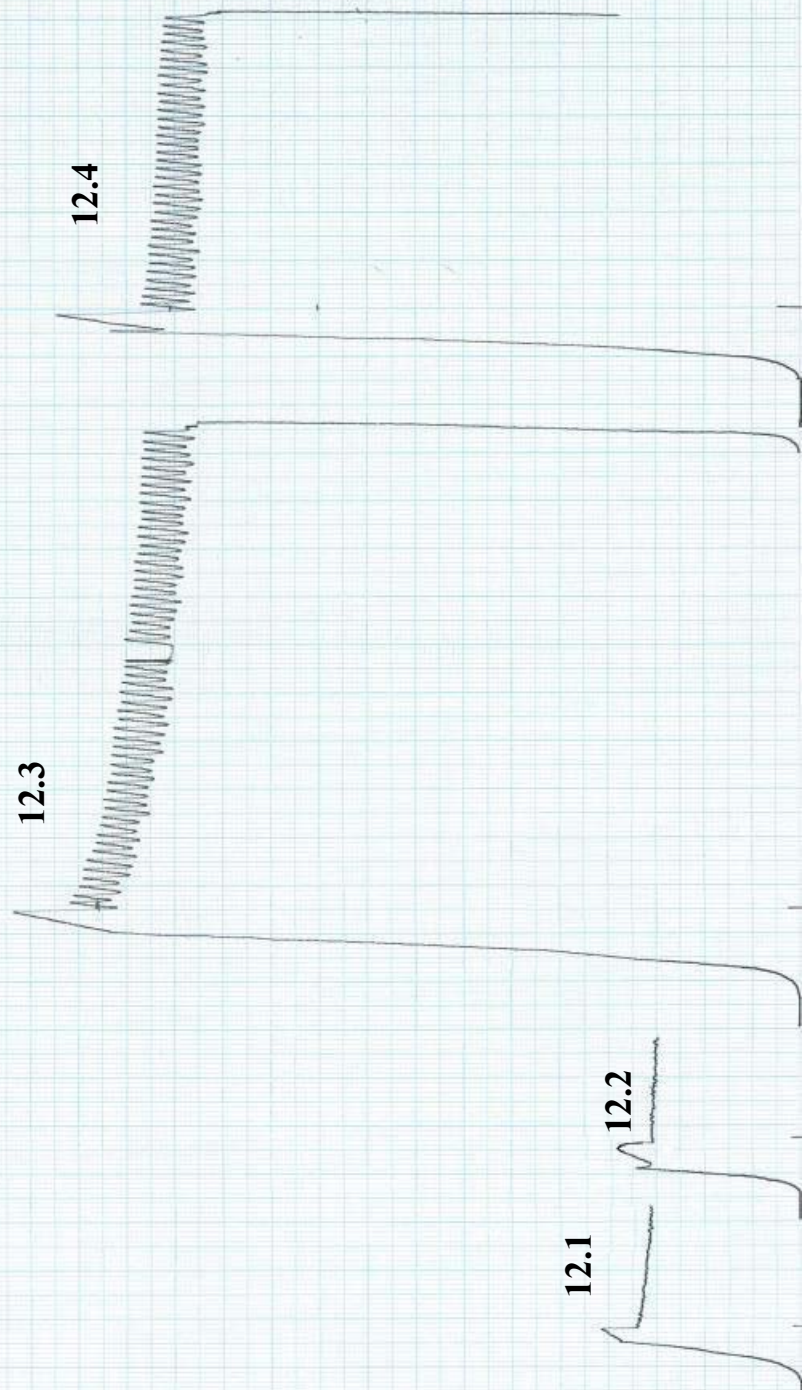


Diagram 12



12.1

		Weight (g)
Board	16	330,8
Board	18	366,2
Board	21	344,3

Moisture Content (%): 11,25

Horsontal Load (N): 400

Max Vertical Load, Vmax (N): 168

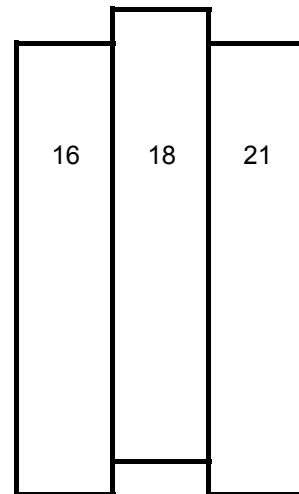
Static Friction Coefficient (μ): 0,21

Displacement at Vmax, d (mm): 0,1375

Load rate (mm/min): 0,6

Previously loaded (digram number): 1.1-1.6

Remarks: none



12.2

		Weight (g)
Board	16	330,8
Board	18	366,2
Board	21	344,3

Moisture Content (%): 11,25

Horsontal Load (N): 400

Max Vertical Load, Vmax (N): 156

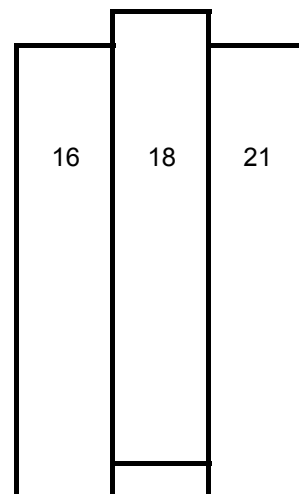
Static Friction Coefficient (μ): 0,195

Displacement at Vmax, d (mm): 0,1375

Load rate (mm/min): 0,6

Previously loaded (digram number): 1.1-1.6 12.1

Remarks: none



12.3

		Weight (g)
Board	16	330,8
Board	18	366,2
Board	21	344,3

Moisture Content (%): 11,25

Horsontal Load (N): 1200

Max Vertical Load, Vmax (N): 652

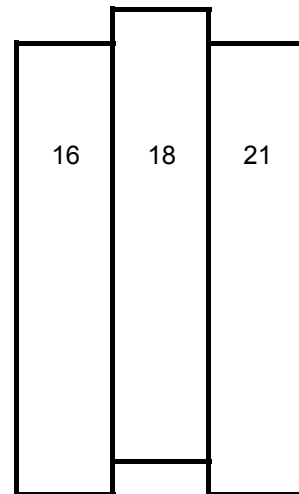
Static Friction Coefficient (μ): 0,271666667

Displacement at Vmax, d (mm): 0,2375

Load rate (mm/min): 0,6

Previously loaded (digram number): 1.1-1.6 12.1-12.2

Remarks: none



12.4

		Weight (g)
Board	16	330,8
Board	18	366,2
Board	21	344,3

Moisture Content (%): 11,25

Horsontal Load (N): 1200

Max Vertical Load, Vmax (N): 616

Static Friction Coefficient (μ): 0,256666667

Displacement at Vmax, d (mm): 0,1875

Load rate (mm/min): 0,6

Previously loaded (digram number): 1.1-1.6 12.1-12.3

Remarks: none

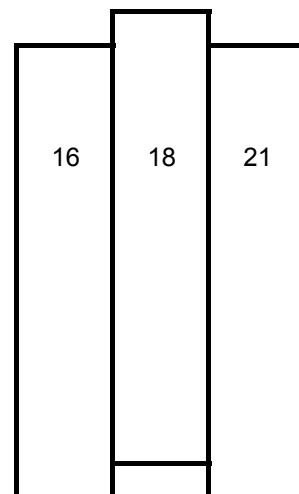
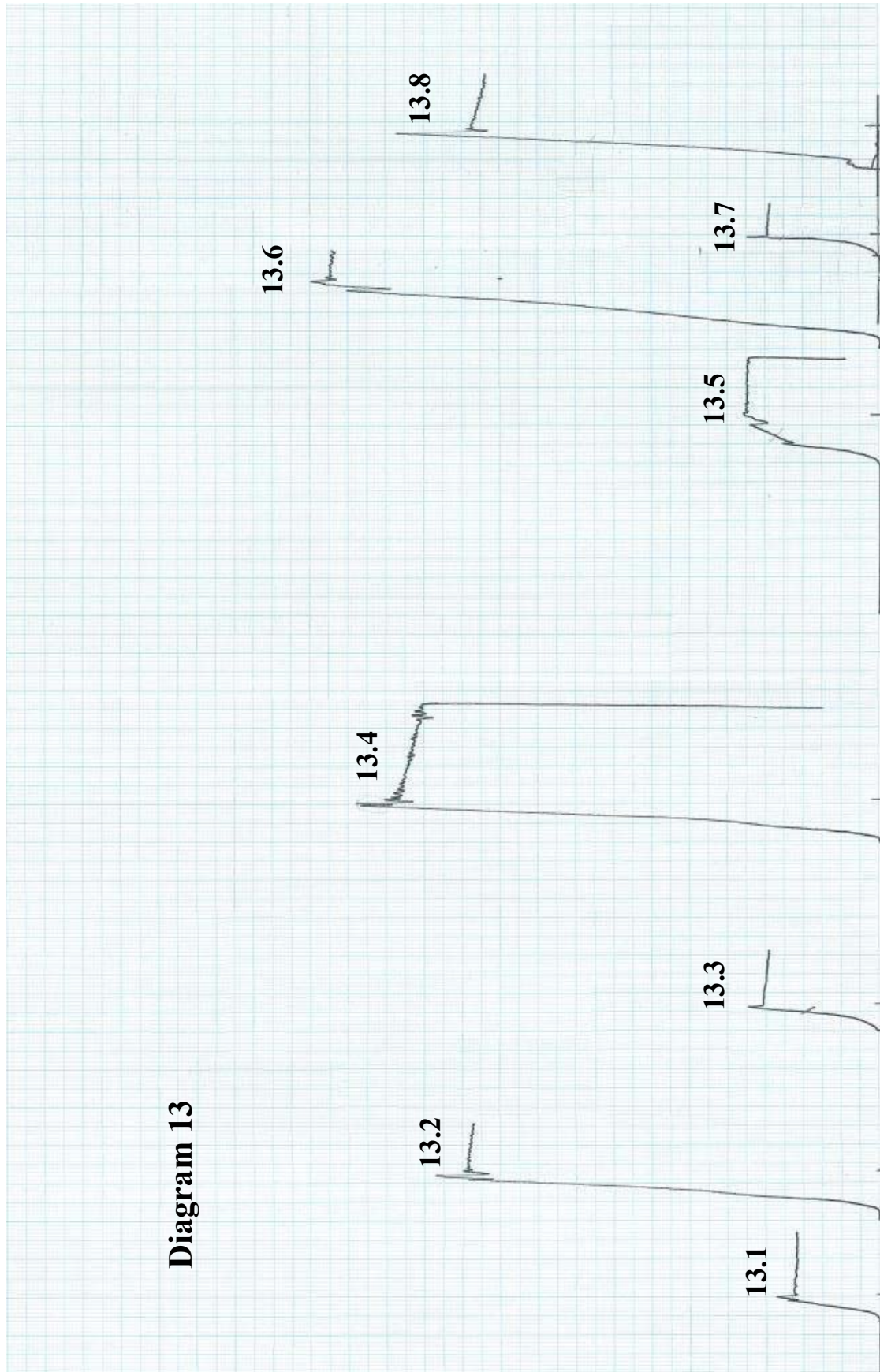


Diagram 13



13.1

		Weight (g)
Board	17	328
Board	24	393,6
Board	20	337,7

Moisture Content (%): 9,76

Horsontal Load (N): 400

Max Vertical Load, Vmax (N): 108

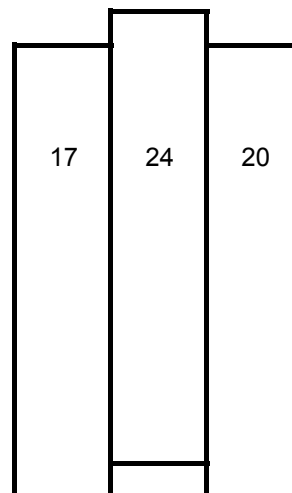
Static Friction Coefficient (μ): 0,135

Displacement at Vmax, d (mm): 0,0875

Load rate (mm/min): 0,3

Previously loaded (digram number): 3.1-3.5 10.1-10.5

Remarks: none



13.2

		Weight (g)
Board	17	328
Board	24	393,6
Board	20	337,7

Moisture Content (%): 9,76

Horsontal Load (N): 1200

Max Vertical Load, Vmax (N): 468

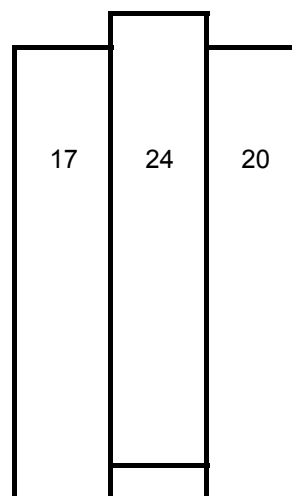
Static Friction Coefficient (μ): 0,195

Displacement at Vmax, d (mm): 0,125

Load rate (mm/min): 0,3

Previously loaded (digram number): 3.1-3.5 10.1-10.5 13.1

Remarks: none



13.3

		Weight (g)
Board	26	375,6
Board	27	333,5
Board	29	346,3

Moisture Content (%): 9,76

Horsontal Load (N): 400

Max Vertical Load, Vmax (N): 140

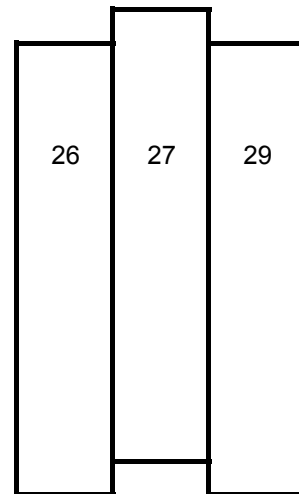
Static Friction Coefficient (μ): 0,175

Displacement at Vmax, d (mm): 0,0875

Load rate (mm/min): 0,3

Previously loaded (digram number): 4.1-4.4 9.1-9.4

Remarks: none



13.4

		Weight (g)
Board	26	375,6
Board	27	333,5
Board	29	346,3

Moisture Content (%): 9,76

Horsontal Load (N): 1200

Max Vertical Load, Vmax (N): 552

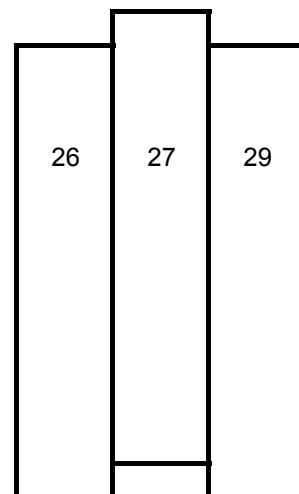
Static Friction Coefficient (μ): 0,23

Displacement at Vmax, d (mm): 0,125

Load rate (mm/min): 0,3

Previously loaded (digram number): 4.1-4.4 9.1-9.4 13.3

Remarks: none



13.5

		Weight (g)
Board	1	324,5
Board	25	340,4
Board	15	399,6

Moisture Content (%): 9,76

Horsontal Load (N): 400

Max Vertical Load, Vmax (N): 140

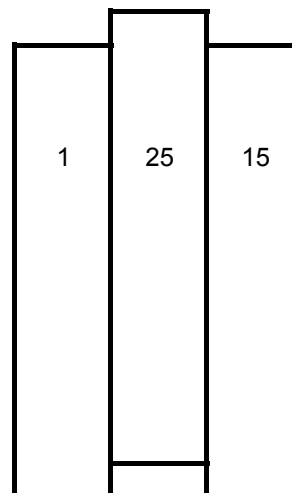
Static Friction Coefficient (μ): 0,175

Displacement at Vmax, d (mm): 0,1625

Load rate (mm/min): 0,3

Previously loaded (digram number): 2.1-2.6 11.1-11.6

Remarks: none

**13.6**

		Weight (g)
Board	1	324,5
Board	25	340,4
Board	15	399,6

Moisture Content (%): 9,76

Horsontal Load (N): 1200

Max Vertical Load, Vmax (N): 600

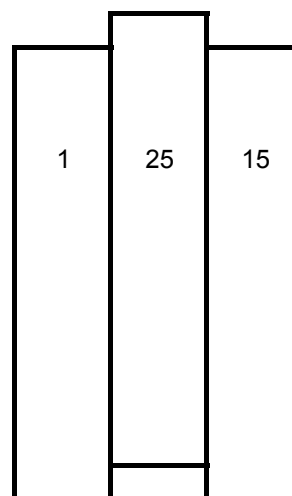
Static Friction Coefficient (μ): 0,25

Displacement at Vmax, d (mm): 0,1875

Load rate (mm/min): 0,3

Previously loaded (digram number): 2.1-2.6 11.1-11.6 13.5

Remarks: none



13.7

	Weight (g)	
Board	16	-
Board	18	328
Board	21	336,4

Moisture Content (%): 9,76

Horsontal Load (N): 400

Max Vertical Load, Vmax (N): 140

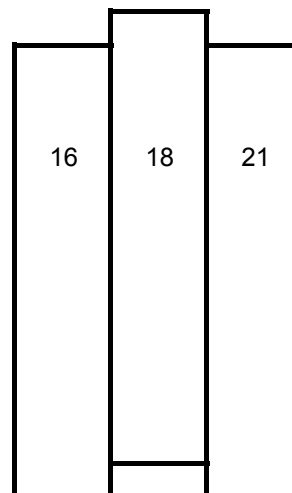
Static Friction Coefficient (μ): 0,175

Displacement at Vmax, d (mm): 0,075

Load rate (mm/min): 0,3

Previously loaded (digram number): 1.1-1.6 12.1-12.4

Remarks: none

**13.8**

	Weight (g)	
Board	16	-
Board	18	328
Board	21	336,4

Moisture Content (%): 9,76

Horsontal Load (N): 1200

Max Vertical Load, Vmax (N): 508

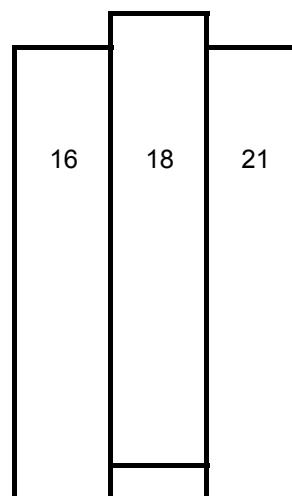
Static Friction Coefficient (μ): 0,211666667

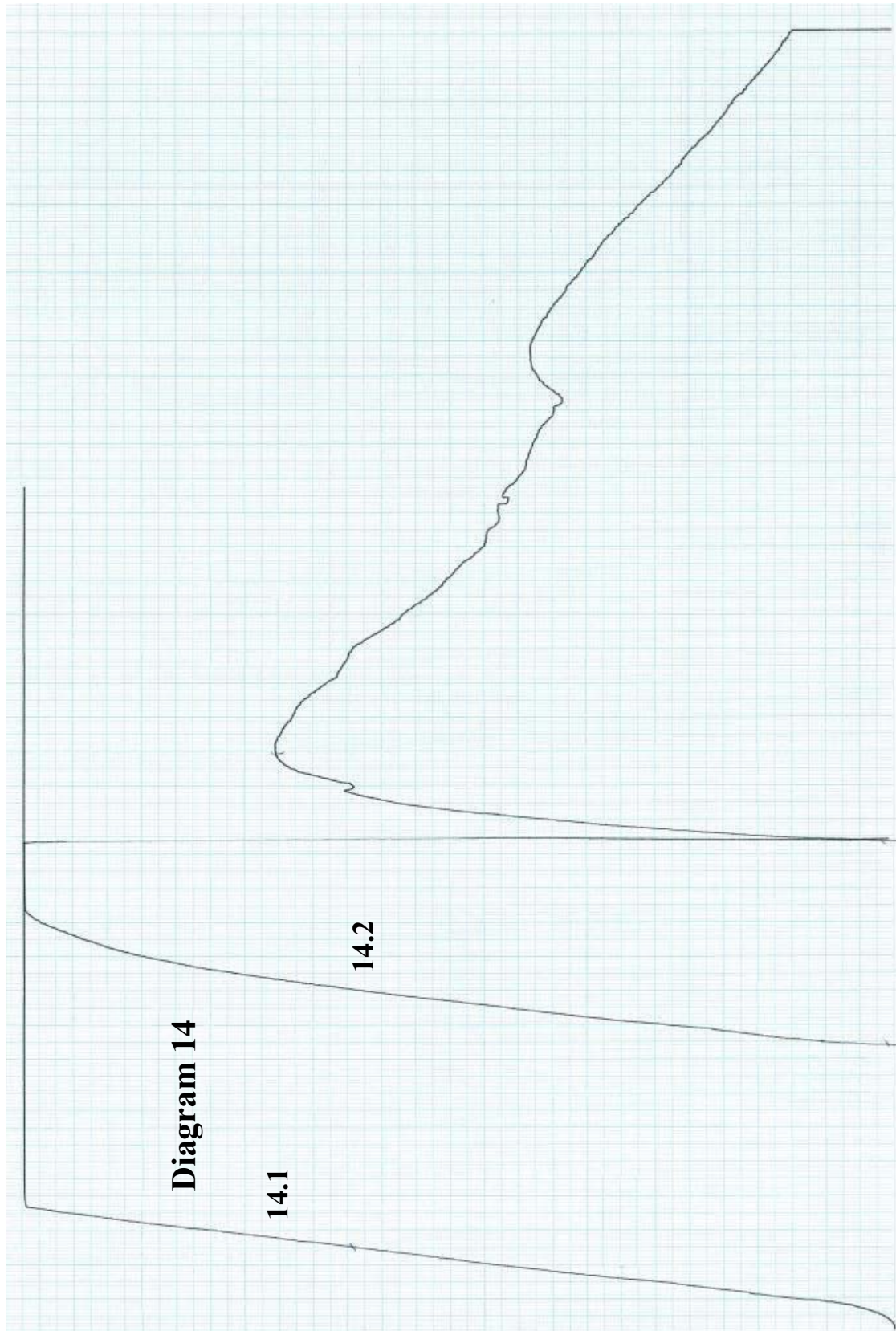
Displacement at Vmax, d (mm): 0,1375

Load rate (mm/min): 0,3

Previously loaded (digram number): 1.1-1.6 12.1-12.4 13.7

Remarks: none





14.1

	Weight (g)	
Board	14	-
Board	7	-
Board	9	-

Moisture Content (%): 9,76

Horsontal Load (N): 400

Max Vertical Load, Vmax (N): 1960

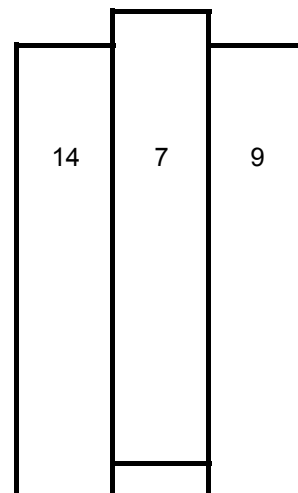
Static Friction Coefficient (μ): 2,45

Displacement at Vmax, d (mm): unknown

Load rate (mm/min): 0.3

Previously loaded (digram number): 7.1 - 7.8

Remarks: Wallpaper used



14.2

	Weight (g)	
Board	19	-
Board	22	-
Board	23	-

Moisture Content (%): 9,76

Horsontal Load (N): 400

Max Vertical Load, Vmax (N): 2260

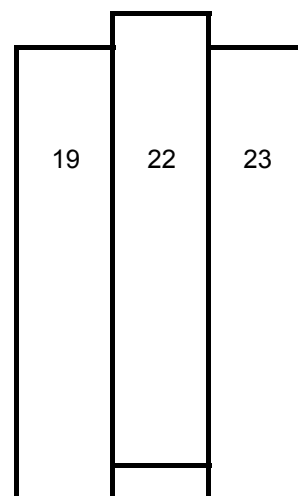
Static Friction Coefficient (μ): 2,825

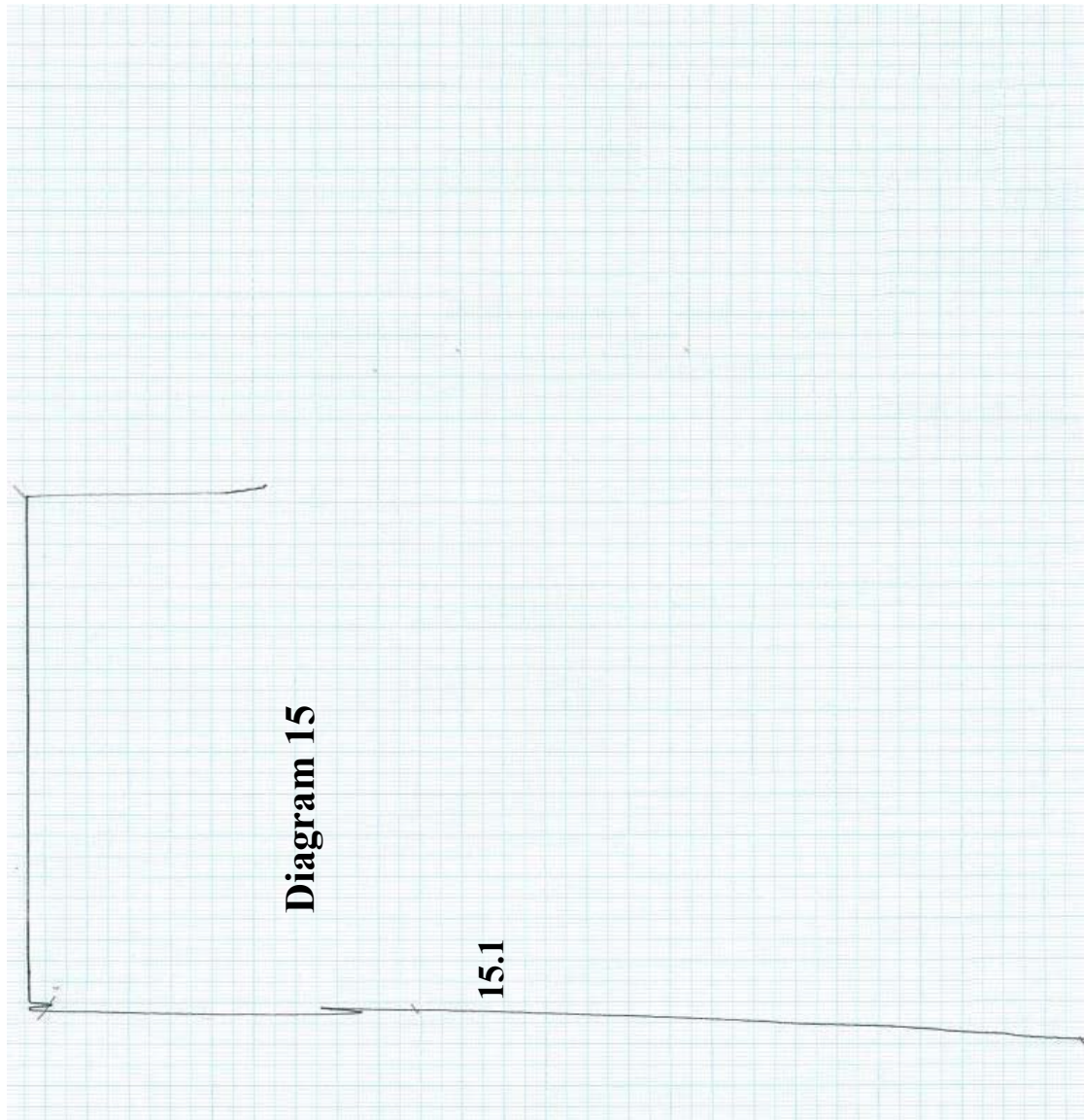
Displacement at Vmax, d (mm): unknown

Load rate (mm/min): 0,3

Previously loaded (digram number): 8.1-8.4

Remarks: Wallpaper used





15.1

	Weight (g)	
Board 13	-	
Board 12	-	
Board 10	-	

Moisture Content (%): 9,76

Horsonal Load (N): 1200

Max Vertical Load, Vmax (N): 3100

Static Friction Coefficient (μ): 1,291666667

Displacement at Vmax, d (mm): unknown

Load rate (mm/min): 0,3

Previously loaded (digram number): 6.1-6.5

Remarks: Wallpaper used, The max capacity reached 4100 rapidly but after a click it was reduced to 3100, probably glue in slot between boards

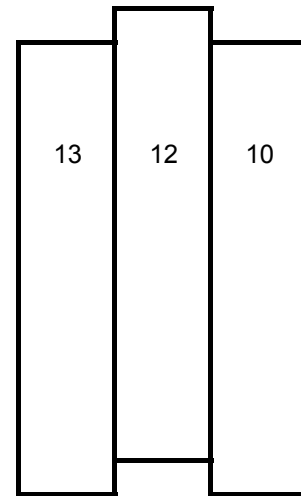
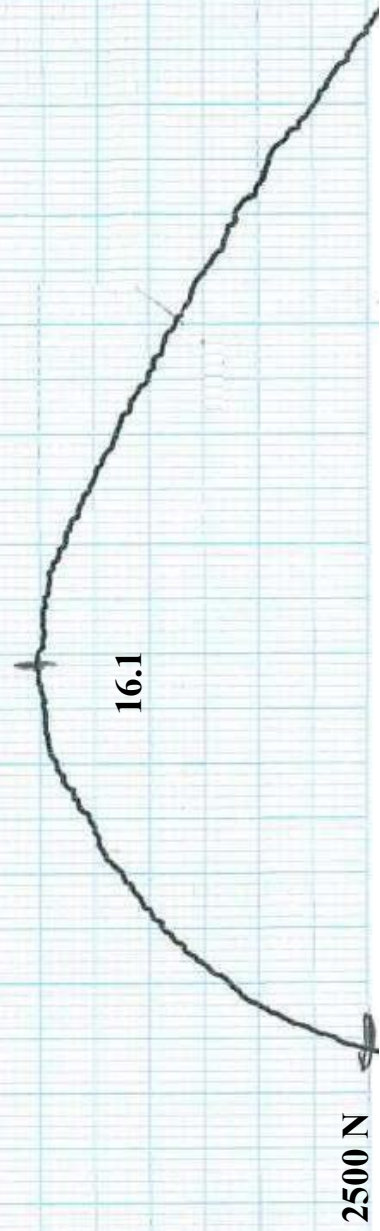


Diagram 16



16.1

	Weight (g)	
Board	11	-
Board	6	-
Board	8	-

Moisture Content (%): 9,76

Horsonal Load (N): 1200

Max Vertical Load, Vmax (N): 2670

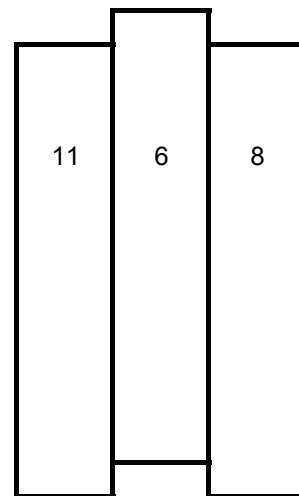
Static Friction Coefficient (μ): 1,1125

Displacement at Vmax, d (mm): unknown

Load rate (mm/min): 0,3

Previously loaded (digram number): 5.1-5.11

Remarks: Wallpaper used



11 Appendix B - Repeated loading

no. 1.1 and 1.2 the static friction coefficient varies from 0,35 to 0,345

peak values on both and the kinetic follows the figure above.

Peak value 1.1 = 2,86%

Peak value 1.2 = 7,25%

no. 1.5 and 1.6 the static friction coefficient varies from 0,407 to 0,407

peak values on both and the kinetic follows the figure above.

Peak value 1.5 = 2,46%

Peak value 1.6 = 8,2%

no. 2.1 and 2.2 the static friction coefficient varies from 0,5 to 0,52

peak values on 2.2 only and the kinetic follows the figure above.

Peak value 2.1 = 0%

Peak value 2.2 = 5,7%

no. 5.1 - 5.5 the static friction coefficient varies in following order

0,58 ; 0,62 ; 0,6 ; 0,61 ; 0,63

peak values on all but 5.1 only and the kinetic follows the figure above (5.2 5.3), different load rate.

Peak value 5.1 = 0%

Peak value 5.2 = 11,29%

Peak value 5.3 = 11,67%

Peak value 5.4 = 6,56%

Peak value 5.5 = 12,7%

no. 5.6 and 5.7 the static friction coefficient varies from 0,38 to 0,38

peak values both and the kinetic follows the figure above.

Peak value 5,6 = 5,26%

Peak value 5,7 = 9,21%

no. 5,8 and 5,9 the static friction coefficient varies from 0,395 to 0,4275

peak values on 5,9 only and the kinetic follows the figure above.

Peak value 5,8 = 0%

Peak value 5,9 = 7,6%

no. 9,1 and 9,2 the static friction coefficient varies from 0,23 to 0,25

peak values both and the kinetic follows the figure above.

Peak value 9,1 = 10,87%

Peak value 9,2 = 18%

no. 9,3 and 9,4 the static friction coefficient varies from 0,262 to 0,275

peak values both and the kinetic follows the figure above.

Peak value 9,3 = 1,91%

Peak value 9,4 = 10,3%

no. 10,1 and 10,2 the static friction coefficient varies from 0,21 to 0,215

peak values both and the kinetic follows the figure above.

Peak value 10,1 = 2,38%

Peak value 10,2 = 11,63%

no. 10,3 - 10,5 the static friction coefficient varies in following order

0,31 ; 0,29 ; 0,275

peak values on all and the kinetic follows the figure above.

Peak value 10,3 = 3,3%

Peak value 10,4 = 7,87%

Peak value 10,5 = 4,85%

no. 11,3 - 11,5 the static friction coefficient varies in following order

0,287 ; 0,307 ; 0,278

peak values on all and the kinetic follows the figure above.

Peak value 11,3 = 1,16%

Peak value 11,4 = 13%

Peak value 11,5 = 12%

no. 12,1 and 12,2 the static friction coefficient varies from 0,21 to 0,195

peak values both and the kinetic follows the figure above.

Peak value 10,1 = 19%

Peak value 10,2 = 20,5%

no. 12,3 and 12,4 the static friction coefficient varies from 0,272 to 0,257

peak values both and the kinetic follows the figure above.

Peak value 10,1 = 9,82%

Peak value 10,2 = 14,94%